Jinchao Xu

Deep Learning Algorithms and Analysis

Summer 2020

Contributors:

This set of notes are based on contributions from many of graduate students, post-doctoral fellows and other collaborators. Here is a partial list:

Juncai He, Qingguo Hong, Li Jiang, Jonathan Siegel, Limin Ma, Lian Zhang, Shenglan Zhao.....

Contents

1

Machine Learning and Image Classification

In this chapter, we give a general introduction to image classification, which is one of the basic machine learning problems and we also discuss some popular datasets: MNIST, CIFAR and ImageNet.

1.1 Introduction to machine learning

Machine learning, a subset of the field of artificial intelligence (AI), is a field that uses the algorithms to explore the underlying patterns in the data. It is an interdisciplinary field involving many majors such as mathematics, statistics and computer science.

Mitchell [**?**] gives a formal definition of learning "A computer program is said to learn from experience E with respect to some class of tasks T and performance measure P, if its performance at tasks in T, as measured by P, improves with experience E." Here the experience E, task T and performance measure P can be chosen from a broad range.

The machine learning algorithms can be broadly categorized into three divisions based on the approach, the data type and the task to be solved: supervised learning algorithms, unsupervised learning algorithms and reinforcement learning algorithms. We will focus on the supervised learning algorithms here.

A typical supervised machine learning task consists of the dataset, the model and the learning algorithm. The data can be selected from a wide variety like digits, pictures, words, etc. The dataset includes the training set, validation set and test set. For the clarification problem, we call the dataset involved in training the model the training set, the dataset used for selecting the optimal model the validation set and the dataset to be applied with the optimal model to measure the corresponding generalization ability the test set. The data is used to help the algorithm to build a mathematical model to extract the patterns or learn the experience. This process is called training the model. The main task of the model is to extract the features and characteristics from the training set for learning and generalize it to the previously unseen test set for inferring. The generalization ability is defined as the performance of the model when making inferences on the previously unseen data.

Supervised learning algorithms try to build a mathematical model of a set of data that contains both the inputs and the desired outputs [**?**]. The inputs, which are also called the predictors or the independent variables, are used to predict the values of the outputs, which are also called the responses, the labels or the dependent variables [**?**]. If the the range of the outputs is categorical or has finite numbers, the supervised learning algorithm is used for classification. If there are infinite many numbers in the the range of the outputs, the supervised learning algorithm is used for regression.

The no free lunch theorem [**?**] for machine learning states that, averaged over all possible data generating distributions, every classification algorithm has the same error rate when classifying previously unseen examples. It means no machine learning algorithm is universally any better than any other in some sense [**?**]. Therefore we need to select the optimal algorithm based on the specific problem, dataset and task since no model dominates all the time.

There are many classic supervised learning algorithms that are widely used in various fields. For example, linear regression, logistic regression, support vector machine (SVM), K nearest neighbor (KNN) and so on. For these supervised learning algorithms, the procedure includes 6 steps to be performed [**?**].

1. The type of data to be used as the training set needs to be determined by the people. For instance, the data can be an image, a word or a vector.
2. Collect a training set and test set representative of the real-world use of the model.
3. Resolve the input feature representation of the learned model. For example, the input obtained from measurements can be transformed to a feature vector while an image can be transformed to a matrix.
4. Choose the structure of the learned model and the corresponding learning algorithm. This is to determine which model to use and how to optimize the model.
5. Finish the experiment design and execute the learning algorithm on the training set.
6. Evaluate the accuracy of the learned model on the test set.

1.2 A basic machine learning problem: image classification

Classification problem is a very important part of machine learning. Its goal is to determine which class a new data belongs to based on a set of training data whose class is known. For example, in mail management, classifying an e-mail as “spam” or “non-spam” is a typical binary classification problem, and the classification of credit rating of credit card customers by banks belong to multiple classification problems. More specifically, in order to understand image classification problem, let us pose the following question:

- Given a set of images of cat, dog and rabbit, how does a machine classify the three different classes?

First of all, we introduce how an image is represented on computer. Mathematically, gray-scale image can be considered as a matrix in $\mathbb{R}^{n_0 \times n_0}$ shown below, where the left one is the image from human vision and the right one is the matrix represented in computer. Each entry in this $\mathbb{R}^{n_0 \times n_0}$ corresponds to the value of a pixel belong to $[0, 255]$.

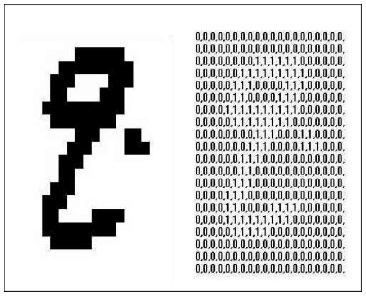

A color image can be taken as 3D tensor (matrix with 3 channels (RGB)) in $\mathbb{R}^{n_0 \times n_0 \times 3}$

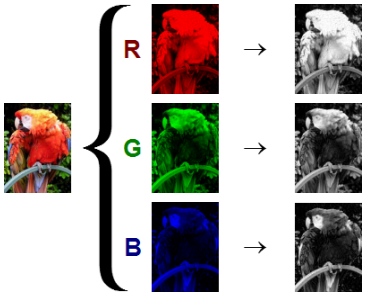

Then, let us think about the image classification problem of cat, dog and rabbit. Each image is a big vector of pixel values, for example

$$d = 1280 \times 720 \times 3(\text{width} \times \text{height} \times \text{RGB channel}) \approx 3\text{M},$$

which can be considered as a point $x \in \mathbb{R}^d$. The question becomes: given 3 different sets of points (cat, dog and rabbit) in $\mathbb{R}^d$, how does a machine classify them?

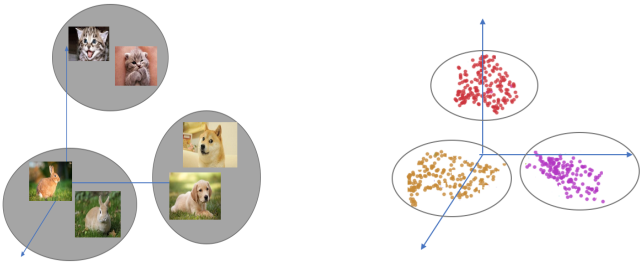

To answer this question, we consider a mathematical problem: Find $f(\cdot;\boldsymbol{\theta}) : \mathbb{R}^d \to \mathbb{R}^3$ such that:

$$f(\text{  };\Theta) \approx \begin{pmatrix}1\\0\\0\end{pmatrix}, \quad f(\text{  };\Theta) \approx \begin{pmatrix}0\\1\\0\end{pmatrix}, \quad f(\text{  };\Theta) \approx \begin{pmatrix}0\\0\\1\end{pmatrix}.$$

$f(\cdot;\boldsymbol{\theta})$ maps a given image to a 3-dimensional vector, which is a probability distribution $\begin{pmatrix}p_1\\p_2\\p_3\end{pmatrix}$, where p_1, p_2, p_3 are probabilities of the given image being cat, dog, rabbit, respectively. For example

$$f(\text{  };\boldsymbol{\theta}) = \begin{pmatrix}0.7\\0.2\\0.1\end{pmatrix} \quad \Longrightarrow \quad \text{  } = \text{cat}.$$

f is a classifier that can be used to classify what a given image is.

1.3 Some popular data sets in image classification

In this subsection, we will introduce some popular and standard data sets in image classification. The most popular four data sets, MNIST, CIFAR-10, CIFAR-100 and ImageNet are shown in Table 1.1.

dataset	training (N)	test (M)	classes (k)	channels (c)	input size (d)
MNIST	60K	10K	10	Greyscale	28*28
CIFAR-10	50K	10K	10	RGB	32*32
CIFAR-100	50K	10K	100	RGB	32*32
ImageNet	1.2M	50K	1000	RGB	224*224

Table 1.1. Basic descriptions about popular datasets

1.3.1 MNIST (Modified National Institute of Standards and Technology Database)

MNIST[**?**] is a database for handwritten digits. It is a simple database for people who want to try learning techniques and pattern recognition methods on real-world data while spending minimal efforts on preprocessing and formatting. In order to use MNIST for the classification problem, the following setup is often used:

- Training set : $N = 60,000$;
- Test set : $M = 10,000$;
- Image size : $d = 28 * 28 * 1 = 784$;
- Classes: $k = 10$;

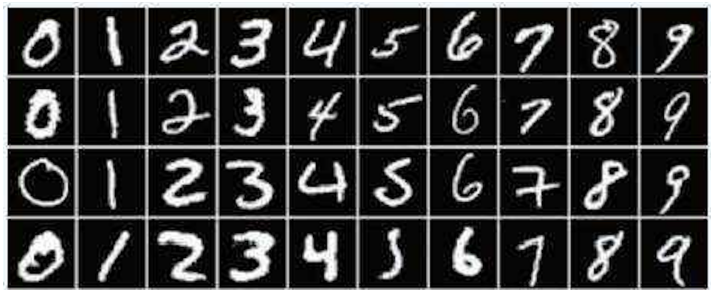

Fig. 1.1. Some images in MNIST.

The following example shows an image of handwritten digits is represented mathematically

$$x = \boxed{2} = \begin{pmatrix} x_1 \\ x_2 \\ \vdots \\ x_{784} \end{pmatrix} \in \mathbb{R}^{784}.$$

MNIST has 10 classes denoted by $\{A_k\}_{k=1}^{10}$ as shown in the following, where A_k is the set of handwritten digits k for $k = 1, 2, 3, ..., 9$ and A_{10} is the set of handwritten digits 0

$$(1.1)\quad A_2 = \left\{\boxed{2}, \boxed{2}, \cdots\right\},\ A_9 = \left\{\boxed{9}, \boxed{9}, \cdots\right\},\ A_{10} = \left\{\boxed{0}, \boxed{0}, \cdots\right\} \subset \mathbb{R}^{784}.$$

1.3.2 CIFAR

CIFAR-10

CIFAR-10[**?**] is a set of images that can be used to teach a computer how to recognize objects. It contains 60,000 32x32 color images in 10 different classes, with 6000

images per class. The 10 different classes represent airplanes, cars, birds, cats, deer, dogs, frogs, horses, ships, and trucks. In order to use CIFAR-10 for the classification problem, people usually use the following setup:

- Training set : $N = 50,000$
- Test set : $M = 10,000$
- Image size : $d = 32 * 32 * 3$
- Classes: $k = 10$

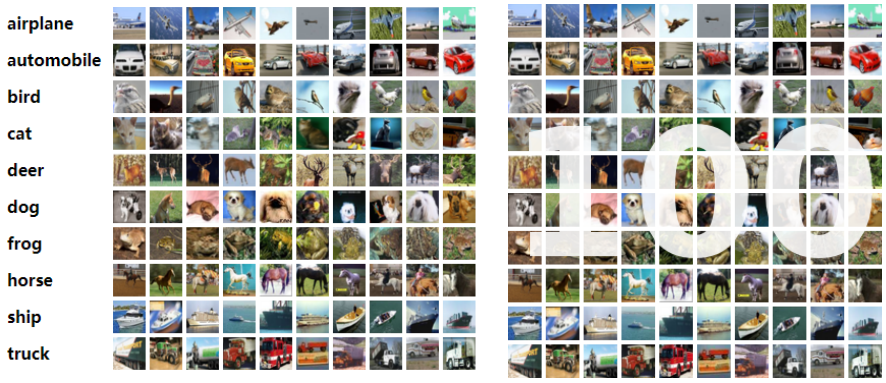

Fig. 1.2. Left: Some images in CIFAR-10. Right: Some images in CIFAR-100.

CIFAR-100

CIFAR-100[**?**] is just like the CIFAR-10, except it has 100 classes containing 600 images each. There are 500 training images and 100 testing images per class. The 100 classes in the CIFAR-100 are grouped into 20 superclasses and each superclass has 5 classes. Each image comes with a "fine" label (the class to which it belongs) and a "coarse" label (the superclass to which it belongs). In order to use CIFAR-100 for the classification problem, people usually use the following setup:

- Training set : $N = 50,000$
- Test set : $M = 10,000$
- Image size : $d = 32 * 32 * 3$
- Classes: $k = 100$

1.3.3 ImageNet

The ImageNet[**?**] project is a large visual database designed for use in visual object recognition software research. More than 1 million images have been hand labeled to indicate what objects are pictured. It is organized according to the WordNet hierarchy

(currently only the nouns), in which each node of the hierarchy is depicted by hundreds and thousands of images. Since 2010, the ImageNet runs an annual software contest, the ImageNet Large Scale Visual Recognition Challenge (ILSVRC), where software programs compete to correctly classify and detect objects and scenes. In order to use ImageNet for the classification problem, we list the setup of ILSVRC2012 in the following

- Training set : $N = 1,200,000$
- Test set : $M = 50,000$
- Image size : $d = 224 * 224 * 3$
- Classes: $k = 1,000$

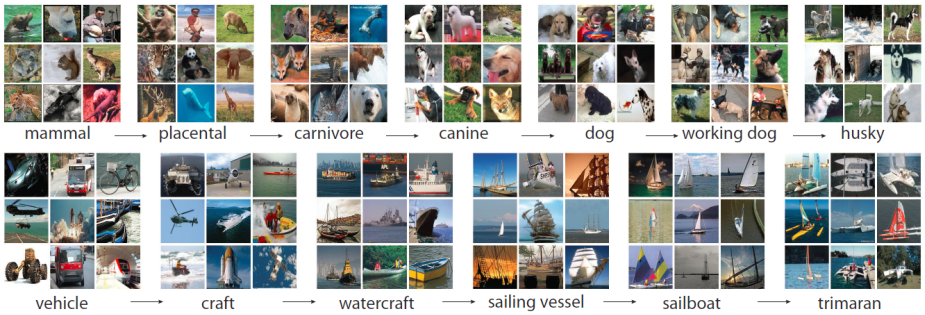

Fig. 1.3. Some images in ImageNet.

2

Linear Machine Learning Models

In this chapter, we will mainly consider two statistic models, namely logistic regression for linearly separable sets, and support vector machine (SVM). These two linear models form the foundation of deep learning, since the final fully connected output layer of a deep neural network is often given by one of these two linear classifiers. One main objective in this chapter is that these linear classification models can be used to classify a collection of linearly separable classes.

In the presentation of this chapter, we treat both logistic regression and support vector machine as pure mathematical techniques for linearly separable sets. In the later chapters, we will relate these techniques in the context of machine learning, especially deep learning.

2.1 Definition of linearly separable sets

In this section, we consider a special class of k linearly separable sets for $k \geq 2$. Let us first introduce the following definition for binary classification.

For $k = 2$, there is a very simple geometric interpretation of two linearly separable sets.

Definition 1. *The two sets A_1, $A_2 \subset \mathbb{R}^d$ are linearly separable if there exists a hyperplane*

$$H_0 = \{x : wx + b = 0\}, \tag{2.1}$$

such that $wx + b > 0$ if $x \in A_1$ and $wx + b < 0$ if $x \in A_2$.

Lemma 1. *The two sets A_1, $A_2 \subset \mathbb{R}^d$ are linearly separable if there exists*

$$W = \begin{pmatrix} w_1 \\ w_2 \end{pmatrix} \in \mathbb{R}^{2\times d}, b = \begin{pmatrix} b_1 \\ b_2 \end{pmatrix} \in \mathbb{R}^{2\times d}, \tag{2.2}$$

such that,

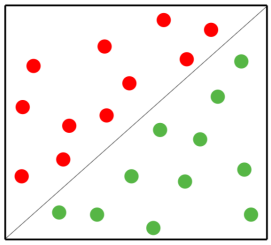

Fig. 2.1. One linearly separable set

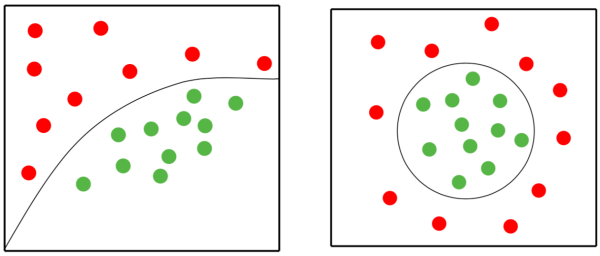

Fig. 2.2. Two non-linearly separable sets

$$w_1 x + b_1 > w_2 x + b_2, \ \forall x \in A_1, \tag{2.3}$$

and

$$w_1 x + b_1 < w_2 x + b_2, \ \forall x \in A_2. \tag{2.4}$$

Proof. Here, we can just take $w = w_1 - w_2$ and $b = b_1 - b_2$, then we can check that the hyperplane $wx + b$ satisfies the definition as presented before. □

Now let us consider multi-class classification. To begin with the definition, let us assume that the data space is divided into k classes represented by k disjoint sets $A_1, A_2, \cdots, A_k \subset \mathbb{R}^d$, which means

$$A = A_1 \cup A_2 \cup \cdots \cup A_k, \ A_i \cap A_j = \emptyset, \forall i \neq j. \tag{2.5}$$

Definition 2 (Linearly Separable). *A collection of subsets $A_1, ..., A_k \subset \mathbb{R}^d$ are linearly separable if there exist*

$$W = \begin{pmatrix} w_1 \\ \vdots \\ w_k \end{pmatrix} \in \mathbb{R}^{k \times d}, b = \begin{pmatrix} b_1 \\ \vdots \\ b_k \end{pmatrix} \in \mathbb{R}^{k \times d}, \tag{2.6}$$

such that, for each $1 \leq i \leq k$ and $j \neq i$

$$w_i x + b_i > w_j x + b_j, \ \forall x \in A_i. \tag{2.7}$$

namely, each pairs of A_i and A_j are linearly separable by the plane

$$H_{ij} = \{(w_i - w_j) \cdot x + (b_i - b_j) = 0\}, \quad \forall j \neq i. \tag{2.8}$$

The geometric interpretation for linearly separable sets is less obvious when $k > 2$.

Lemma 2. *Assume that $A_1, ..., A_k$ are linearly separable and $W \in \mathbb{R}^{k\times d}$ and $b \in \mathbb{R}^k$ satisfy (2.6). Define*

$$\Gamma_i(W, b) = \{x \in \mathbb{R}^d : (Wx + b)_i > (Wx + b)_j, \ \forall j \neq i\} \tag{2.9}$$

Then for each i,

$$A_i \subset \Gamma_i(W, b) \tag{2.10}$$

We note that each $\Gamma_i(W, b)$ is a polygon whose boundary consists of hyperplanes given by (2.8).

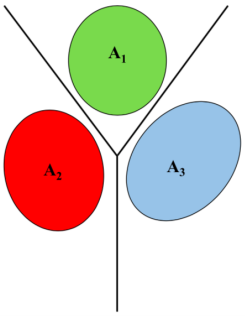

Fig. 2.3. Linearly separable sets in 2-d space (k = 3)

We next introduce two more definitions of linearly separable sets that have more clear geometric interpretation.

Definition 3 (All-vs-One Linearly Separable). *A collection of subsets $A_1, ..., A_k \subset \mathbb{R}^d$ is all-vs-one linearly separable if for each $i = 1, ..., k$, A_i and $\cup_{j\neq i} A_j$ are linearly separable.*

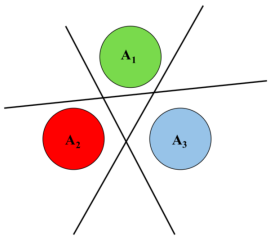

Fig. 2.4. All-vs-One linearly separable sets (k = 3)

Definition 4 (Pairwise Linearly Separable). *A collection of subsets $A_1, ..., A_k \subset \mathbb{R}^d$ is pairwise linearly separable if for each pair of indices $1 \le i < j \le k$, A_i and A_j are linearly separable.*

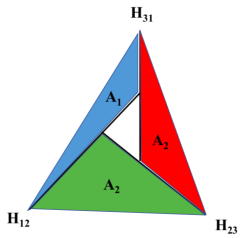

Fig. 2.5. Pairwise linearly separable sets in 2-d space (k = 3)

We begin by comparing our notion of linearly separable to the two other previously introduced geometric definitions of all-vs-one linearly separable and pairwise lineaerly separable. Obviously, in the case of two classes, they are all equivalent, however, with more than two classes this is no longer the case. We do have the following implications, though.

Lemma 3. *If $A_1, ..., A_k \subset \mathbb{R}^d$ are all-vs-one linearly separable, then they are linearly separable as well.*

Proof. Assume that $A_1, ..., A_k$ are all-vs-one linearly separable. For each i, let w_i, b_i be such that $w_i x + b_i$ separates A_i from $\cup_{j\neq i} A_j$, i.e. $w_i x + b_i > 0$ for $x \in A_i$ and $w_i x + b_i < 0$ for $x \in \cup_{j\neq i} A_j$.

Set $W = (w_1^T, w_2^T, \cdots, w_k^T)^T$, $b = (b_1, b_2, \cdots, b_k)^T$ and observe that if $x \in A_i$, then $(Wx + b)_i > 0$ while $(Wx + b)_j < 0$ for all $j \neq i$. □

Lemma 4. *If $A_1, ..., A_k \subset \mathbb{R}^n$ are linearly separable, then they are pairwise linearly separable as well.*

Proof. If $A_1, ..., A_k \subset \mathbb{R}^d$ are linearly separable, suppose that $W = (w_1^T, w_2^T, \cdots, w_k^T)^T$, $b = (b_1, b_2, \cdots, b_k)^T$. So we have

$$\begin{cases} w_i x + b_i > w_j x + b_j & x \in A_i \\ w_i x + b_i < w_j x + b_j & x \in A_j \end{cases} \tag{2.11}$$

Take $w_{i,j} = w_i - w_j, b_{i,j} = b_i - b_j$, then we have

$$w_{i,j} x + b_{i,j} \begin{cases} > 0 & x \in A_i \\ < 0 & x \in A_j \end{cases} \tag{2.12}$$

So $A_1, ..., A_k$ are pairwise linearly separable. □

However, the converses of both of these statements are false, as the following examples show.

Example 1 (Linearly separable but not all-vs-one linearly separable). Consider the sets $A_1, A_2, A_3 \subset \mathbb{R}$ given by $A_1 = [-4, -2]$, $A_2 = [-1, 1]$, and $A_3 = [2, 4]$. These sets are clearly not one-vs-all linearly separable because A_2 cannot be separated from both A_1 and A_3 by a single plane (in $\mathbb{R}$ this is just cutting the real line at a given number, and A_2 is in the middle).

However, these sets are linearly separated by $W = [-2, 0, 2]^T$ and $b = [-3, 0, -3]^T$, for example.

Example 2 (Pairwise linearly separable but not linearly separable). Consider the sets $A_1, A_2, A_3 \subset \mathbb{R}^2$ shown in figure 2.5. Note that A_i and A_j are separated by hyperplane $H_{i,j}$ (drawn in the figure) and so these sets are pairwise linearly separable. We will show that they are not linearly separable.

Assume to the contrary that $W \in \mathbb{R}^{3\times 2}$ and $b \in \mathbb{R}^2$ separate A_1, A_2, and A_3. Then $(w_i - w_j)x + (b_i - b_j)$ must be a plane which separates A_i and A_j. Now consider a point z bounded by A_1, A_2 and A_3 in figure 2.5. We see from the figure that given any plane separating A_1 from A_2, z must be on the same side as A_2, given any plane separating A_2 from A_3, z must be on the same side as A_3, and given any plane separating A_3 from A_1, z must be on the same side as A_1.

This means that $(w_2 - w_1)z + (b_2 - b_1) > 0$, $(w_3 - w_2)z + (b_3 - b_2) > 0$, and $(w_1 - w_3)z + (b_1 - b_3) > 0$. Adding these together, we obtain $0 > 0$, a contradiction.

The essence behind this example is that although the sets A_1, A_2, and A_3 are pairwise linearly separable, no possible pairwise separation allows us to consistently classify arbitrary new points. However, a linear separation would give us a consistent scheme for classifying new points.

So the notion of linear separability is sandwiched in between the more intuitive notions of all-vs-one and pairwise separability. It turns out that linear separability is the notion which is most useful for the k-class classification problem and so we focus on this notion of separability from now on.

2.2 Introduction to logistic regression

In this section, we introduce techniques related to basic logistic regression, see [**?**] for more details.

2.2.1 Logistic regression

Assume that we are given k linearly separable sets $A_1, A_2, \cdots, A_k \in \mathbb{R}^d$, we define the set of classifiable weights as

$$\boldsymbol{\Theta} = \{\boldsymbol{\theta} = (W, b) : w_i x + b_i > w_j x + b_j,\ \forall x \in A_i,\ j \neq i, i = 1, \cdots, k\} \tag{2.13}$$

which means those (W, b) can separate $A_1, A_2, \cdots, A_k$ correctly.

Our linearly separable assumption implies that $\boldsymbol{\Theta} \neq \emptyset$. Now we know the existence of linearly classifiable weights. But how can we find one element in $\boldsymbol{\Theta}$?

Definition 5 (soft-max). *Given $s = (s_1, s_2, \cdots, s_k)^T \in \mathbb{R}^k$, we define the soft-max mapping $\sigma : \mathbb{R}^k \to \mathbb{R}^k$ as*

$$\sigma(s) = \frac{e^s}{e^s \cdot \mathbf{1}} = \frac{1}{\sum_{i=1}^{k} e^{s_i}} \begin{pmatrix} e^{s_1} \\ e^{s_2} \\ \vdots \\ e^{s_k} \end{pmatrix} \tag{2.14}$$

where $e^s = \begin{pmatrix} e^{s_1} \\ e^{s_2} \\ \vdots \\ e^{s_k} \end{pmatrix}$, $\mathbf{1} = \begin{pmatrix} 1 \\ 1 \\ \vdots \\ 1 \end{pmatrix} \in \mathbb{R}^k$.

Definition 6. *Given parameter $\boldsymbol{\theta} = (W, b)$, we define a feature mapping $\boldsymbol{p} : \mathbb{R}^d \to \mathbb{R}^k$ as*

$$\boldsymbol{p}(x; \boldsymbol{\theta}) = \sigma(Wx + b) = \frac{1}{\sum_{i=1}^{k} e^{w_i x + b_i}} \begin{pmatrix} e^{w_1 x + b_1} \\ e^{w_2 x + b_2} \\ \vdots \\ e^{w_k x + b_k} \end{pmatrix} = \begin{pmatrix} p_1(x; \boldsymbol{\theta}) \\ p_2(x; \boldsymbol{\theta}) \\ \vdots \\ p_k(x; \boldsymbol{\theta}) \end{pmatrix} \tag{2.15}$$

where the i-th component

$$p_i(x; \boldsymbol{\theta}) = \frac{e^{w_i x + b_i}}{\sum_{i=1}^{k} e^{w_i x + b_i}}. \tag{2.16}$$

The soft-max mapping have several important properties.

1. $0 < p_i(x;\boldsymbol{\theta}) < 1,\ \sum_i p_i(x;\boldsymbol{\theta}) = 1.$

   This implies that $\boldsymbol{p}(x;\boldsymbol{\theta})$ can be regarded as a probability distribution of data points which means that given $x \in \mathbb{R}^d$, we have $x \in A_i$ with probability $p_i(x;\boldsymbol{\theta})$, $i = 1, \cdots, k$.
2. $p_i(x;\boldsymbol{\theta}) > p_j(x;\boldsymbol{\theta}) \Leftrightarrow w_i x + b_i > w_j x + b_j$.
   This implies that the linearly classifiable weights have an equivalent description as

$$\boldsymbol{\Theta} = \left\{\boldsymbol{\theta} : p_i(x;\boldsymbol{\theta}) > p_j(x;\boldsymbol{\theta}),\ \forall x \in A_i,\ j \neq i, i = 1, \cdots, k\right\} \tag{2.17}$$

3. We usually use the max-out method to do classification. For a given data point x, we first use a soft-max mapping to map it to $\boldsymbol{p}(x;\boldsymbol{\theta})$, then we attach x to the class $i = \arg\max_j p_i(x;\boldsymbol{\theta})$.
   This means that we pick the label i as the class of x such that $x \in A_i$ has the biggest probability $p_i(x;\boldsymbol{\theta})$.

More detailed discussion of logistic regression from the probability perspective will be presented in the nearly future.

From the above properties, we can define the following likelihood function to help find elements in $\boldsymbol{\Theta}$:

$$P(\boldsymbol{\theta}) = \prod_{i=1}^{k} \prod_{x \in A_i} p_i(x;\boldsymbol{\theta}). \tag{2.18}$$

Based on the property that

$$p_i(x;\boldsymbol{\theta}) = \max_{1 \leq j \leq k} p_j(x;\boldsymbol{\theta}), \quad \forall x \in A_i,\ \boldsymbol{\theta} \in \Theta, \tag{2.19}$$

we may use the next optimization problem

$$\max_{\boldsymbol{\theta} \in \boldsymbol{\Theta}} P(\boldsymbol{\theta}). \tag{2.20}$$

to find an element in $\boldsymbol{\Theta}$. More precisely, let us introduce the next lemmas (properties) of $P(\boldsymbol{\theta})$.

Lemma 5. *Assume that the sets $A_1, A_2, \cdots, A_k$ are linearly separable. Then we have*

$$\left\{\boldsymbol{\theta} :\ P(\boldsymbol{\theta}) > \frac{1}{2}\right\} \subset \boldsymbol{\Theta}. \tag{2.21}$$

Proof. It suffices to show that if $\boldsymbol{\theta} \notin \boldsymbol{\Theta}$, we must have $P(\boldsymbol{\theta}) \leq \frac{1}{2}$. For any $\boldsymbol{\theta} \notin \boldsymbol{\Theta}$, there must exist an i_0 ,an $x_0 \in A_{i_0}$ and a $j_0 \neq i_0$ such that

$$w_{i_0} x_0 + b_{i_0} \leq w_{j_0} x_0 + b_{j_0}. \tag{2.22}$$

Then we have

$$p_{i_0}(x_0;\boldsymbol{\theta}) \le \frac{e^{w_{i_0}x_0+b_{i_0}}}{e^{w_{i_0}x_0+b_{i_0}}+e^{w_{j_0}x_0+b_{j_0}}} \le \frac{1}{2}. \tag{2.23}$$

Notice that $p_i(x;\boldsymbol{\theta}) < 1$ for all $i = 1,\cdots,k$, $x \in A$. So

$$P(\boldsymbol{\theta}) < p_{i_0}(x_0;\boldsymbol{\theta}) \le \frac{1}{2}. \tag{2.24}$$

□

Lemma 6. *If $A_1, A_2, \cdots, A_k$ are linearly separable and $\boldsymbol{\theta} \in \boldsymbol{\Theta}$, we have*

$$\lim_{\alpha\to+\infty} p_i(x;\alpha\boldsymbol{\theta}) = 1 \Leftrightarrow x \in A_i. \tag{2.25}$$

Proof. We first note that if $x \in A_i$,

$$p_i(x,\boldsymbol{\theta}) = \frac{1}{1+\sum\limits_{j\neq i} e^{\alpha[(w_jx+b_j)-(w_ix+b_i)]}} \to 1, \quad \text{as} \quad \alpha\to\infty. \tag{2.26}$$

On the other hand, if $x \notin A_i$,

$$p_i(x;\boldsymbol{\alpha\theta}) = \frac{1}{1+\sum\limits_{j\neq i} e^{\alpha[(w_jx+b_j)-(w_ix+b_i)]}} \le \frac{1}{2}. \tag{2.27}$$

This implies that if $x \notin A_i$, $\lim_{\alpha\to\infty} p_i(x;\alpha\boldsymbol{\theta}) \neq 1$ which is equivalent to the proposition that if $\lim_{\alpha\to\infty} p_i(x;\alpha\boldsymbol{\theta}) = 1$, then $x \in A_i$. □

Lemma 7. *If $A_1, A_2, \cdots, A_k$ are linearly separable,*

$$\boldsymbol{\Theta} = \left\{\boldsymbol{\theta} : \lim_{\alpha\to+\infty} P(\alpha\boldsymbol{\theta}) = 1\right\}. \tag{2.28}$$

Proof. We first note that if $\boldsymbol{\theta} \in \boldsymbol{\Theta}$, we have $\lim\limits_{\alpha\to+\infty} p_i(x;\alpha\boldsymbol{\theta}) = 1$ for all $x \in A_i$. So

$$\lim_{\alpha\to+\infty} P(\alpha\boldsymbol{\theta}) = \lim_{\alpha\to+\infty} \prod_{i=1}^{k}\prod_{x\in A_i} p_i(x;\alpha\boldsymbol{\theta}) = \prod_{i=1}^{k}\prod_{x\in A_i}\lim_{\alpha\to+\infty} p_i(x;\alpha\boldsymbol{\theta}) = 1. \tag{2.29}$$

On the other hand, if $\lim\limits_{\alpha\to+\infty} P(\alpha\boldsymbol{\theta}) = 1$, there must exist one $\alpha_0 > 0$ such that $P(\alpha_0\boldsymbol{\theta}) > \frac{1}{2}$. From Lemma 5, we have $\alpha_0\boldsymbol{\theta} \in \boldsymbol{\Theta}$, which means $\boldsymbol{\theta} \in \boldsymbol{\Theta}$. □

These properties above imply that if we can obtain a classifiable weight through maximizing $P(\boldsymbol{\theta})$, while lemma 7 tells us that $P(\boldsymbol{\theta})$ will not have a global minimum actually.

More specifically, we just need to find some $\boldsymbol{\theta} \in \boldsymbol{\Theta}$ such that

$$P(\boldsymbol{\theta}) > \frac{1}{2} \Leftrightarrow L(\boldsymbol{\theta}) := -\log P(\boldsymbol{\theta}) < \log(2). \tag{2.30}$$

2.2.2 Regularized logistic regression

Here, we start from the regularization term $e^{-\lambda R(\|\boldsymbol{\theta}\|)}$ with these next properties:

1. $\lambda > 0$.
2. $R(t)$ is a strictly increasing function on $\mathbb{R}^+$ with $R(0) = 0$, $\lim_{t\to+\infty} R(t) = +\infty$. For example, $R(t) = t^2$.
3. $\|\cdot\|$ is a norm on $R^{k\times(d+1)}$, a commonly used norm is the following Frobenius norm:

$$\|\boldsymbol{\theta}\|_F = \sqrt{\sum_{i,j} W_{ij}^2 + \sum_i b_i^2}. \tag{2.31}$$

Based on this regularization term, we may consider the following regularized likelihood function $P_\lambda(\boldsymbol{\theta})$ as

$$P_\lambda(\boldsymbol{\theta}) = P(\boldsymbol{\theta})e^{-\lambda R(\|\boldsymbol{\theta}\|)}. \tag{2.32}$$

Here, let us define

$$\boldsymbol{\Theta}_\lambda = \arg\max_{\boldsymbol{\theta}} P_\lambda(\boldsymbol{\theta}), \tag{2.33}$$

where

$$\arg\max_{\boldsymbol{\theta}} P_\lambda(\boldsymbol{\theta}) = \left\{\boldsymbol{\theta} \ : \ P_\lambda(\boldsymbol{\theta}) = \max_{\boldsymbol{\theta}} P_\lambda(\boldsymbol{\theta})\right\}. \tag{2.34}$$

The next lemma show that the maximal set of modified objective is not empty.

Lemma 8. *Suppose that $A_1, A_2, \cdots, A_k$ are linearly separable, then*

1. *if $\lambda = 0$, $\boldsymbol{\Theta}_0 = \emptyset$,*
2. *$\boldsymbol{\Theta}_\lambda$ must be nonempty for all $\lambda > 0$.*

Proof. Lemma 7 shows the first proposition. For the second proposition, we notice that

1. $P_\lambda(\mathbf{0}) = \frac{1}{k^N}$.
2. $\exists\, M_\lambda > 0$ such that $e^{-\lambda R(\|\boldsymbol{\theta}\|)} < \frac{1}{k^N}$ whenever $\|\boldsymbol{\theta}\| > M_\lambda$ because of the properties of $R(\|\boldsymbol{\theta}\|)$.

So a maxima on $\{\boldsymbol{\theta} : \|\boldsymbol{\theta}\| \le M_\lambda\}$ must be a global maxima. Then we can easily obtain the result in the lemma from the boundedness and closeness of $\{\boldsymbol{\theta} : \|\boldsymbol{\theta}\| \le M_\lambda\}$. □

Furthermore, we have the next theorem which shows that we can indeed get $\boldsymbol{\Theta}$ by maximizing $P_\lambda(\boldsymbol{\theta})$.

Theorem 1. *If $A_1, A_2, \cdots, A_k$ are linearly separable,*

$$\boldsymbol{\Theta}_\lambda \subset \boldsymbol{\Theta}, \tag{2.35}$$

when $\lambda > 0$ and sufficiently small.

Proof. By Lemma 5, we can take $\boldsymbol{\theta}_0 \in \boldsymbol{\Theta}$ such that $P(\boldsymbol{\theta}_0) > \frac{3}{4}$. Then, for any $\lambda < \frac{\log \frac{3}{2}}{R(\|\boldsymbol{\theta}_0\|)}$, $\boldsymbol{\theta}_\lambda \in \boldsymbol{\Theta}_\lambda$, we have

$$P(\boldsymbol{\theta}_\lambda) \geq P_\lambda(\boldsymbol{\theta}_\lambda) \geq P_\lambda(\boldsymbol{\theta}_0) = P(\boldsymbol{\theta}_0) e^{-\lambda R(\|\boldsymbol{\theta}_0\|)} > \frac{3}{4} \cdot \frac{2}{3} = \frac{1}{2},$$

which implies that $\boldsymbol{\theta}_\lambda \in \Theta$. Thus, for any $0 < \lambda < \frac{\log \frac{3}{2}}{R(\|\boldsymbol{\theta}_0\|)}$, $\boldsymbol{\Theta}_\lambda \subset \boldsymbol{\Theta}$.

□

The design of logistic regression is that maximize $P_\lambda(\boldsymbol{\theta})$ is equivalent to minimize $-\log P_\lambda(\boldsymbol{\theta})$, i.e.,

$$\max_{\boldsymbol{\theta}} \{P_\lambda(\boldsymbol{\theta})\} \Leftrightarrow \min_{\boldsymbol{\theta}} \{-\log P_\lambda(\boldsymbol{\theta})\}, \tag{2.36}$$

while the second one is more convenient to evaluate the gradient. Meanwhile, we add a regularization term $R(\boldsymbol{\theta})$ to the objective function which makes the optimization problem has a unique solution.

Mathematically, we can formulate Logistic regression as

$$\min_{\boldsymbol{\theta}} L_\lambda(\boldsymbol{\theta}), \tag{2.37}$$

where

$$L_\lambda(\boldsymbol{\theta}) := -\log P_\lambda(\boldsymbol{\theta}) = -\log P(\boldsymbol{\theta}) + \lambda R(\|\boldsymbol{\theta}\|) = L(\boldsymbol{\theta}) + \lambda R(\|\boldsymbol{\theta}\|), \tag{2.38}$$

with

$$L(\boldsymbol{\theta}) = -\sum_{i=1}^{k} \sum_{x \in A_i} \log p_i(x; \boldsymbol{\theta}). \tag{2.39}$$

Then we have the next logistic regression algorithm.

Algorithm 1 Logistic Regression

Given data $A_1, A_2, \cdots, A_k$, find

$$\boldsymbol{\theta}^* = \arg\min_{\boldsymbol{\theta}} L_\lambda(\boldsymbol{\theta}), \tag{2.40}$$

for some sufficient small $\lambda > 0$.

Remark 1. Here

$$L(\boldsymbol{\theta}) = -\log P(\boldsymbol{\theta}), \tag{2.41}$$

is known as the loss function of logistic regression model. The next reasons may show that why $L(\boldsymbol{\theta})$ is popular.

1. It is more convenient to take gradient for $L(\boldsymbol{\theta})$ than $P(\boldsymbol{\theta})$.
2. $L(\boldsymbol{\theta})$ is related the so-called cross-entropy loss function which will be discussed in the next section.
3. $L(\boldsymbol{\theta})$ is a convex function which will be discussed later.

2.3 KL divergence and cross-entropy

Cross-entropy minimization is frequently used in optimization and rare-event probability estimation. When comparing a distribution against a fixed reference distribution, cross-entropy and KL divergence are identical up to an additive constant. See more details in [**? ? ?**] and the reference therein.

The KL(Kullback–Leibler) divergence defines a special distance between two discrete probability distributions

$$p = \begin{pmatrix} p_1 \\ \vdots \\ p_k \end{pmatrix}, \quad q = \begin{pmatrix} q_1 \\ \vdots \\ q_k \end{pmatrix}$$

with $0 \le p_i, q_i \le 1$ and $\sum_{i=1}^k p_i = \sum_{i=1}^k q_i = 1$ by

$$D_{\mathrm{KL}}(q, p) = \sum_{i=1}^{k} q_i \log \frac{q_i}{p_i}. \tag{2.42}$$

Lemma 9. *$D_{\mathrm{KL}}(q, p)$ works like a "distance" without the symmetry:*

1. *$D_{\mathrm{KL}}(q, p) \ge 0$;*
2. *$D_{\mathrm{KL}}(q, p) = 0$ if and only if $p = q$;*

Proof. We first note that the elementary inequality

$$\log x \le x - 1, \quad \text{for any } x \ge 0, \tag{2.43}$$

and the equality holds if and only if $x = 1$.

$$-D_{\mathrm{KL}}(q, p) = -\sum_{i=1}^{c} q_i \log \frac{q_i}{p_i} = \sum_{i=1}^{k} q_i \log \frac{p_i}{q_i} \le \sum_{i=1}^{k} q_i (\frac{p_i}{q_i} - 1) = 0. \tag{2.44}$$

And the equality holds if and only if

$$\frac{p_i}{q_i} = 1 \quad \forall i = 1 : k. \tag{2.45}$$

□

Define cross-entropy for distribution p and q by

$$H(q, p) = -\sum_{i=1}^{k} q_i \log p_i, \tag{2.46}$$

and the entropy for distribution q by

$$H(q) = -\sum_{i=1}^{k} q_i \log q_i. \tag{2.47}$$

Note that

$$D_{\mathrm{KL}}(q,p)=\sum_{i=1}^{k}q_i\log\frac{q_i}{p_i}=\sum_{i=1}^{k}q_i\log q_i-\sum_{i=1}^{k}q_i\log p_i \tag{2.48}$$

Thus,

$$H(q,p)=H(q)+D_{\mathrm{KL}}(q,p). \tag{2.49}$$

It follows from the relation (2.49) that

$$\arg\min_{p}D_{\mathrm{KL}}(q,p)=\arg\min_{p}H(q,p). \tag{2.50}$$

The concept of cross-entropy can be used to define a loss function in machine learning and optimization. Let us assume y_i is the true label for x_i, for example $y_i = e_{k_i}$ if $x_i \in A_{k_i}$. Consider the predicted distribution

$$\boldsymbol{p}(x;\boldsymbol{\theta})=\frac{1}{\sum_{i=1}^{k}e^{w_i x+b_i}}\begin{pmatrix}e^{w_1x+b_1}\\ e^{w_2x+b_2}\\ \vdots\\ e^{w_kx+b_k}\end{pmatrix}=\begin{pmatrix}p_1(x;\boldsymbol{\theta})\\ p_2(x;\boldsymbol{\theta})\\ \vdots\\ p_k(x;\boldsymbol{\theta})\end{pmatrix} \tag{2.51}$$

for any data $x \in A$. By (2.50), the minimization of KL divergence is equivalent to the minimization of the cross-entropy, namely

$$\arg\min_{\theta}\sum_{i=1}^{N}D_{\mathrm{KL}}(y_i,\boldsymbol{p}(x_i;\boldsymbol{\theta}))=\arg\min_{\theta}\sum_{i=1}^{N}H(y_i,\boldsymbol{p}(x_i;\boldsymbol{\theta})). \tag{2.52}$$

Recall that we have all data $D = \{(x_1, y_1), (x_2, y_2), \cdots, (x_N, y_N)\}$. Then, it is natural to consider the loss function as following:

$$\sum_{j=1}^{N}H(y_i,\boldsymbol{p}(x_i;\boldsymbol{\theta})), \tag{2.53}$$

which measures the distance between the real label and predicted one for all data. In the meantime, we can check that

$$\begin{aligned}\sum_{j=1}^{N}H(y_j,\boldsymbol{p}(x_j;\boldsymbol{\theta}))&=-\sum_{j=1}^{N}y_j\cdot\log\boldsymbol{p}(x_j;\boldsymbol{\theta})\\ &=-\sum_{j=1}^{N}\log p_{i_j}(x_i;\boldsymbol{\theta})\quad(\text{because } y_j=e_{i_j}\text{ for } x_j\in A_{i_j})\\ &=-\sum_{i=1}^{k}\sum_{x\in A_i}\log p_i(x;\boldsymbol{\theta})\\ &=-\log\prod_{i=1}^{k}\prod_{x\in A_i}p_i(x;\boldsymbol{\theta})\\ &=L(\theta)\end{aligned} \tag{2.54}$$

with $L(\theta)$ defined in (2.39) as

$$L(\boldsymbol{\theta}) = -\sum_{i=1}^{k}\sum_{x\in A_i}\log p_i(x;\boldsymbol{\theta}). \tag{2.55}$$

That is to say, the logistic regression loss function defined by likelihood in (2.39) is exact the loss function defined by measuring the distance between real label and predicted one via cross-entropy. We can note

$$\min_{\boldsymbol{\theta}} L_\lambda(\boldsymbol{\theta}) \Leftrightarrow \min_{\boldsymbol{\theta}} \sum_{j=1}^{N} H(y_i, \boldsymbol{p}(x_i;\boldsymbol{\theta}))+\lambda R(\|\boldsymbol{\theta}\|) \Leftrightarrow \min_{\boldsymbol{\theta}} \sum_{j=1}^{N} D_{\mathrm{KL}}(y_i, \boldsymbol{p}(x_i;\boldsymbol{\theta}))+\lambda R(\|\boldsymbol{\theta}\|). \tag{2.56}$$

2.4 Support vector machine

There is a lot of work about SVM in literature , see [**? ? ? ?**] for example. Given a binary linearly separable classification dataset $(x_i, y_i)_{i=1}^N$, where $x_i \in \mathbb{R}^d, y_i \in \left\{\begin{pmatrix}1\\0\end{pmatrix}, \begin{pmatrix}0\\1\end{pmatrix}\right\}$. We use A_1, A_2 to denote the data with label $\begin{pmatrix}1\\0\end{pmatrix}, \begin{pmatrix}0\\1\end{pmatrix}$, respectively. Our goal is to find a $\theta = (w, b)$ where $w \in \mathbb{R}^{1\times d}, b \in \mathbb{R}$ such that the hyperplane $H_\theta = \{x : wx + b = 0\}$ can separate A_1, A_2.

2.4.1 Binary SVM

Binary Support Vector Machine (SVM for short hereinafter) wants to find the classifiable hyperplane which has the biggest distance with A_1 and A_2. Assume that we have the hyperplanes $wx + b = \pm 1$ with

$$wx_i + b \geq 1 \quad \text{for} \quad x_i \in A_1, \quad wx_i + b \leq -1 \quad \text{for} \quad x_i \in A_2,$$

which is similar to the definition (2.1). Let $y_1 = \begin{pmatrix}1\\0\end{pmatrix}$ for $x_i \in A_1$ and $y_2 = \begin{pmatrix}0\\1\end{pmatrix}$ for $x_i \in A_2$. Note that w is normal to the hyperplane and the distance between the points satisfying

$$wx_i + b = \pm 1$$

and the hyperplane $wx + b = 0$ is $\dfrac{1}{\|w\|_2}$. Thus, the width of the margin is $\dfrac{2}{\|w\|_2}$ as shown in Figure 2.6. For any w and b, the smallest distance between points and the hyperplane is

$$\frac{\min_i \ell_i(wx_i + b)}{\|w\|_2}, \tag{2.57}$$

where $\ell_i = 1 - 2e_2^T y_i$. Note that

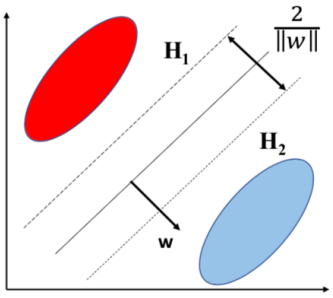

Fig. 2.6. SVM

$$\ell_i = \begin{cases} 1 & \text{if } y_i = \begin{pmatrix} 1 \\ 0 \end{pmatrix}, \\ -1 & \text{if } y_i = \begin{pmatrix} 0 \\ 1 \end{pmatrix}. \end{cases}$$

Consider the problem

$$\max_{w,b} \frac{\min_i \ell_i(wx_i + b)}{\|w\|_2}. \tag{2.58}$$

Intuitively, the best separating hyperplane H is only determined by those data points who are closest to H. Those data points are called support vector, and this method are called support vector machine.

Without loss of generality, we may restrict the norm of $\|w\|$ to be 1, which leads to a equivalent optimization problem

$$\max_{\|w\|_2=1} \min_i \ell_i(wx_i + b) \tag{2.59}$$

Actually, we can prove $\operatorname{argmax}_{\|w\|_2=1} \min_i \ell_i(wx_i + b)$ is nonempty, but here we just admit this fact and only prove the uniqueness of the solution.

Lemma 10. *If A_1, A_2 are linearly separable, then*

$$\operatorname*{argmax}_{\|w\|_2=1} \min_i \ell_i(wx_i + b) \tag{2.60}$$

is nonempty.

Proof. Take $x_{i_1} \in A_1$ and $x_{i_2} \in A_2$, given $(w, b) \in \{(w, b) : l_i(wx_i + b) > 0, \forall i\}$, we have

$$\begin{cases} wx_{i_1} + b > 0, \\ wx_{i_2} + b < 0 \end{cases} \tag{2.61}$$

which implies $|b| < \max_i \|x_i\|_2$. So we have

$$\operatorname*{argmax}_{\|w\|_2=1} \min_i \ell_i(wx_i + b) = \operatorname*{argmax}_{\|w\|_2=1,\ |b|\le\max_i \|x_i\|_2} \min_i \ell_i(wx_i + b) \neq \emptyset. \tag{2.62}$$

□

Lemma 11. *If A_1, A_2 are linearly separable, then*

$$\operatorname*{argmax}_{\|w\|_2=1} \min_i \ell_i(wx_i + b) \tag{2.63}$$

is a singleton set.

Proof. Denote $m(w, b) = \min_i \ell_i(wx_i + b)$. Notice that $m(w, b)$ is a concave homogeneous function w.r.t w, b and $\|\cdot\|_2$ is a strictly convex norm. Suppose there are two solution (w_1, b_1) and (w_2, b_2) such that $w_1 \neq w_2$, take $\overline{w} = \frac{w_1+w_2}{2}, \overline{b} = \frac{b_1+b_2}{2}$, we must have

$$m(\overline{w}, \overline{b}) \ge \frac{m(w_1, b_1) + m(w_2, b_2)}{2} = \max_{\|w\|_2=1} m(w, b), \tag{2.64}$$

and

$$\|\overline{w}\|_2 < 1. \tag{2.65}$$

So

$$m(\frac{\overline{w}}{\|\overline{w}\|_2}, \frac{\overline{b}}{\|\overline{w}\|_2}) = \frac{m(\overline{w}, \overline{b})}{\|\overline{w}\|_2} > \max_{\|w\|_2=1} m(w, b), \tag{2.66}$$

which leads to a contradiction. So all the solutions must have the same w, we denote it as w^*. Then if (w^*, b^*) is a solution of problem (2.60), we must have

$$b^* \in \operatorname*{argmax}_b m(w^*, b) \tag{2.67}$$

Actually,

$$m(w^*, b) = \min\{b + \min_{x\in A_1} w^* x, -b + \min_{x\in A_2}(-w^* x)\}. \tag{2.68}$$

It is easy to observe that $\operatorname*{argmax}_b m(w^*, b)$ is a singleton set and

$$b^* = \frac{\min_{x\in A_2}(-w^* x) - \min_{x\in A_1} w^* x}{2}. \tag{2.69}$$

□

Denote

$$\theta^*_{SVM} = (w^*_{SVM}, b^*_{SVM}) = \operatorname*{argmax}_{\|w\|_2=1} \min_i \ell_i(wx_i + b). \tag{2.70}$$

Theorem 2 (Representation Theorem). *Let $\theta^*_{SVM} = (w^*_{SVM}, b^*_{SVM})$ be the solution of (2.70). Then, w^*_{SVM} must be a linear combination of $x_i^T, i = 1, 2, \cdots, N$.*

Proof. Denote

$$S = \text{span}\{x_i^T\}_{i=1}^N. \tag{2.71}$$

Then we have

$$\mathbb{R}^{1\times d} = S \oplus^{\perp} S^{\perp}. \tag{2.72}$$

So w^*_{SVM} can be uniquely decomposed as $w^*_{SVM} = w^*_S + w^*_{S^\perp}$ where $w_S \in S$ and $w^*_{S^\perp} \in S^\perp$. We will prove that $w^*_{S^\perp} = 0$. Suppose not, we have

$$\|w^*_S\|_2 < \|w^*_{SVM}\|_2 = 1. \tag{2.73}$$

Notice that

$$w^*_{SVM} x_i = w^*_S x_i, \ \forall i = 1, 2, \cdots, N. \tag{2.74}$$

Thus we have

$$\min_i \ell_i(w^*_{SVM} x_i + b^*_{SVM}) = \min_i \ell_i(w^*_S x_i + b^*_{SVM}). \tag{2.75}$$

So

$$\min_i \ell_i(w^*_{SVM} x_i + b^*_{SVM}) < \frac{\min_i \ell_i(w^*_S x_i + b^*_{SVM})}{\|w^*_S\|} = \min_i \ell_i(\frac{w^*_S}{\|w^*_S\|_2} x_i + \frac{b^*_{SVM}}{\|w^*_S}\|_2), \tag{2.76}$$

which leads to a contradiction to the definition of θ^*_{SVM}. □

2.4.2 Soft margin maximization and kernel methods

We may rewrite the SVM problem as

$$\max_{w,b} \frac{2}{\|w\|}, \tag{2.77}$$

$$s.t. \ \ell_i(wx_i + b) \geq 1, \ \forall i. \tag{2.78}$$

or equivalently,

$$\min_{w,b} \|w\|^2, \tag{2.79}$$

$$s.t. \ \ell_i(wx_i + b) \geq 1, \ \forall i. \tag{2.80}$$

Notice that the feasible domain of margin maximization is nonempty if and only if dataset is linearly separable. So when the data is linearly nonseparable, this method

can't even get a classifier even though it may not be good. One way to handle this problem is to relax the constraint by adding relaxation variables.

Define soft margin maximization problem

$$\min_{w,b,\xi} \|w\|^2 + \lambda^{-1} \sum_{i=1}^{N} \xi_i, \tag{2.81}$$

$$s.t.\ \ell_i(wx_i + b) + \xi_i \geq 1,\ \forall i. \tag{2.82}$$

$$\xi_i \geq 0. \tag{2.83}$$

where $\lambda > 0$. The above problem is equivalent to

$$\min_{w,b} \|w\|^2 + \lambda^{-1} \sum_{i=1}^{N} \mathrm{ReLU}(1 - \ell_i(wx_i + b)). \tag{2.84}$$

Thus, soft margin maximization problem (2.81) can be reformulated as

$$\min_{w,b} \sum_{i=1}^{N} \mathrm{ReLU}(1 - \ell_i(wx_i + b)) + \lambda\|w\|^2. \tag{2.85}$$

We can still prove that the solution of (2.85) satisfies the representation theorem. Thus we can restrict w to be in the set S. Assume that

$$w = \sum_{i=1}^{N} \alpha_i x_i^T, \tag{2.86}$$

Denote $\alpha = (\alpha_1, \cdots, \alpha_N)^T$. We can rewrite the problem (2.85) as

$$\min_{\alpha} \sum_{i=1}^{N} \mathrm{ReLU}(1 - \ell_i(\sum_{j=1}^{N} \langle x_i, x_j \rangle \alpha_j + b)) + \lambda \alpha^T (\langle x_i, x_j \rangle)_{N\times N} \alpha \tag{2.87}$$

We can see that the whole problem is only determined by the inner product of data points but not the data itself directly.

Use the above formulation, we can induce nonlinearity in SVM. Denote the input space as X where $\{x_i\}_{i=1}^N \subset X$. We use two steps to obtain a nonlinear classification model. First, we use a nonlinear feature mapping $\phi : X \to \mathcal{H}$ to map input space X to a feature space $\mathcal{H}$. Second, we use linear SVM to do classification on $\{\phi(x_i)\}_{i=1}^N \subset \mathcal{H}$.

We may just asssume dataset after feature mapping ϕ is linearly separable. Then, the SVM problem after doing feature mapping can be formulated as problem (2.85) as

$$\min_{\alpha} \sum_{i=1}^{N} \mathrm{ReLU}(1 - \ell_i(\sum_{j=1}^{N} \langle \phi(x_i), \phi(x_j) \rangle \alpha_j + b)) + \lambda \alpha^T (\langle \phi(x_i), \phi(x_j) \rangle)_{N\times N} \alpha \tag{2.88}$$

Notice that to obtain the above problem we don't really need to know what exactly is the nonlinear mapping ϕ, but only need to compute the value of $< \phi(x_i), \phi(x_j) >$. So we define a kernel function $k : X \times X \to \mathbb{R}$ such that

$$k(x,y) = \langle \phi(x), \phi(y) \rangle, \ \ x, y \in X. \tag{2.89}$$

Then the kernel SVM can be formulated as

$$\min_{\alpha} \sum_{i=1}^{N} \mathrm{ReLU}(1 - \ell_i(\sum_{j=1}^{N} k(x_i, x_j)\alpha_j + b)) + \lambda \alpha^T (k(x_i, x_j))_{N\times N}\alpha \tag{2.90}$$

In practice, we just need to find a proper kernel function instead of a good nonlinear feature mapping. Here we list some common used kernel functions:

- Polynomial kernel: $k(x,y) = (a\langle x, y\rangle + b)^n, a > 0, b \geq 0, n \in \mathbb{N}^+$.
- Gaussian kernel: $k(x,y) = e^{-\gamma \|x-y\|^2}, \gamma > 0$.
- Laplacian kernel: $k(x,y) = e^{-\gamma \|x-y\|}, \gamma > 0$
- Tanh kernel: $k(x,y) = \tanh(a\langle x, y\rangle + b), a > 0, b \geq 0$.

2.4.3 Binary logistic regression

In multi-class Logistic regression, if we use $\|W\|$ to replace $\|\boldsymbol{\theta}\|$ in regularization term, we can get another version of logistic regression:

$$\mathcal{L}_\lambda(\boldsymbol{\theta}) = -\sum_{i=1}^{k} \sum_{x\in A_i} \log p_i(x;\boldsymbol{\theta}) + \lambda R(\|W\|), \tag{2.91}$$

where $p_i(x;\boldsymbol{\theta})$ and $R(\cdot)$ share the same definitions as in previous sections of logistic regression. Let

$$\boldsymbol{\Theta}_\lambda = \arg\min_{\boldsymbol{\theta}} \mathcal{L}_\lambda(\boldsymbol{\theta}). \tag{2.92}$$

The following lemma follows directly from the definition of $p_i(x;\boldsymbol{\theta})$.

Lemma 12. *For any $W \in \mathbb{R}^{k\times d}, b \in \mathbb{R}^k, \alpha \in \mathbb{R}$, we have*

$$\mathcal{L}_\lambda(W, b) = \mathcal{L}_\lambda(W, b + \alpha \mathbf{1}), \tag{2.93}$$

where $\mathbf{1} = (1, 1, \cdots, 1)^T \in \mathbb{R}^k$.

Binary logistic regression refers to the case when $k = 2$.

Lemma 13. *If $k = 2$, given any $\boldsymbol{\theta}_\lambda = \begin{pmatrix} w_1 & b_1 \\ w_2 & b_2 \end{pmatrix} \in \boldsymbol{\Theta}_\lambda$, we have*

$$w_1 = -w_2.$$

According to the above two lemmas, we can restrict $\boldsymbol{\theta}$ to have the form

$$\boldsymbol{\theta} = \begin{pmatrix} \frac{w}{2} & \frac{b}{2} \\ -\frac{w}{2} & -\frac{b}{2} \end{pmatrix}, \tag{2.94}$$

so our score mapping can be written as

$$\boldsymbol{p}(x;\theta) = \begin{pmatrix} \frac{1}{1+e^{-(wx+b)}} \\ \frac{1}{1+e^{wx+b}} \end{pmatrix}. \tag{2.95}$$

Denote $\theta = (w, b)$ where $w \in \mathbb{R}^d, b \in \mathbb{R}$, correspondingly, we have

$$P(\theta) = \prod_{i=1}^{N} \frac{1}{1 + e^{-y_i(wx+b)}}. \tag{2.96}$$

Here we have the new "label" y_i defined by

$$y_i = \begin{cases} 1, & \text{if} \quad x_i \in A_1 \\ -1, & \text{if} \quad x_i \in A_2 \end{cases}. \tag{2.97}$$

Thus we have

$$L(\theta) = -\log P(\theta) = \sum_{i=1}^{N} \log(1 + e^{-y_i(wx+b)}), \tag{2.98}$$

and take $R(t) = t^2$, we have

$$\mathcal{L}_\lambda(\theta) = L(\theta) + \lambda\|w\|_2^2 = \sum_{i=1}^{N} \log(1 + e^{-y_i(wx+b)}) + \lambda\|w\|_2^2. \tag{2.99}$$

Here $L(\theta)$ is a strictly convex function without any global minima.

Lemma 14. *Assume that A_1, A_2 are linearly separable, and we follow the same definition of linearly classifiable weights:*

$$\boldsymbol{\Theta} = \left\{ \boldsymbol{\theta} : p_i(x;\boldsymbol{\theta}) > p_j(x;\boldsymbol{\theta}),\ \forall x \in A_i, j \neq i, i = 1, 2 \right\}, \tag{2.100}$$

where

$$\boldsymbol{p}(x;\theta) = \begin{pmatrix} \frac{1}{1+e^{-(wx+b)}} \\ \frac{1}{1+e^{wx+b}} \end{pmatrix}. \tag{2.101}$$

Then, we have the following statement:

1. *$\theta = (w, b) \in \boldsymbol{\Theta}$ if and only if*

$$\frac{1}{1 + e^{-y_i(wx+b)}} > \frac{1}{2},\ \forall i = 1, 2 \cdots, N.$$

2. *If $P(\theta) > \frac{1}{2}$, then θ must be classifiable, i.e.*

$$\{\theta : P(\theta) > \frac{1}{2}\} \subset \boldsymbol{\Theta}.$$

3. Prove that

$$\boldsymbol{\Theta} = \{\theta : \lim_{\alpha \to +\infty} P(\alpha\theta) = 1\}.$$

If A_1, A_2 are linearly separable, then $\operatorname{argmin}_{w,b} \mathcal{L}_\lambda(\theta)$ is nonempty for λ sufficiently small.

Lemma 15. *If A_1, A_2 are linearly separable, then*

$$\operatorname*{argmin}_{w,b} \mathcal{L}_\lambda(\theta) \tag{2.102}$$

is a singleton set for λ sufficiently small.

Proof. Because $L(\theta)$ is strictly convex w.r.t. θ and $\|w\|^2$ is convex w.r.t. θ, so $\mathcal{L}(\theta, \lambda) = L(\theta) + \lambda\|w\|_2^2$ is stricly convex w.r.t. θ, which implies our result directly. □

For λ sufficiently small, denote

$$\theta_{LR}(\lambda) = (w_{LR}(\lambda), b_{LR}(\lambda)) = \operatorname*{argmin}_{w,b} \mathcal{L}_\lambda(\theta). \tag{2.103}$$

Lemma 16. *If A_1, A_2 are linearly separable,*

1. *$\mathcal{L}_\lambda(\theta) \to 0$ as $\lambda \to 0$.*
2. *$\|w_{LR}(\lambda)\| \to \infty$ as $\lambda \to 0$.*
3. *$\min_i y_i(w_{LR}(\lambda)x_i + b_{LR}(\lambda)) \to \infty$ as $\lambda \to 0$.*
4. *If A_1, A_2 are also nonempty,*

$$\|b_{LR}(\lambda)\| \le \max_i \|x_i\| \|w_{LR}(\lambda)\| \tag{2.104}$$

for λ sufficiently small.

The above lemma implies that $\theta_{LR}(\lambda)/\|w_{LR}(\lambda)\|$ is bounded for λ sufficiently small.

Theorem 3. *If A_1, A_2 are linearly separable, then $\frac{\theta_{LR}(\lambda)}{\|w_{LR}(\lambda)\|}$ converge to θ^*_{SVM} as $\lambda \to 0$, i.e.*

$$\theta^*_{SVM} = \lim_{\lambda \to 0} \frac{\theta_{LR}(\lambda)}{\|w_{LR}(\lambda)\|}. \tag{2.105}$$

Proof. Because $\frac{\theta_{LR}(\lambda)}{\|w_{LR}(\lambda)\|}$ is bounded for λ sufficiently small, we only need to prove that it has no convergence points other than θ^*_{SVM} as $\lambda \to 0$. We first introduce a soft margin function $m : \mathbb{R}^n \to \mathbb{R}$ such that

$$m(\theta) = \min_i y_i(wx_i + b). \tag{2.106}$$

Suppose that there exist a sequence $\{\lambda_n\}_{n=1}^\infty$ and $\bar{\theta} = (\bar{w}, \bar{b}) \neq \theta^*_{SVM}$ so that $\lambda_n \downarrow 0$ and $\frac{\theta_{LR}(\lambda_n)}{\|w_{LR}(\lambda_n)\|} \to \bar{\theta}$ as $n \to \infty$. Obviously $\|\bar{w}\| = 1$, and

$$0 \leq m(\bar{\theta}) < m(\theta^*_{SVM}). \tag{2.107}$$

Take a positive number $\epsilon < m(\theta^*_{SVM}) - m(\bar{\theta})$. Then there exists $K_0 \in \mathbb{N}^+$ such that

$$0 < m(\frac{\theta_{LR}(\lambda_n)}{\|w_{LR}(\lambda_n)\|}) < m(\theta^*_{SVM}) - \epsilon, \tag{2.108}$$

for all $n \geq K_0$.

Consider $\theta_n = (w_n, b_n) = \|w_{LR}(\lambda_n)\|\theta^*_{SVM}$. Then

$$\lim_{n\to\infty} \frac{\log(1 + e^{-m(\theta_n)})}{\log(1 + e^{-m(\theta_{LR}(\lambda_n))})} = \lim_{n\to\infty} e^{\|w_{LR}(\lambda_n)\|(m(\frac{\theta_{LR}(\lambda_n)}{\|w_{LR}(\lambda_n)\|}) - m(\theta^*_{SVM}))} \leq \lim_{n\to\infty} e^{-\|w_{LR}(\lambda_n)\|\epsilon} = 0. \tag{2.109}$$

So there exists a $K_1 \in \mathbb{N}^+$ such that

$$N \log(1 + e^{-m(\theta_n)}) < \log(1 + e^{-m(\theta_{LR}(\lambda_n))}) \tag{2.110}$$

for all $n \geq K_1$. Take $K = \max\{K_0, K_1\}$. Then for all $n \geq K$, we have

$$\mathcal{L}(\theta_n) \leq N \log(1 + e^{-m(\theta_n)}) + \lambda\|w_{\lambda_n}\|^2 < \log(1 + e^{-m(\theta_{LR}(\lambda_n))}) + \lambda\|w_{\lambda_n}\|^2 \leq \mathcal{L}(\theta_{LR}(\lambda_n)), \tag{2.111}$$

which contradicts the definition of $\theta_{LR}(\lambda)$. □

For the proof of the above theorem, you can also refer to the paper by Rosset Saharon, Zhu Ji and Trevor J. Hastie [**?**].

3

Probability

3.1 Introduction to probability

Introduction to Probability: https://link-springer-com.ezaccess.libraries.psu.edu/book/10.1007%2F978-0-387-21736-9

3.2 Basic probability

3.3 Basic Probability Theory

- Outcome — Set of possible outcomes
- Event — Subset of possible outcomes, an event is something which can happen or not happen
- Distribution — measure on the outcome space, just give the probability of each outcome
- Independence — "Events that are unrelated", depends on the distribution

3.3.1 Discrete Examples

- Coin Flip:
  - Outcomes: $\{H, T\}$
  - Event: If we toss a coin once, there are two possible events: $\{H\}$ and $\{T\}$; If we toss a coin twice, the event that the first toss is heads is $A = \{HH, HT\}$; If we toss a coin three times, the event that the second toss is heads is $B = \{HHH, THT, HHT, THT\}$.
  - Distribution: If we toss a coin, the possibility that it is H and the possibility that it is T are the same, that is $p(\{H\}) = p(\{T\}) = 0.5$.
- Rolling a Die:
  - Outcomes:$\{1, 2, 3, 4, 5, 6\}$

- Event: some examples $E_1 = \{3\}$— rolling a 3 $E_2 = \{1, 3, 5\}$ — rolling an odd number$E_3 = \{2, 4, 6\}$ — rolling an even number$E_4 = \{1, 2\}$— rolling either a 1 or 2
- Distribution: $p(\{1\}) = p(\{2\}) = ... = p(\{6\}) = \frac{1}{6}$(most common case) $p(\{1\}) = \frac{1}{2}, p(\{2\}) = ... = p(\{6\}) = \frac{1}{10}$ (for some special die)
- Independence: Given events E_1 and E_2, they are independent if$p(E_1 \bigwedge E_2) = p(E_1)p(E_2)$(the probability that both events appear is equal to the product of the probability that one event appears) $p(E_1|E_2) = \frac{p(E_1 \bigwedge E_2)}{p(E_2)} = p(E_1)$ (the conditional probability of E_1 given the event E_2 is equal to the probability of E_1)
- example of independence: The die roll 2 and 3 are independent; Events E_2 and E_4 are also independent: $E_2 \bigwedge E_4 = \{1, 3, 5\} \bigwedge \{1, 2\} = \{1\}$ $p(E_2 \bigwedge E_4) = p(\{1\}) = \frac{1}{6}$ $p(E_2)p(E_4) = p(\{1, 3, 5\})p(\{1, 2\}) = \frac{1}{2}\frac{1}{3} = \frac{1}{6}$

3.3.2 Independent Copies

- Coin Flip: 2 independent copies: $C_1 = \{H, T\}, C_2 = \{H, T\} \Rightarrow$ $C_1 \times C_2$

	H^{P_H}	T^{P_T}
$P_H H$	HH	HT
$P_T T$	TH	TT

  - Event: $\{HT, HT\} \Rightarrow$ exactly one head $\{HT, HH, TH\} \Rightarrow$at least one head
  - Distribution: $p((H, T)) = p_1(H)p_2(T)$
  - Generalized: K-coins **independent**. $\{H, T\}^K = \{K - tuples\ of\ H, T\}$ Distribution. $p((H, ..., T)) = p_1(H)...p_k(T)$ Can generalize this to infinite protucts as well. (Doesn't hold for dependent events)

3.3.3 Continuous Distributions

- Ex: Uniform Distribution on $[0, 1]$. Outcomes: $[0, 1]$ Events: Ex: the event $[0, 0.5]$ means random number ≤ 0.5 Ex: the event $[0, 0.25] \bigcup [0.5, 0.75]$ means random number less than 0.025 or between 0.5 and 0.75

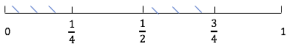

- Distribution: A distribution a rule which gives the probability of any event. Properties to satisfy: if events $E_1, E_2, ..., E_n, ...$satisfy that $E_i \bigcap E_j = \varnothing$, then
  1. $p(E_1 \bigcup ... \bigcup E_n \bigcup ...) = \sum_{i=1}^{\infty} p(E_j)$
  2. $p(E) = \int_E d_x$, "length of E"
  3. examples 1: $E_1 = [0, 0.5]$

$$P(E_1) = \int_{E_1} d_x = \int_0^{1/2} dx = \frac{1}{2}.$$

4. examples 2: $E_2 = [0, 0.25] \bigcup [0.5, 0.75]$

$$p(E_2) = \int_{E_2} dx = \int_0^{1/4} dx + \int_{1/2}^{3/4} dx = \frac{1}{4} + \frac{1}{4} = \frac{1}{2}$$

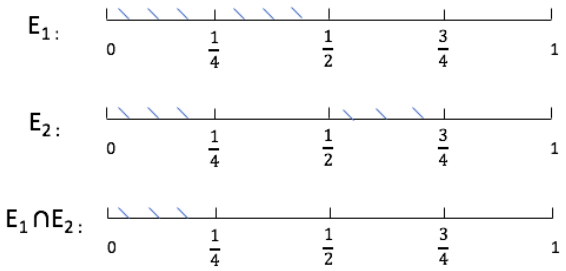

- Independence: Two events E_1, E_2 are independent if

$$p(E_1 \cap E_2) = p(E_1)\, p(E_2)$$

For example, $E_1 \cap E_2 = [0, 0.5] \cap \left(\left[0, \frac{1}{4}\right] \cup \left[\frac{1}{2}, \frac{3}{4}\right]\right)$

$$p\left(E_1 \bigcap E_2\right) = \frac{1}{4} = \frac{1}{2} \cdot \frac{1}{2} = p(E_1)\, p(E_2)$$

Frist two binary digits are like two independent coin flips. Every binary digit is like an independent coin flip, so we ca think of the random number as being an infinite sequence of coin flips. In general, we'll consider distribution defined by a probability density function p(x). The probability of an event is given by $P(E) = \int_{E_1} p(x) d_x$

– Outcomes: $[0, 1]$
– Density function: $p(x) = 1$ ($\int_0^1 p(x) = 1$)

3.3.4 Gaussian/ Normal Distribution

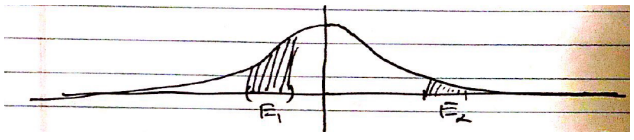

- Outcomes:

- Events: Subsets of R
- Density function: $P(x) = \frac{1}{\sqrt{2\pi}} e^{-x^2/2}$ Means that for any event E,

$$p(E) = \int_E \frac{1}{\sqrt{2\pi}} e^{-x^2/2} dx.$$

- Cummulative distribution Function

$$F(x) = \int_{-\infty}^{x} p(t)dt = p(t < x)$$

Note that $\lim_{x\to\infty} F(x) = 1$.

3.4 Random, Variable, Mean, Variance

- Recall:
  - Set if outcomes: Ω
  - Event: Subset of outcomes: E
  - Probability Distribution: $p(x)$

3.4.1 Random Variable

- Defin: A random variable X is a function $X : \Omega \to S$ Here $S = R, R^d$, but could be arbitrary.
- Ex: Rolling a die:
  - Outcomes: $\Omega = 1, 2, ..., 6$
  - Events are subsets of Ω
  - Distribution: $p(1) = p(2) = ... = p(6) = \frac{1}{6}$ Suppose we roll the die, then if the die comes up d times, you win d dollars, minus 1 dollar if it's even. The amount you win is a random variable. $X_1 : \Omega \to R$, $X_1(1) = 1$, $X_1(2) = 1$, $X_1(3) = 3$, $X_1(4) = 3$, $X_1(5) = 5$, $X_1(6) = 5$ Can define multiple random variables on a single outcome space Ω.
- Ex: Rolling a die. If the die comes up d times, you get d dollars. If d is even, then you give a dollar to your friend. $X_1 \leftarrow$ your winnings, $X_2 \leftarrow$ your friends winnings.

$$X_2 : \Omega \to \mathbb{R}, X_2(1) = 0, \quad X_2(2) = 1$$
$$X_2(3) = 0, \quad X_2(4) = 1$$
$$X_2(5) = 0, \quad X_2(6) = 1$$

From here on out Ω will be fixed, we talk about different random variables on Ω.

3.4.2 Mean of random variable

- Defin: Mean of a random variable X. Expectation of X:

$$\mathbb{E}[X] = \sum_{\omega\in\Omega} p(\omega)X(\omega)\left(= \int_{\Omega} X(\omega)p(\omega)d\omega\right)$$

- Ex:

$$\mathbb{E}[X_1] = \frac{1}{6}(1+1+3+3+5+5) = 3$$
$$\mathbb{E}[X_2] = \frac{1}{6}(0+1+0+1+0+1) = \frac{1}{2}$$

3.4.3 Variance of Random Variables

- Defin: Variance of a Random Variable X:

$$V[X] = \mathbb{E}\left[X^2\right] - \mathbb{E}[X]^2 = \mathbb{E}\left[(X - \mathbb{E}[X])^2\right]$$

- Ex:

$$\begin{aligned} &V[X_1] = \mathbb{E}\left[X_1^2\right] - (3)^2 \\ &= \tfrac{1}{6}\left(1^2+1^2+3^2+3^2+5^2+5^2\right) - 9 \\ &= \tfrac{1}{3}(1+9+25) - 9 \\ &= \tfrac{35}{3} - 9 = \tfrac{8}{3} \end{aligned}$$

Variance measures "how much X deviates from it's average".

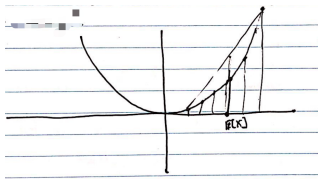

3.4.4 Independenve of Random variables

- Defin: Two random variables X_1, X_2 are independent if for any α,β, $E_1 = \{w : X_1(\omega) < \alpha\}, E_2 = \{w : X_2(\omega) < \beta\}$ are independent events.
- Ex: X_1, X_2 are independent: if (α,β) $\alpha = 4$, $\beta = \frac{1}{2}$,

$$E_1 = \{w : X_1(u) < 4\} = \{1,2,3,4\}$$
$$E_2 = \left\{w : X_2(\omega) < \tfrac{1}{2}\right\} = \{1,3,5\}$$

$$p(E_1 \bigcap E_2) = p(E_1)\,p(E_2)$$
$$p(\{1,3\}) = p(E_1)\,p(E_2)$$

3.4.5 Properties of E, V, Independence

– If X_1, X_2 are random variable, then

$$(a_1X_1 + a_2x_2)(w) = a_1x_1(w) + a_2x_2(w)$$

$$\mathbb{E}[a_1X_1 + a_2X_2] = a_1\mathbb{E}[X_1] + a_2\mathbb{E}[X_2]$$

– If X_1, X_2 are independent random variables, then

$$\mathbb{E}[X, X_2] = \mathbb{E}[X_1]\mathbb{E}[X_2]$$

– From this, we get if X_1, X_2 are independent,

$$V[X_1 + X_2] = V[X_1] + V[X_2]$$

$$V[a_1x_1 + a_2x_2] = a_1^2V[x_1] + a_2^2V[x_2]$$

3.5 Probability interpretation of logistic regression

Logistic regression models the probabilities for classification problems with two possible outcomes. It's an extension of the linear regression model for classification problems.

- Input: d-dimension feature vector $x \in R^d$
- Output: a class or label $l \in \{1, \ldots, k\}$ (how to classify)
- Example 1: Image classfication: Given input image $x \in R^{n\times n}$, predict a label for the image. e.g. cat/ dog; MNIST: $\{0, \ldots, 9\}$; CIFAR-10, $\{0, \ldots, 9\}$
- Example 2: Binary Classfication: Given some medical data $x \in R^d$(features, like heart pressure, resting heart rate, family history, etc), we try to predict incidence of heart disease. The label will be binary $\{0, 1\}$, called binary classification.

3.5.1 Logistic Regression Model

Given input feature vector $x \in R^n$, the model predicts a probability distribution over the labels $\{0, \ldots, k\}$.

$$\text{affine linear map: } Ax + b: \quad R^n \to R^k$$

with $A \in R^{k\times n}$, $x \in R^n$, $b \in R^k$.

$$\text{softmax}(Ax + b): \quad R^n \to R^k \xrightarrow{softmax} P(\{1, \ldots, k\})$$

Softmax:

1. Input: $y \in \mathbb{R}^k = \begin{pmatrix} y_1 \\ \vdots \\ y_k \end{pmatrix}$

2. Output: Distribution $p(j) = \frac{e^{y_j}}{\sum_{i=1}^{n} e^{y_i}}$
3. Take exponential and normalize

Logistic Regression Model: Given input (feature/data) $x \in R^n$, we return the distribution softmax $(Ax + b)$ where A, b are parameters.

- Example 1: Divide data into two classes: parameters are $\mathbf{a} \in \mathbb{R}^n, b \in \mathbb{R}$

$$A \in \mathbb{R}^{1\times n}, \quad Ax + b \in \mathbb{R}.$$

The probability that the data x belongs to class 1 is

$$P(1) = \frac{e^{\mathbf{a}\cdot x+b}}{e^{\mathbf{a}\cdot x+b} + 1},$$

and the probability that the data x belongs to class 2 is

$$P(2) = \frac{1}{e^{\mathbf{a}\cdot x+b} + 1}.$$

If $\mathbf{a} \cdot x + b = 0$, $P(1) = P(2) = \frac{1}{2}$. We don't know how to classify the data lying on the line $\mathbf{a} \cdot x + b = 0$ as shown in the figure below. Note that

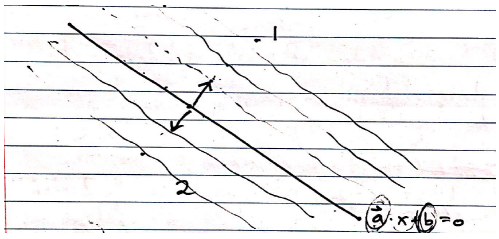

$$\frac{p(1)}{p(2)} = e^{\mathbf{a}\cdot x+b}, \quad \log\left(\frac{p(1)}{p(2)}\right) = \mathbf{a} \cdot x + b.$$

By the above equation, $\mathbf{a}$ means which feature is important. Logarithm of the odds: $\log\left(\frac{p(1)}{p(2)}\right)$. Assumption: $\log\left(\frac{p(1)}{p(2)}\right)$ is linear in the feature vector

3.5.2 Learning the parameters a, *b* from data

Data: feature vectors x and corresponding labels l. Given data

$$\{(x_1, l_1), \ldots, (x_n, l_1)\} = D$$

How can we estimate A, b?

3.6 Maximamum Likelihood

If parameters A and b are known, for any data $x_1 \in \mathbb{R}^n$, model gives softmax $(Ax_1 + b)$

$$\frac{1}{\sum_{i=1}^{k} e^{\mathbf{a_i} \cdot x_i + b_i}} \begin{pmatrix} e^{\mathbf{a}_1 \cdot x_1 + b_1} \\ \vdots \\ e^{a_k \cdot x_1 + b_k} \end{pmatrix} = \begin{pmatrix} p(1) \\ \vdots \\ p(k) \end{pmatrix}$$

This means that the probability that the model assigns to l_1 is

$$p(l) = \frac{1}{\sum_{i=1}^{k} e^{a_i \cdot x_i + b_i}} \cdot e^{\mathbf{a}_l \cdot x_1 + b_l}$$

Instead of considering this probability, we consider its negtive logarithm:

$$-\log p(l) = \log\left(\sum_{i=1}^{k} e^{a_i \cdot x_i + b_i}\right) - (\mathbf{a}_l \cdot x_1 + b_l)$$

Since data points are independent, so we take product of the probability which leads to the logistic regression loss. Logistic Regression Loss:

$$L_D(A, b) = \sum_{(x,l) \in D} \left[\log\left(\sum_{i=1}^{k} a_i \cdot x + b_i\right) - (\mathbf{a}_l \cdot x + b_l)\right]$$

We want to maximize the probability that the model assigns to l, that means we need to minimize $-\log p(l)$. So we need to find

$$(A, b) = \min_{A,b} L_D(A, b).$$

3.7 Basic Statistical Learning Theory

- Goal: Estimate an unknown probability distribution D on a set X from samples (i, i, d) $x_1, \ldots, x_n \in X$
- Introduce a family of distributions P_θ for $\theta \in \Theta$ and try to choose θ to "match" the samples.
  - Maximum Likelihood Estimate: Choose θ to maximize the probability of the samples.
  - Example: Let $X = R$, have some samples $x_1, \ldots, x_n$ drawn from a distribution D, say P_θ is a Gaussian with variance 1, centered at $\theta \in \mathbb{R} = \Theta$, i.e. density $p_\theta(x) = \frac{1}{\sqrt{2\pi}} e^{-(x-\theta)^2/2}$
  - Use the samples to find the center θ.

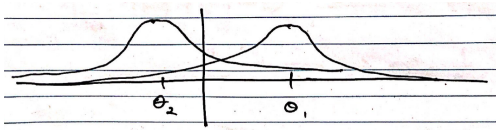

3.7.1 Maximum Likelihood Estimate(MLE)

- Given $\theta \in \Theta (= \mathbb{R}$ for this example), what is the probability of the data $\left\{x_j\right\}_{j=1}^n$?
  - Samles independent: Likelihood function(as a function of σ)

$$P_\theta\left(\left\{x_j\right\}_{j=1}^n\right) = \prod_{j=1}^n p_\theta\left(x_j\right) = \frac{1}{(\sqrt{2\pi})^n}\prod_{j=1}^n e^{-\left(x_j-\theta\right)^2/2} = \frac{1}{(2\pi)^{n/2}} e^{-\sum_{j=1}^n \left(x_j-\theta\right)^2/2}$$

  - MLE: Choose θ to maximize this!
  - Often it's useful to consider log likelihood function $\log\left(P_\theta\left(\left\{x_j\right\}_{j=1}^n\right)\right)$

$$\theta^* = \text{argmax}_{\theta\in\Theta} \log\left(P_\theta\left(\left\{x_j\right\}_{j=1}^n\right)\right)$$
$$\left(\text{argmin}_{\theta\in\Theta} - \log\left(P_\theta\left(\left\{x_j\right\}_{j=1}^n\right)\right)\right)$$

- For this example:

$$\log\left(P_\theta\left(\left\{x_j\right\}_{j=1}^n\right)\right) = -\log(2\pi)\cdot\left(\frac{n}{2}\right) - \sum_{j=1}^n \frac{\left(x_j-\theta\right)^2}{2}$$

$$\theta^* = \text{argmin}_{\theta\in\mathbb{R}} \sum_{j=1}^n \frac{\left(x_j-\theta\right)^2}{2}.$$

$$\theta^* = \frac{1}{n}\sum_{j=1}^n x_j.$$

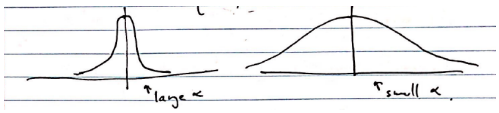

3.8 Classfication/ Logistic Regression

- For Classification: X is feature space and Y is label space

$$\widetilde{X} = X \times Y$$

- We have samples $\left\{\left(x_j, y_j\right)\right\}_{j=1}^n$
- Suppose that D is an unknown distribution on $\widetilde{X}$, but we're only trying to estimate $D_{Y|X}$ as a function of X. (Given the feature X, what is the possible label.)
- Introduce parameters $\theta \in \Theta$, we define $p(y|x,\theta)$ (called the model)
- Now choose θ to match the data $\left\{\left(x_j, y_j\right)\right\}_{j=1}^n$
- MLE:

$$\begin{aligned}\theta^* &= \text{argmax}_{\theta\in\Theta}\, p\left(\{y_i\}_{j=1}^n \,|\, \left\{x_j\right\}_{j=1}^n, \theta\right)\\ &= \text{argmax}_{\theta\in\Theta} \prod_{j=1}^n p\left(y_j|x_j,\theta\right)\\ &= \text{argmin}_{\theta\in\Theta} \sum_{j=1}^n -\log\left(p\left(y_j|x_j,\theta\right)\right)\end{aligned}$$

- Example: Logistic Regression:
  - Model
    $$p(y|x,\theta) = p(y|x,w,b)$$
    with $W \in \mathbb{R}^{d\times d}$ and $b \in \mathbb{R}^k$ (parameters for affine linear map)
  - d: dimension of features, i.e. number of pixels
  - k: number of classes

$$p(y|x,w,b) = \text{ softmax}\,(Wx+b) = \frac{1}{\sum_{i=1}^k e^{w_i\cdot x+b_i}}\begin{pmatrix} e^{w_1\cdot x+b_1}\\ \vdots \\ e^{w_k\cdot x+b_k}\end{pmatrix}$$

- Need to calculate:

$$\begin{aligned}&-\log\left(p\left(y_i|x_i,w,b\right)\right)\\ &= -\log\left(\frac{1}{e^{wx_i+b}\cdot\mathbb{I}}e^{wx_i+b}\cdot y_i\right)\\ &= \log\left(e^{wx_i+b}\cdot 1\right) - \log\left(e^{wx_i+b}\cdot y_i\right)\end{aligned} \tag{3.1}$$

  with $y_i = (0,\cdots,0,1,0,\cdots,0)$(only the i-th entry is 1, all others are 0) and all the entries of $\mathbb{I}$ are 1.

$$(w,b)^* = \underset{w,b}{\text{argmin}} \sum_{i=1}^n \log\left(e^{wx_i+b}\cdot\mathbb{I}\right) - \log\left(e^{wx_i+b}\cdot y_i\right)$$

3.9 Bayesian Approach to Machine Learning

3.9.1 Goal

- Goal: Estimate an unknown distribution on X from data $\left\{x_j\right\}_{j=1}^n$

  - Build a model
    - Set of parameters Θ
    - Family of distribution on X,

$$p(x|\theta) \quad \text{with} \quad \theta \in \Theta$$

    - Prior distribution on the parameters Θ,

$$q(\theta).$$

  - Use Bayes' Law

$$p(\theta|x)p(x) = p(x \text{ and } \theta) = p(x|\theta)p(\theta)$$

  - Recall if A_1, A_2 are events:

$$p(A_1|A_2) = \frac{P(A_1 \cap A_2)}{P(A_2)}$$

$$p(\theta|x) = \frac{p(x|\theta)q(\theta)}{p(x)}$$

$$p(\theta|x) \sim p(x|\theta)q(\theta)$$

    where $p(\theta|x)$ is the posteriori distribution, $q(\theta)$ is the prior distribution and $p(x|\theta)$ is the likelihood function.

- Stant with: prior $q(\theta)$
- Add data x, replace q with the posterior

$$p(\theta|x) \sim p(x|\theta)q(\theta)$$

- More data: multiply by likelihood function and then normalize
- Left with a posterior distribution
  - Sample from posterion distribution to approximate

$$P_{pred}(x) = \int_{\Theta} p(x|\theta)p(\theta)d\theta$$

  - Choose θ to maximize posterior distribution

$$\begin{aligned}
\theta^* &= \arg\max_{\theta\in\Theta} p(\theta|x) \\
&= \arg\min_{\theta\in\Theta} -\log p(\theta|x) \\
&= \arg\min_{\theta\in\Theta} -\log(p(x|\theta)) - \log(q(\theta)) + \log(p(x)) \\
&= \arg\min_{\theta\in\Theta} -\log(p(x|\theta)) - \log(q(\theta))
\end{aligned}$$

    where $-\log(p(x|\theta))$ is the negative log likelihood and $-\log(q(\theta))$ is the regularization coming from prior.

3.9.2 Example: Image Classification/ Logistic Regression

- Images $x \in X = \mathbb{R}^d$
- Labels $y \in Y = \{e_1, \ldots, e_k\}$ with k is the dimension of labels
- Data $\left\{(x_j, y_j)\right\}_{j=1}^n$
- Model $\theta = (W, b) \in \mathbb{R}^{k\times d} \times \mathbb{R}^k$. By (3.1),

$$p(y|x, \theta) = \frac{e^{Wx+b} \cdot y}{e^{Wx+b} \cdot \mathbb{I}}$$

- Prior distribution: suppose it is a Gaussian,

$$q(W, b) = Ce^{-\alpha\left(\|W\|_2^2 + \|b\|_2^2\right)}$$

  – Calculate the posterior: here $q(W, b) = p(W, b|x)$,

$$p(W, b|x, y) = \frac{p(y|x, W, b)p(W, b|x)}{p(y|x)}$$

$$p(y|x) = \int_\Theta p(y|x, W, b)q(W, b)d\theta$$

$$\begin{aligned}
(W, b)^* &= \arg\min_{W,b} -\log\left(p\left(W, b|\left\{x_j, y_j\right\}_{j=1}^n\right)\right) \\
&= \arg\min_{W,b} -\log\left(p\left(\left\{y_j\right\}_{j=1}^n | \left\{x_j\right\}_{j=1}^n, W, b\right)\right) - \log(q(W, b)) \\
&= \arg\min_{W,b} -\log\left(\prod_{i=1}^n p\left(y_j|x_j, W, b\right)\right) - \log(q(W, b)) \\
&= \operatorname*{argmin}_{W,b} \sum_{j=1}^n \log\left(e^{Wx+b} \cdot \mathbb{I}\right) - \log\left(e^{Wx_j+b} \cdot y_j\right) + \alpha\left(\|W\|_2^2 + \|b\|_2^2\right).
\end{aligned}$$

3.10 General Covariance

Let $X \in V$ be a random variable living in an inner product space V with $E[X] = 0$ Define: The covariance of X is the quadratic form $\mathrm{Cov}(X) : V \to R$ defined by

$$\mathrm{Cov}(X)(v) = E\left[\langle X, v\rangle^2\right]$$

If V is finite dimensional and $e_1, \ldots, e_n$ is an orthonormal matrix then

$$\langle X, v\rangle = X^\top v = v^\top X$$

and so

$$\mathrm{Cov}(X)(v) = \mathbb{E}\left[v^\top X X^\top v\right] = v^\top \mathbb{E}\left[XX^\top\right] v$$

Sometimes, we may define a scalar variance

$$\mathrm{Var}(X) = \mathbb{E}\left[\|X\|^2\right] = \mathrm{tr}\left(\mathbb{E}\left[XX^\top\right]\right)$$

3.10.1 Whitening

Consider transforming the random variable X with a linear transformation matrix A. Then

$$Cov(AX) = \mathbb{E}\left[AXX^\top A^\top\right] = A\mathbb{E}\left[XX^\top\right]A^\top = AVA^T$$

where $V = \mathbb{E}\left[XX^\top\right]$ is the coveriance of X. So if we choose A s.t.

$$AVA^\top = I \Leftrightarrow V = A^{-1}A^{-T},$$

then

$$Cov(AX) = I,$$

so AX is "white noise". Clearly there are many choice for A. Namely given an A, OA also works for any orthonormal O.

3.10.2 Batch Normalization

- Calculating an appropriate A is generally competationally too expensive. The most efficient way to do it is likely a Cholesky factorization.
- In BN, we instead choose A diagonal so that

$$\text{diag}\left(A \cup A^T\right) = (1, 1, \ldots, 1)$$

- Of course the off-diagonal entries of $A \cup A^T$ will generally not be O.

3.10.3 Central Limiting Theorem

Let $X_1, X_2, \ldots, X_n$ be independent copies of $X \in \Omega$ with $E[X] = 0$. Then $V = E\left[XX^T\right]$. Consider

$$\bar{X}_n = \frac{1}{\sqrt{n}} \sum_{i=1}^{n} X_i.$$

As $n \to \infty$, $\bar{X}_n$ converges to a Gaussian distribution, namely,

$$\lim_{n\to\infty} \bar{X}_n = \text{Gaussian}(0, V)$$

with distribution

$$P(X) = \frac{1}{(\sqrt{2n}\det(V))^d} e^{\frac{-x^T V^{-1} x}{2}} dx.$$

4

Training Algorithms

4.1 Line search and gradient descent method

4.1.1 Gradient descent method

For simplicity, let us just consider a general optimization problem

$$\min_{x\in\mathbb{R}^n} f(x). \tag{4.1}$$

A general approach: line search method

Given any initial guess x_1, the line search method uses the following algorithm

$$\eta_t = \arg\min_{\eta\in\mathbb{R}^1} f(x_t - \eta p_t) \qquad \text{(1D minimization problem)}$$

to produce $\{x_t\}_{t=1}^{\infty}$

$$x_{t+1} = x_t - \eta_t p_t. \tag{4.2}$$

Here η_t is called the step size in optimization and also learning rate in machine learning, p_t is called the descent direction, which is the critical component of this algorithm. And x_t tends to

$$x^* = \arg\min_{x\in\mathbb{R}^n} f(x) \iff f(x^*) = \min_{x\in\mathbb{R}^n} f(x)$$

as t tends to infinity. There is a series of optimization algorithms which follow the above form just using different choices of p_t.

Then, the next natural question is what a good choice of p_t is? We have the following theorem to show why gradient direction is a good choice for p_t.

Lemma 17. *Given $x \in \mathbb{R}^n$, if $\nabla f(x) \neq 0$, the fast descent direction of f at x is the negative gradient direction, namely*

$$-\frac{\nabla f(x)}{\|\nabla f(x)\|} = \arg\min_{p\in\mathbb{R}^n,\|p\|=1} \left.\frac{\partial f(x+\eta p)}{\partial \eta}\right|_{\eta=0}. \tag{4.3}$$

It means that $f(x)$ decreases most rapidly along the negative gradient direction.

Proof. Let p be a direction in $\mathbb{R}^n, \|p\| = 1$. Consider the local decrease of the function $f(\cdot)$ along direction p

$$\Delta(p) = \lim_{\eta\downarrow 0} \frac{1}{\eta}(f(x+\eta p) - f(x)) = \left.\frac{\partial f(x+\eta p)}{\partial \eta}\right|_{\eta=0}.$$

Note that

$$\left.\frac{\partial f(x+\eta p)}{\partial \eta}\right|_{\eta=0} = \sum_{i=1}^{n} \frac{\partial f}{\partial x_i}(x+\eta p)p_i\Big|_{\eta=0} = (\nabla f, p), \tag{4.4}$$

which means that

$$f(x+\eta p) - f(x) = \eta(\nabla f(x), p) + o(\eta).$$

Therefore

$$\Delta(p) = (\nabla f(x), p).$$

Using the Cauchy-Schwarz inequality $-\|x\| \cdot \|y\| \leq (x, y) \leq \|x\| \cdot \|y\|$, we obtain

$$-\|\nabla f(x)\| \leq (\nabla f(x), p) \leq \|\nabla f(x)\|.$$

Let us take

$$\bar{p} = -\nabla f(x)/\|\nabla f(x)\|.$$

Then

$$\Delta(\bar{p}) = -(\nabla f(x), \nabla f(x))/\|\nabla f(x)\| = -\|\nabla f(x)\|.$$

The direction $-\nabla f(x)$ (the antigradient) is the direction of the fastest local decrease of the function $f(\cdot)$ at point x. □

Here is a simple diagram for this property.

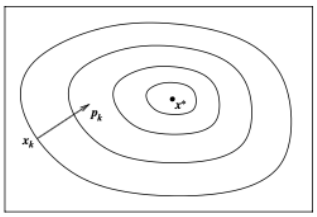

Fig. 4.1. Negative Gradient Direction: x_t is current point, p_t is the negative gradient of x_t, i.e., $-\nabla f(x_t)$.

Since at each point, $f(x)$ decreases most rapidly along the negative gradient direction, it is then natural to choose the search direction in (4.2) in the negative gradient direction and the resulting algorithm is the so-called gradient descent method.

Algorithm 2 Gradient Descent Method

Given the initial guess x_0, learning rate $\eta_t > 0$
For t=1,2,$\cdots$,

$$x_{t+1} = x_t - \eta_t \nabla f(x_t), \tag{4.5}$$

In practice, we need a "stopping criterion" that determines when the above gradient descent method to stop. One possibility is

While $S(x_t; f) = \|\nabla f(x_t)\| \leq \epsilon$ or $t \geq T$

for some small tolerance $\epsilon > 0$ or maximal number of iterations T. In general, a good stopping criterion is hard to come by and it is a subject that has called a lot of research in optimization for machine learning.

In the gradient method, the scalar factors for the gradients, η_t, are called the step sizes. Of course, they must be positive. There are many variants of the gradient method, which differ one from another by the step-size strategy. Let us consider the most important examples.

1. The sequence $\{\eta_t\}_{t=0}^{\infty}$ is chosen in advance. For example, (constant step)

$$\eta_t = \frac{\eta}{\sqrt{t+1}};$$

2. Full relaxation:

$$\eta_t = \arg\min_{\eta \geq 0} f\left(x_t - \eta \nabla f\left(x_t\right)\right);$$

3. The Armijo rule: Find $x_{t+1} = x_t - \eta \nabla f(x_t)$ with $\eta > 0$ such that

$$\alpha \left(\nabla f(x_t), x_t - x_{t+1}\right) \leq f(x_t) - f(x_{t+1}),$$

$$\beta \left(\nabla f(x_t), x_t - x_{t+1}\right) \geq f(x_t) - f(x_{t+1}),$$

where $0 < \alpha < \beta < 1$ are some fixed parameters.

Comparing these strategies, we see that

1. The first strategy is the simplest one. It is often used in the context of convex optimization. In this framework, the behavior of functions is much more predictable than in the general nonlinear case.
2. The second strategy is completely theoretical. It is never used in practice since even in one-dimensional case we cannot find the exact minimum in finite time.
3. The third strategy is used in the majority of practical algorithms. It has the following geometric interpretation. Let us fix $x \in \mathbb{R}^n$ assuming that $\nabla f(x) \neq 0$. Consider the following function of one variable:

$$\phi(\eta) = f(x - \eta \nabla f(x)), \quad \eta \geq 0.$$

Then the step-size values acceptable for this strategy belong to the part of the graph of ϕ which is located between two linear functions:

$$\phi_1(\eta) = f(x) - \alpha\eta \|\nabla f(x)\|^2, \quad \phi_2(\eta) = f(x) - \beta\eta \|\nabla f(x)\|^2$$

Note that $\phi(0) = \phi_1(0) = \phi_2(0)$ and $\phi'(0) < \phi_2'(0) < \phi_1'(0) < 0$. Therefore, the acceptable values exist unless $\phi(\cdot)$ is not bounded below. There are several very fast one-dimensional procedures for finding a point satisfying the Armijo conditions. However, their detailed description is not important for us now.

4.1.2 Convergence of Gradient Descent method

Now we are ready to study the rate of convergence of unconstrained minimization schemes. For the optimization problem (4.1),

$$\min_{x \in \mathbb{R}^n} f(x). \tag{4.6}$$

We assume that $f(x)$ is convex. Then we say that x^* is a minimizer if

$$f(x^*) = \min_{x \in \mathbb{R}^n} f(x).$$

For minimizer x^*, we have

$$\nabla f(x^*) = 0. \tag{4.7}$$

We have the next two properties of the minimizer for convex functions:

1. If $f(x) \geq c_0$, for some $c_0 \in \mathbb{R}$, then we have

$$\arg\min f \neq \emptyset. \tag{4.8}$$

2. If $f(x)$ is λ-strongly convex, then $f(x)$ has a unique minimizer, namely, there exists a unique $x^* \in \mathbb{R}^n$ such that

$$f(x^*) = \min_{x \in \mathbb{R}^n} f(x). \tag{4.9}$$

To investigate the convergence of gradient descent method, let us recall the gradient descent method:

Algorithm 3 FGD

For: $t = 1, 2, \cdots$

$$x_{t+1} = x_t - \eta_t \nabla f(x_t), \tag{4.10}$$

where η_t is the stepsize / learning rate.

We have the next theorem about the convergence of gradient descent method under the Assumption **??**.

Theorem 4. *For Gradient Descent Algorithm 3, if $f(x)$ satisfies Assumption* **??**, *then*

$$\|x_t - x^*\|^2 \leq \alpha^t \|x_0 - x^*\|^2 \tag{4.11}$$

if $0 < \eta_t < \frac{2\lambda}{L^2}$ *and* $\alpha < 1$.

Particularly, if $\eta_t = \frac{\lambda}{L^2}$, *then*

$$\|x_t - x^*\|^2 \leq \left(1 - \frac{\lambda^2}{L^2}\right)^t \|x_0 - x^*\|^2. \tag{4.12}$$

Proof. Note that

$$x_{t+1} - x = x_t - \eta_t \nabla f(x_t) - x. \tag{4.13}$$

By taking L^2 norm for both sides, we get

$$\|x_{t+1} - x\|^2 = \|x_t - \eta_t \nabla f(x_t) - x\|^2. \tag{4.14}$$

Let $x = x^*$. It holds that

(4.15)

$$\begin{aligned}
\|x_{t+1} - x^*\|^2 &= \|x_t - \eta_t \nabla f(x_t) - x^*\|^2 \\
&= \|x_t - x^*\|^2 - 2\eta_t \nabla f(x_t)^\top (x_t - x^*) + \eta_t^2 \|\nabla f(x_t) - \nabla f(x^*)\|^2 && \text{(by } \nabla f(x^*) = 0\text{)} \\
&\leq \|x_t - x^*\|^2 - 2\eta_t \lambda \|x_t - x^*\|^2 + \eta_t^2 L^2 \|x_t - x^*\|^2 && \text{(by } \lambda\text{- strongly convex (??) and Lipschitz)} \\
&\leq (1 - 2\eta_t \lambda + \eta_t^2 L^2) \|x_t - x^*\|^2 = \alpha \|x_t - x^*\|^2,
\end{aligned}$$

where

$$\alpha = \left(L^2(\eta_t - \frac{\lambda}{L^2})^2 + 1 - \frac{\lambda^2}{L^2} \right) < 1 \text{ if } 0 < \eta_t < \frac{2\lambda}{L^2}.$$

Particularly, if $\eta_t = \frac{\lambda}{L^2}$,

$$\alpha = 1 - \frac{\lambda^2}{L^2},$$

which finishes the proof. □

This means that if the learning rate is chosen appropriatly, $\{x_t\}_{t=1}^{\infty}$ from the gradient descent method will converge to the minimizer x^* of the function.

There are some issues on Gradient Descent method:

- $\nabla f(x_t)$ is very expensive to compute.
- Gradient Descent method does not yield generalization accuracy.

The stochastic gradient descent (SGD) method in the next section will focus on these two issues.

4.2 Stochastic gradient descent method and convergence theory

The next optimization problem is the most common case in machine learning.

Problem 1.

$$\min_{x \in \mathbb{R}^n} f(x) \quad \text{and} \quad f(x) = \frac{1}{N} \sum_{i=1}^{N} f_i(x). \tag{4.16}$$

One version of stochastic gradient descent (SGD) algorithm is:

Algorithm 4 SGD

Input: initialization x_0, learning rate η_t.
For: t = 0,1,2,...
Randomly pick $i_t \in \{1, 2, \cdots, N\}$ independently with probability $\frac{1}{N}$

$$x_{t+1} = x_t - \eta_t \nabla f_{i_t}(x_t). \tag{4.17}$$

4.2.1 Convergence of SGD

Theorem 5. *Assume that each $f_i(x)$ is λ-strongly convex and $\|\nabla f_i(x)\| \leq M$ for some $M > 0$. If we take $\eta_t = \frac{a}{\lambda(t+1)}$ with sufficiently large a such that*

$$\|x_0 - x^*\|^2 \leq \frac{a^2 M^2}{(a-1)\lambda^2} \tag{4.18}$$

then

$$\mathbb{E}e_t^2 \leq \frac{a^2M^2}{(a-1)\lambda^2(t+1)}, \quad t \geq 1, \tag{4.19}$$

where $e_t = \|x_t - x^*\|$.

Proof. The L^2 error of SGD can be written as

$$\begin{aligned}
\mathbb{E}\|x_{t+1} - x^*\|^2 &\leq \mathbb{E}\|x_t - \eta_t \nabla f_{i_t}(x_t) - x^*\|^2 \\
&\leq \mathbb{E}\|x_t - x^*\|^2 - 2\eta_t \mathbb{E}(\nabla f_{i_t}(x_t) \cdot (x_t - x^*)) + \eta_t^2 \mathbb{E}\|\nabla f_{i_t}(x_t)\|^2 \\
&\leq \mathbb{E}\|x_t - x^*\|^2 - 2\eta_t \mathbb{E}(\nabla f(x_t) \cdot (x_t - x^*)) + \eta_t^2 M^2 \\
&\leq \mathbb{E}\|x_t - x^*\|^2 - \eta_t \lambda \mathbb{E}\|x_t - x^*\|^2 + \eta_t^2 M^2 \\
&= (1 - \eta_t \lambda)\mathbb{E}\|x_t - x^*\|^2 + \eta_t^2 M^2
\end{aligned} \tag{4.20}$$

The third line comes from the fact that

$$\begin{aligned}
\mathbb{E}(\nabla f_{i_t}(x_t) \cdot (x_t - x^*)) &= \mathbb{E}_{i_1 i_2 \cdots i_t}(\nabla f_{i_t}(x_t) \cdot (x_t - x^*)) \\
&= \mathbb{E}_{i_1 i_2 \cdots i_{t-1}} \frac{1}{N} \sum_{i=1}^{N} \nabla f_i(x_t) \cdot (x_t - x^*) \\
&= \mathbb{E}_{i_1 i_2 \cdots i_{t-1}} \nabla f(x_t) \cdot (x_t - x^*) \\
&= \mathbb{E}\nabla f(x_t) \cdot (x_t - x^*),
\end{aligned} \tag{4.21}$$

and

$$\mathbb{E}\|\nabla f_{i_t}(x_t)\|^2 \leq \mathbb{E}M^2 = M^2. \tag{4.22}$$

Note when $t = 0$, we have

$$\mathbb{E}e_0^2 = \|x_0 - x^*\|^2 \leq \frac{a^2M^2}{(a-1)\lambda}, \tag{4.23}$$

based on the assumption.

In the case of SDG, by the inductive hypothesis,

$$\begin{aligned}
\mathbb{E}e_{t+1}^2 &\leq (1 - \eta_t\lambda)\mathbb{E}e_t^2 + \eta_t^2 M^2 \\
&\leq (1 - \frac{a}{t+1})\frac{a^2M^2}{(a-1)\lambda^2(t+1)} + \frac{a^2M^2}{\lambda^2(t+1)^2} \\
&\leq \frac{a^2M^2}{(a-1)\lambda^2}\frac{1}{(t+1)^2}(t+1-a+a-1) \\
&= \frac{a^2M^2}{(a-1)\lambda^2}\frac{t}{(t+1)^2} \\
&\leq \frac{a^2M^2}{(a-1)\lambda^2(t+2)}. \quad \left(\frac{t}{(t+1)^2} \leq \frac{1}{t+2}\right),
\end{aligned} \tag{4.24}$$

which completes the proof. □

4.2.2 SGD with mini-batch

Firstly, we will introduce a natural extended version of the SGD discussed above with introducing mini-batch.

Algorithm 5 SGD with mini-batch

Input: initialization x_0, learning rate η_t.
For: t = 0,1,2,...

Randomly pick $B_t \subset \{1, 2, \cdots, N\}$ independently with probability $\frac{m!(N-m)!}{N!}$ and $\#B_t = m$.

$$x_{t+1} = x_t - \eta_t g_t(x_t). \tag{4.25}$$

where

$$g_t(x_t) = \frac{1}{m} \sum_{i \in B_t} \nabla f_i(x_t)$$

Now we introduce the SGD algorithm with mini-batch without replacement which is the most commonly used version of SGD in machine learning.

Algorithm 6 Shuffle SGD with mini-batch

Input: learning rate η_k, mini-batch size m, parameter initialization x_0 and denote $M = \lceil \frac{N}{m} \rceil$.
For Epoch $k = 1, 2, \ldots$

Randomly pick $B_t \subset \{1, 2, \cdots, N\}$ without replacement with $\#B_t = m$ for $t = 1, 2, \cdots, M$.

For mini-batch $t = 1 : M$
Compute the gradient on B_t:

$$g_t(x) = \frac{1}{m} \sum_{i \in B_t} \nabla f_i(x)$$

Update x:

$$x \leftarrow x - \eta_k g_t(x),$$

EndFor
EndFor

To "randomly pick $B_i \subset \{1, 2, \cdots, N\}$ without replacement with $\#B_i = m$ for $i = 1, 2, \cdots, t$", we usually just randomly shuffle the index set first and then consec-

utively pick every m elements in the shuffled index set. That is the reason why we would like to call the algorithm as shuffled SGD while this is the mostly used version of SGD in machine learning.

Remark 2. Let us recall a general machine learning loss function

$$L(\theta) = \frac{1}{N}\sum_{i=1}^{N} \ell(h(X_i;\theta), Y_i), \tag{4.26}$$

where $\{(X_i, Y_i)\}_{i=1}^N$ correspond to these data pairs. For example, $\ell(\cdot,\cdot)$ takes cross-entropy and $h(x;\theta) = \boldsymbol{p}(x;\theta)$ as we discussed in Section 2.2.1. Thus, we have the following corresponding relation

$$f(x) \leftrightsquigarrow L(\theta), \quad f_i(x) \leftrightsquigarrow \ell(h(X_i;\theta), Y_i).$$

5

Polynomials and Weierstrass theorem

5.1 Weierstrass Theorem

To approximate any continuous function, a very simple idea is to approximate the function in a polynomial space. An important property of this space is that polynomials can approximate any reasonable function!

- $P_n(\mathbb{R}^d)$ is dense in $C(\Omega)$ [Weierstrass theorem]
- $P_n(\mathbb{R}^d)$ is dense in all Sobolev spaces: $L^2(\Omega), W^{m,p}(\Omega), \ldots$

Theorem 6. *Let $\Omega \subset R^n$ be a closed and bounded set. Given any continuous function $f(x)$ on Ω, there exists a sequence of polynomials $\{p_n(x)\}$ such that*

$$\lim_{n\to\infty} \max_{x\in\Omega} |f(x) - p_n(x)| = 0 \tag{5.1}$$

Proof. Let us first give the proof for $d = 1$ and $\Omega = [0, 1]$. Given $f : [0, 1] \to R$ be a continuous function.

Let

$$\tilde{f}(x) = f(x) - l(x) \tag{5.2}$$

where $l(x) = f(0) + x(f(1) - f(0))$. Then $\tilde{f}(0) = \tilde{f}(1) = 0$. Noting that $l(x)$ is a linear function, hence without lose of generality, we can only consider the case $f : [0, 1] \to R$ with $f(0) = f(1) = 0$. Since f is continuous on the closed interval $[0, 1]$, then f is uniformly continuous on $[0, 1]$.

First we extend f to be zero outside of $[0, 1]$ and obtain $f : R \to R$, then it is obviously that f is still uniformly continuous.

Next for $0 \le x \le 1$, we construct

$$p_n(x) = \int_{-1}^{1} f(x + t)Q_n(t)dt = \int_{-x}^{1-x} f(x + t)Q_n(t)dt = \int_{0}^{1} f(t)Q_n(t - x)dt \tag{5.3}$$

where $Q_n(x) = c_n(1 - x^2)^n$ and

$$\int_{-1}^{1} Q_n(x)dx = 1. \tag{5.4}$$

Thus $\{p_n(x)\}$ is a sequence of polynomials.

Since

$$\int_{-1}^{1}(1-x^2)^n dx = 2\int_{0}^{1}(1-x^2)^n dx = 2\int_{0}^{1}(1-x)^n(1+x)^n dx \tag{5.5}$$

$$\geq 2\int_{0}^{1}(1-x)^n dx = \frac{2}{n+1} > \frac{1}{n}. \tag{5.6}$$

Combing with $\int_{-1}^{1} Q_n(x)dx = 1$, we obtain $c_n < n$ implying that for any $\delta > 0$

$$0 \leq Q_n(x) \leq n(1-\delta^2)^n \quad (\delta \leq |x| \leq 1), \tag{5.7}$$

so that $Q_n \to 0$ uniformly in $\delta \leq |x| \leq 1$ as $n \to \infty$.

Given any $\epsilon > 0$, since f in uniformly continuous, there exists $\delta > 0$ such that for any $|y - x| < \delta$, we have

$$|f(y) - f(x)| < \frac{\epsilon}{2}. \tag{5.8}$$

Finally, let $M = \max|f(x)|$, using (5.8), (5.4) and (5.7), we have

$$\big|p_n(x) - f(x)\big| = \Big|\int_{-1}^{1}(f(x+t) - f(t))Q_n(t)dt\Big| \leq \int_{-1}^{1}\big|f(x+t) - f(t)\big|Q_n(t)dt \tag{5.9}$$

$$\leq 2M\int_{-1}^{-\delta} Q_n(t)dt + \frac{\epsilon}{2}\int_{-\delta}^{\delta} Q_n(t)dt + 2M\int_{\delta}^{1} Q_n(t)dt \tag{5.10}$$

$$\leq 4Mn(1-\delta^2)^n + \frac{\epsilon}{2} < \epsilon \tag{5.11}$$

for all large enough n, which proves the theorem.

The above proof generalize the high dimensional case easily. We consider the case that

$$\Omega = [0,1]^d.$$

By extension and using cut off function, W.L.O.G. that we assume that $f = 0$ on the boundary of Ω and we then extending this function to be zero outside of Ω.

Let us consider the special polynomial functions

$$Q_n(x) = c_n\prod_{k=1}^{d}(1-x_k^2) \tag{5.12}$$

Similar proof can then be applied. □

$d =$	2	4	8
$N =$	5×10^3	4.6×10^6	3.5×10^{11}

5.1.1 Curse of dimensionality

Number of coefficients for polynomial space $P_n(\mathbb{R}^d)$ is

$$N = \binom{d+n}{n} = \frac{(n+d)!}{d!n!}.$$

For example $n = 100$: As the this table shows, the dimension of the polynomial space $P_n(\mathbb{R}^d)$ increases rapidly as the degree n increases. This leads to an extremely large space therefore very expensive to approximate functions in polynomial spaces in high dimensions.

5.1.2 Runge's phenomenon

A natural way to approximate a given function on any interval $[a, b]$ is to use an n-degree polynomial $p_n(x)$ by $n + 1$ equispaced points, namely

$$x_i = a + \frac{b-a}{n}, \quad i = 0, 1, 2, \cdots, n.$$

By Weierstrass' theorem, we expect a more accurate reconstruction of $f(x)$ by using more points. But this is not always true as shown in the following example.

Consider the Runge function (a scaled version of the Witch of Agnesi)

$$f(x) = \frac{1}{1 + 25x^2}.$$

Runge found that if this function is interpolated at equidistant points x_i between -1 and 1 such that:

$$x_i = \frac{2i}{n} - 1, \quad i \in \{0, 1, \ldots, n\}$$

with a polynomial $p_n(x)$ of degree $\leq n$, the resulting interpolation oscillates toward the ends of the interval, i.e. close to -1 and 1. It can even be proven that the interpolation error increases (without bound) when the degree of the polynomial is increased:

$$\lim_{n\to\infty} \left(\max_{-1\leq x\leq 1} |f(x) - p_n(x)| \right) = +\infty.$$

This shows that high-degree polynomial interpolation at equidistant points can be troublesome.

The experiment shows that the polynomials $p_n(x)$ produced in this manner may in fact diverge away from $f(x)$ as n increases. This typically occurs in an oscillating pattern that magnifies near the ends of the interpolation points. This phenomenon is attributed to Runge.

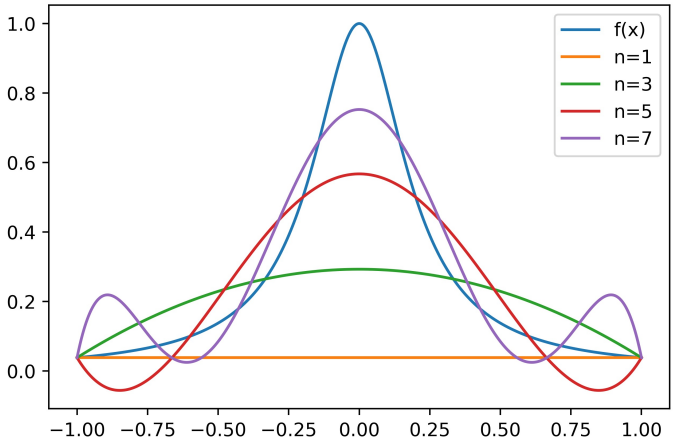

Fig. 5.1. Runge's phenomenon: Runge function $f(x) = \frac{1}{1+25x^2}$ and its polynomial interpolation $p_n(x)$.

Thus, this particular set of polynomial functions $p_n(x)$ is not guaranteed to have the property of uniform convergence. In other words, Weierstrass' theorem guarantees the existence of the polynomial functions, but how to find such polynomials is not provided.

5.2 Fourier transform and Fourier series

We make use of the theory of tempered distributions (see [**?**] for an introduction) and we begin by collecting some results of independent interest, which will also be important later.

5.2.1 Fourier transform

Before studying the Fourier transform, we first consider Schwartz space which is defined below.

Definition 7. *The Schwartz space $\mathcal{S}(\mathbb{R}^n)$ is the topological vector space of functions $f : \mathbb{R}^n \to \mathbb{C}$ such that $f \in C^\infty(\mathbb{R}^n)$ and*

$$x^\alpha \partial^\beta f(x) \to 0 \quad \text{as } |x| \to \infty$$

for every pair of multi-indices $\alpha, \beta \in \mathbb{N}_0^n$. For $\alpha, \beta \in \mathbb{N}_0^n$ and $f \in \mathcal{S}(\mathbb{R}^n)$ let (5.10)

$$\|f\|_{\alpha,\beta} = \sup_{\mathbb{R}^n} \left| x^\alpha \partial^\beta f \right|$$

A sequence of functions $\{f_k : k \in \mathbb{N}\}$ converges to a function f in $\mathcal{S}(\mathbb{R}^n)$ if

$$\|f_n - f\|_{\alpha,\beta} \to 0 \quad \text{as } k \to \infty$$

for every $\alpha, \beta \in \mathbb{N}_0^n$.

The Schwartz space consists of smooth functions whose derivatives and the function itself decay at infinity faster than any power. Schwartz functions are rapidly decreasing. When there is no ambiguity, we will write $\mathcal{S}(\mathbb{R}^n)$ as $\mathcal{S}$. Roughly speaking, tempered distributions grow no faster than a polynomial at infinity.

Definition 8. *A tempered distribution T on $\mathbb{R}^n$ is a continuous linear functional $T : \mathcal{S}(\mathbb{R}^n) \to \mathbb{C}$. The topological vector space of tempered distributions is denoted by $\mathcal{S}'(\mathbb{R}^n)$ or $\mathcal{S}'$. If $\langle T, f\rangle$ denotes the value of $T \in \mathcal{S}'$ acting on $f \in \mathcal{S}$ then a sequence $\{T_k\}$ converges to T in $\mathcal{S}'$, written $T_k \to T$, if*

$$\langle T_k, f\rangle \to \langle T, f\rangle$$

for every $f \in \mathcal{S}$.

Since $\mathcal{D} \subset \mathcal{S}$ is densely and continuously imbedded, we have $\mathcal{S}' \subset \mathcal{D}'$. Moreover, a distribution $T \in \mathcal{D}'$ extends uniquely to a tempered distribution $T \in \mathcal{S}'$ if and only if it is continuous on $\mathcal{D}$ with respect to the topology on $\mathcal{S}$. Every function $f \in L^1_{\text{loc}}$ defines a regular distribution $T_f \in \mathcal{D}'$ by

$$\left\langle T_f, \phi \right\rangle = \int f\phi dx \quad \text{for all } \phi \in \mathcal{D}.$$

If $|f| \le p$ is bounded by some polynomial p, then T_f extends to a tempered distribution $T_f \in \mathcal{S}'$, but this is not the case for functions f that grow too rapidly at infinity.

The Schwartz space is a natural one to use for the Fourier transform. Differentiation and multiplication exchange roles under the Fourier transform and therefore so do the properties of smoothness and rapid decrease. As a result, the Fourier transform is an automorphism of the Schwartz space. By duality, the Fourier transform is also an automorphism of the space of tempered distributions.

Definition 9. *The Fourier transform of a function $f \in \mathcal{S}(\mathbb{R}^n)$ is the function $\hat{f} : \mathbb{R}^n \to \mathbb{C}$ defined by*

$$\hat{f}(\omega) = \int f(x) e^{-2\pi i \omega \cdot x} dx.$$

The inverse Fourier transform of f is the function $\check{f} : \mathbb{R}^n \to \mathbb{C}$ defined by

$$\check{f}(x) = \int f(\omega) e^{2\pi i \omega \cdot x} dk.$$

Definition 10. *The Fourier transform of a tempered distribution $f \in \mathcal{S}'$ is defined by*

$$\langle \hat{f}, \phi\rangle = \langle f, \hat{\phi}\rangle, \quad \forall \phi \in \mathcal{S}.$$

The support of a continuous function f is the closure of the set $\{x \in \mathbb{R} : f(x) \neq 0\}$.

Properties 7 *The Fourier transform has the following properties*

1. *If $f \in \mathcal{S}'$ and the support of $\hat{f}$ is $\{0\}$, then f is a polynomial.*
2. *If $f \in \mathcal{S}'$ and the support of $\hat{f}$ is a single point $\{a\}$, then $f(x) = e^{2\pi i a x} P(x)$, where $P(x)$ is a polynomial.*

5.2.2 Poisson summation formula

Theorem 8. *Let $f \in L^1(\mathbb{R})$ and f is continuous. Then we have for almost all $(x, \omega) \in \mathbb{R} \times \hat{\mathbb{R}}$ that*

$$T \sum_{n\in\mathbb{Z}} f(x+nT) e^{-2\pi i \omega (x+nT)} = \sum_{n\in\mathbb{Z}} \hat{f}\left(\omega + \frac{n}{T}\right) e^{2\pi i n x/T}$$

where both sides converge absolutely.

In addition, let Λ be the lattice in $\mathbb{R}^d$ consisting of points with integer coordinates. For a function f in $L^1\left(\mathbb{R}^d\right)$ and f is continuous, we have

$$\sum_{\omega\in\Lambda} f(x+\omega) = \sum_{\nu\in\Lambda} \hat{f}(\omega) e^{2\pi i x\cdot\omega}.$$

where both series converge absolutely and uniformly on Λ.

Proof. We just give a proof of a simple case that $f : \mathbb{R} \to \mathbb{C}$ is a Schwarz function (see Definition 7). Let:

$$F(x) = \sum_{n\in\mathbb{Z}} f(x+n).$$

Then $F(x)$ is 1-periodic (because of absolute convergence), and has Fourier coefficients:

$$\begin{aligned}
\hat{F}_\omega &= \int_0^1 \sum_{n\in\mathbb{Z}} f(x+n) e^{-2\pi i\omega x}\, \mathrm{d}x \\
&= \sum_{n\in\mathbb{Z}} \int_0^1 f(x+n) e^{-2\pi i\omega x}\, \mathrm{d}x \quad \text{because } f \text{ is Schwarz, so convergence is uniform} \\
&= \sum_{n\in\mathbb{Z}} \int_n^{n+1} f(x) e^{-2\pi i\omega x}\, \mathrm{d}x \\
&= \int_{\mathbb{R}} f(x) e^{-2\pi i\omega x}\, \mathrm{d}x \\
&= \hat{f}(k)
\end{aligned}$$

where $\hat{f}$ is the Fourier transform of f.

Therefore by the definition of the Fourier series of f :

$$F(x) = \sum_{\omega\in\mathbb{Z}} \hat{f}(k) e^{2\pi i\omega x}.$$

Choosing $x = 0$ in this formula:

$$\sum_{n\in\mathbb{Z}} f(n) = \sum_{\omega\in\mathbb{Z}} \hat{f}(\omega)$$

as required. □

5.2.3 A special cut-off function

Let us first state the following simple result that can be obtained by following a calculation given in Section 3 of [**?**].

Lemma 18. *Given $\alpha > 1$, consider*

$$g(t) = \begin{cases} e^{-(1-t^2)^{1-\alpha}} & t \in (-1,1) \\ 0 & \textit{otherwise}. \end{cases} \tag{5.13}$$

then there is a constant c_α such that

$$|\hat{g}(\omega)| \lesssim e^{-c_\alpha |\omega|^{1-\alpha^{-1}}}, \tag{5.14}$$

Proof. Consider the asymptotic behavior of the Fourier transform

$$F(\omega) = \int_{-\infty}^{\infty} g(t) e^{2\pi i\omega t} dt = 2\,\mathrm{Re} \int_0^1 e^{2\pi i\omega t - (1-t^2)^{1-\alpha}} dt$$

for $|\mathrm{Re}\,\omega| \gg 1$. (Without loss of generality, we can restrict ourselves to real $\omega \geq 0$). With a change of variable $x = 1 - t$,

$$F(\omega) = 2\,\mathrm{Re} \int_0^1 e^{f(x)} dx$$

with $f(x) = 2\pi i\omega - 2\pi i\omega x - (2x - x^2)^{1-\alpha} \approx \tilde{f}(x) + O\left(x^{2-\alpha}\right)$ and

$$\tilde{f}(x) = 2\pi i\omega - 2\pi i\omega x - (2x)^{1-\alpha}.$$

The saddle point is the $x = x_0$ where $f'(x_0) = 0$. Since $\tilde{f}'(x) = -2\pi i\omega + (\alpha - 1)2^{1-\alpha} x^{-\alpha}$,

$$x_0 \approx \tilde{x}_0 = \left(2^{-\alpha}(\alpha - 1)/i\omega\pi\right)^{1/\alpha} \sim \omega^{-1/\alpha}.$$

Therefore $\tilde{f}(\tilde{x}_0) \sim \omega^{(\alpha-1)/\alpha}$ asymptotically. The second derivative is

$$\tilde{f}''(\tilde{x}_0) = -2^{1-\alpha}\alpha(\alpha - 1)\tilde{x}_0^{-\alpha-1} = -i^{(\alpha+1)/\alpha} 2A\omega^{(\alpha+1)/\alpha},$$

where

$$A = 2\alpha(\alpha - 1)^{-1/\alpha}\pi^{(\alpha+1)/\alpha}.$$

Now,

$$
\begin{aligned}
\tilde{f}(x) \approx & \tilde{f}(\tilde{x}_0) + \frac{\tilde{f}''(\tilde{x}_0)}{2}(x-\tilde{x}_0)^2 \\
= & 2\pi i\omega - (\alpha-1)^{\frac{1}{\alpha}}(i\omega\pi)^{\frac{\alpha-1}{\alpha}} - (\alpha-1)^{\frac{1-\alpha}{\alpha}}(i\omega\pi)^{\frac{\alpha-1}{\alpha}} \\
& - i^{(\alpha+1)/\alpha}A\omega^{(\alpha+1)/\alpha}(x-2^{-1}(\alpha-1)^{-\frac{1}{\alpha}}(i\omega\pi)^{-\frac{1}{\alpha}})^2.
\end{aligned} \tag{5.15}
$$

Choose a contour $x = i^{-1/\alpha}u$, in which case

$$
\tilde{f}(x) \approx \tilde{f}(\tilde{x}_0) - i^{(\alpha-1)/\alpha}A\omega^{(\alpha+1)/\alpha}\,(u-u_0)^2\,,
$$

which is a path of descent so we can perform a Gaussian integral.

Recall that the integral of

$$
\int_{-\infty}^{\infty} e^{-au^2}du = \sqrt{\pi/a} \tag{5.16}
$$

as long as Re$a > 0$, which is true here. Note also that, in the limit as ω becomes large, the integrand becomes zero except close to $u = \sqrt{1/2\omega}$, so we can neglect the rest of the contour and treat the integral over u as going from $-\infty$ to ∞. (Thankfully, the width of the Gaussian $\Delta u \sim \omega^{-3/4}$ goes to zero faster than the location of the maximum $u_0 \sim \omega^{-1/2}$, so we don't have to worry about the $u = 0$ origin). Also note that the change of variables from x to u gives us the Jacobian factor for

$$
dx = i^{-1/\alpha}du.
$$

Thus, when all is said and done, we obtain the exact asymptotic form of the Fourier integral for $\omega \gg 1$:

$$
\begin{aligned}
F(\omega) \approx & 2\,\mathrm{Re}\int_0^1 e^{\tilde{f}(\tilde{x}_0)-i^{(\alpha-1)/\alpha}A\omega^{(\alpha+1)/\alpha}(u-u_0)^2}dx \\
= & 2\,\mathrm{Re}\,e^{\tilde{f}(\tilde{x}_0)}i^{-1/\alpha}\int_{-\infty}^{\infty} e^{-i^{\frac{(\alpha-1)}{\alpha}}A\omega^{(\alpha+1)/\alpha}(u-u_0)^2}du \\
= & 2\,\mathrm{Re}\,e^{\tilde{f}(\tilde{x}_0)}\pi^{1/2}i^{-1/\alpha}i^{\frac{(1-\alpha)}{2\alpha}}A^{-1/2}\omega^{-(\alpha+1)/2\alpha} \qquad \text{by (5.16)} \\
= & 2\,\mathrm{Re}\left[\sqrt{\frac{\pi}{(i\omega)^{(\alpha+1)/\alpha}A}}e^{\tilde{f}(\tilde{x}_0)}\right] \\
\approx & 2\,\mathrm{Re}\left[\sqrt{\frac{\pi}{(i\omega)^{(\alpha+1)/\alpha}A}}e^{2\pi i\omega-2\pi i\omega\tilde{x}_0-[(2-\tilde{x}_0)\tilde{x}_0]^{1-\alpha}}\right]
\end{aligned} \tag{5.17}
$$

with x_0 and A given above. Notice that $\tilde{x}_0 \sim \omega^{-1/\alpha}$. Thus,

$$
|F(\omega)| \approx e^{-c_\alpha|\omega|^{1-\alpha^{-1}}}.
$$

□

5.2.4 Fourier transform of polynomials

We begin by noting that an activation function σ, which satisfies a polynomial growth condition $|\sigma(x)| \leq C(1+|x|)^n$ for some constants C and n, is a tempered distribution. As a result, we make this assumption on our activation functions in the following theorems. We briefly note that this condition is sufficient, but not necessary (for instance an integrable function need not satisfy a pointwise polynomial growth bound) for σ to be represent a tempered distribution.

We begin by studying the convolution of σ with a Gaussian mollifier. Let η be a Gaussian mollifier

$$\eta(x) = \frac{1}{\sqrt{\pi}} e^{-x^2}. \tag{5.18}$$

Set $\eta_\epsilon = \frac{1}{\epsilon}\eta(\frac{x}{\epsilon})$. Then consider

$$\sigma_\epsilon(x) := \sigma * \eta_\epsilon(x) = \int_{\mathbb{R}} \sigma(x-y)\eta_\epsilon(y)dy \tag{5.19}$$

for a given activation function σ. It is clear that $\sigma_\epsilon \in C^\infty(\mathbb{R})$. Moreover, by considering the Fourier transform (as a tempered distribution) we see that

$$\hat{\sigma}_\epsilon = \hat{\sigma}\hat{\eta}_\epsilon = \hat{\sigma}\eta_{\epsilon^{-1}}. \tag{5.20}$$

We begin by stating a lemma which characterizes the set of polynomials in terms of their Fourier transform.

Lemma 19. *Given a tempered distribution σ, the following statements are equivalent:*

1. *σ is a polynomial*
2. *σ_ϵ given by (7.31) is a polynomial for any $\epsilon > 0$.*
3. *$\mathrm{supp}(\hat{\sigma}) \subset \{0\}$.*

Proof. We begin by proving that (3) and (1) are equivalent. This follows from a characterization of distributions supported at a single point (see [**?**], section 6.3). In particular, a distribution supported at 0 must be a finite linear combination of Dirac masses and their derivatives. In particular, if $\hat{\sigma}$ is supported at 0, then

$$\hat{\sigma} = \sum_{i=1}^{n} a_i \delta^{(i)}. \tag{5.21}$$

Taking the inverse Fourier transform and noting that the inverse Fourier transform of $\delta^{(i)}$ is $c_i x^i$, we see that σ is a polynomial. This shows that (3) implies (1), for the converse we simply take the Fourier transform of a polynomial and note that it is a finite linear combination of Dirac masses and their derivatives.

Finally, we prove the equivalence of (2) and (3). For this it suffices to show that $\hat{\sigma}$ is supported at 0 iff $\hat{\sigma}_\epsilon$ is supported at 0. This follows from equation 7.32 and the fact that $\eta_{\epsilon^{-1}}$ is nowhere vanishing. □

As an application of Lemma 21, we give a simple proof of the result in the next section.

6

Finite Element Method

Finite element method is a classic numerical method for solving partial differential equations. In this chapter, we will give a brief introduction to this method. discuss its basic properties and error estimates. In later chapters, we will show that the neural network functions can be viewed as an extension of finite element function. In this chapter, we discuss the classical linear finite element spaces, the error estimate of the finite element method and adaptivity method to improve the approximation. For shape-regular mesh, we will establish both the upper and lower bound of the approximation error.

6.1 Linear finite element spaces

In this section, we introduce linear finite element spaces. We will walk through the basic setup, and derive some error estimates.

6.1.1 Triangulations

Given a bounded polyhedral domain $\Omega \subset \mathbb{R}^d$, a geometric triangulation (also called mesh or grid) $\mathcal{T}_h = \{\tau\}$ of Ω is a set of d-simplices such that

(1) $\overline{\Omega} = \cup\tau$, where $\overline{\Omega}$ denotes the closure of Ω.

(2) if τ_1 and τ_2 are distinct elements in $\mathcal{T}_h$ then $\mathring{\tau}_1 \cap \mathring{\tau}_2 = \emptyset$, where $\mathring{\tau}_i$ denotes the interior of $\tau_i, i = 1, 2$.

Examples of triangulations for $\Omega = (0, 1)$ $(d = 1)$ and for $\Omega = (0, 1)^2$ $(d = 2)$ are shown in Figure 6.1 and Figure 6.2, respectively.

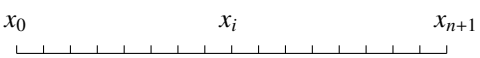

Fig. 6.1. 1D uniform grid

Example 3. Given $\Omega = (0, 1)$, we consider the mesh:

$$0 = x_0 < x_1 < \cdots < x_{n+1} = 1, \quad x_i = \frac{i}{n+1}, \quad (i = 0, \cdots, n+1) \tag{6.1}$$

which is the 1D uniform grid shown in Figure 6.1.

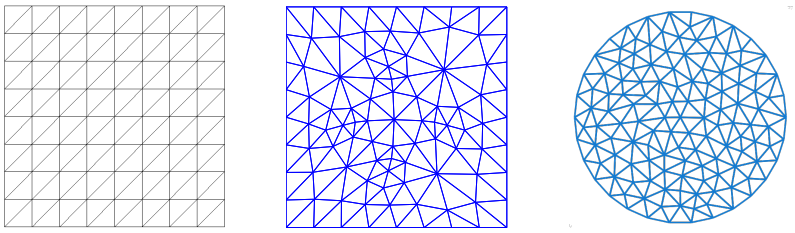

Fig. 6.2. 2D grids

Denote

$$h_\tau = \text{diam}(\tau) \quad \text{(diameter of the smallest sphere containing } \overline{\tau}),$$

and

$$h = \max_{\tau \in \mathcal{T}_h} h_\tau; \quad \underline{h} = \min_{\tau \in \mathcal{T}_h} h_\tau.$$

A set of triangulations $\mathscr{T}$ is called *shape regular* if there exists a constant c_0 such that

$$\max_{\tau \in \mathcal{T}_h} \frac{h_\tau^d}{|\tau|} \leq c_0, \quad \forall \mathcal{T}_h \in \mathscr{T}, \tag{6.2}$$

where $|\tau|$ is the measure of τ in $\mathbb{R}^d$. This assumption can also be represented as

$$\max_{\tau \in \mathcal{T}_h} \frac{h_\tau}{\rho_\tau} \leq \sigma_1, \quad \forall \mathcal{T}_h \in \mathscr{T}, \tag{6.3}$$

where ρ_τ denotes the radius of the ball inscribed in τ. In two dimensions, it is equivalent to the minimal angle of each triange is bounded below uniformly in the shape regular class.

In addition to (6.2), if

$$\frac{\max_{\tau \in \mathcal{T}_h} |\tau|}{\min_{\tau \in \mathcal{T}_h} |\tau|} \leq \rho, \quad \forall \mathcal{T}_h \in \mathscr{T}, \tag{6.4}$$

$\mathscr{T}$ is called *quasi-uniform*. For quasi-uniform grids, $h = \max_{\tau \in \mathcal{T}_h} h_\tau$, the mesh size of $\mathcal{T}_h$, is used to measure the approximation rate.

The assumption (6.3) is a local assumption, as is meant by above definition, for $d = 2$ for example, it assures that each triangle will not degenerate into a segment in the limiting case.

On the other hand, the assumption (6.4) is a global assumption, which says that the smallest mesh size is not too small compared with the largest mesh size of the same triangulation. By the definition, in a quasi-uniform triangulation, all the elements are about the same size asymptotically.

Let $x_i = (x_i^1, \cdots, x_i^d)^t, i = 1, \cdots, d+1$ be $d+1$ points in $\mathbb{R}^d$ which do not all lie in one hyper-plane. The *convex hull* of the $d+1$ points $x_1, \cdots, x_{d+1}$ (See Figure 6.3)

$$\tau := \{x = \sum_{i=1}^{d+1} \lambda_i x_i \,|\, 0 \le \lambda_i \le 1, i = 1 : d+1, \sum_{i=1}^{d+1} \lambda_i = 1\} \tag{6.5}$$

is defined as a *geometric d-simplex* generated (or spanned) by the vertices $x_1, \cdots, x_{d+1}$. For example, a triangle is a 2-simplex and a tetrahedron is a 3-simplex. For an integer $0 \le m \le d-1$, an m-dimensional face of τ is any m-simplex generated by $m+1$ of the vertices of τ. Zero-dimenisonal faces are vertices and one-dimensional faces are called edges of τ. The $(d-1)$-face opposite to the vertex x_i will be denoted by F_i. On the other hand, for any $x \in \tau$, there exist unique numbers $\lambda_1, \cdots, \lambda_{d+1}$ satisfying

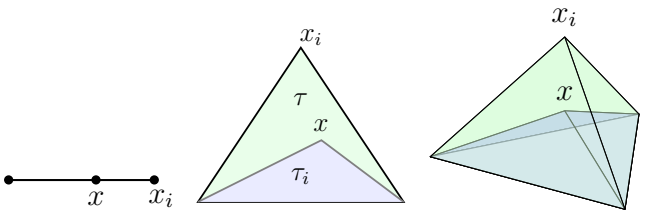

Fig. 6.3. Geometric explanation of barycentric coordinates

$0 \le \lambda_i \le 1, i = 1 : d+1, \sum_{i=1}^{d+1} \lambda_i = 1$ such that $x = \sum_{i=1}^{d+1} \lambda_i x_i$, thus we can denote $\lambda_1, \cdots, \lambda_{d+1}$ as $\lambda_1(x), \cdots, \lambda_{d+1}(x)$. In fact, the numbers $\lambda_1(x), \cdots, \lambda_{d+1}(x)$ are called *barycentric coordinates* of x with respect to the $d+1$ points $x_1, \cdots, x_{d+1}$. There is a simple geometric meaning of the barycentric coordinates. Given a $x \in \tau$, let $\tau_i(x)$ be the simplex with vertices x_i replaced by x. Then it can be easily shown that

$$\lambda_i(x) = |\tau_i(x)|/|\tau|, \tag{6.6}$$

where $|\cdot|$ is the Lebesgure measure in $\mathbb{R}^d$, namely area in two dimensions and volume in three dimensions. Note that $\lambda_i(x)$ is affine function of x and vanishes on the face F_i. We list the four basic properties of barycentric coordinate below:

1. $0 \le \lambda_i(x) \le 1$;
2. $\sum_{i=1}^{d+1} \lambda_i(x) = 1$;
3. $\lambda_i(x) \in P_1(\tau)$, where $P_1(\tau)$ denotes the space of polynomials of degree 1 (linear) on $\tau \in \mathcal{T}_h$;

4. $\lambda_i(x_j) = \delta_{ij} = \begin{cases} 1, & \text{if} \quad i = j \\ 0, & \text{if} \quad i \neq j \end{cases}$.

6.1.2 Continuous linear finite element spaces

A conforming linear finite element function in a domain $\Omega \subset \mathbb{R}^d$ is a continuous function that is piecewise linear function with respect to a grid or mesh consisting of a union of simplices.

Given a shape regular triangulation $\mathcal{T}_h$ of Ω, we define the continuous linear finite element space as

$$V_h := \{v \,|\, v \in C(\overline{\Omega}), \text{ and } v|_\tau \in P_1(\tau), \forall \tau \in \mathcal{T}_h\}, \tag{6.7}$$

where $P_1(\tau)$ denotes the space of polynomials of degree 1 (linear) on $\tau \in \mathcal{T}_h$. Whenever we need to deal with boundary conditions, we further define $V_{h,0} = V_h \cap H_0^1(\Omega)$.

We note here that the global continuity is also necessary in the definition of V_h in the sense that if u has a square interable gradient, that is $u \in H^1(\Omega)$, and u is piecewise smooth, then u is continuous.

We always use n_h to denote the dimension of finite element spaces. For V_h, n_h is the number of vertices of the triangulation $\mathcal{T}_h$ and for $V_{h,0}$, n_h is the number of interior vertices.

Nodal basis functions and dual basis

For linear finite element spaces, we have the so called *a standard nodal basis functions* $\{\varphi_i, i = 1, \cdots n_h\}$ such that φ_i is piecewise linear (with respect to the triangulation) and $\varphi_i(x_j) = \delta_{i,j}$. Note that $\varphi_i|_\tau$ is the corresponding barycentrical coordinates of x_i. See Figure 6.5 for an illustration in 2D. Let $(\varphi_i^*)_{i=1}^{n_h}$ be the dual basis of $(\varphi_i)_{i=1}^{n_h}$,

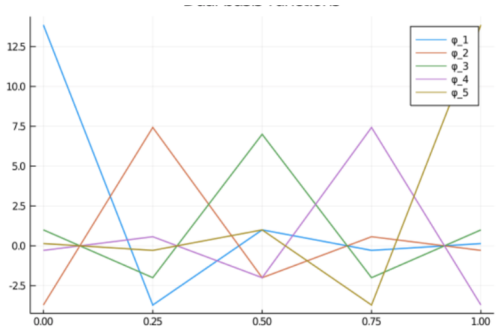

Fig. 6.4. Dual basis functions of V_h in 1D for $n_h = 5$.

namely

$$(\varphi_i^*, \varphi_j) = \delta_{i,j}, \quad i, j = 1, \ldots, n_h. \tag{6.8}$$

We notice that all the nodal basis functions $\{\varphi_i\}$ are locally supported, but their dual basis functions $\{\varphi_i^*\}$ are in general not locally supported (see Figure 6.4). The nodal basis functions $\{\varphi_i\}$ are easily constructed in terms of barycentric coordinate functions. The dual basis $\{\varphi_i^*\}$ are only interesting for theoretical consideration and it is not necessary to know the actual constructions of these functions.

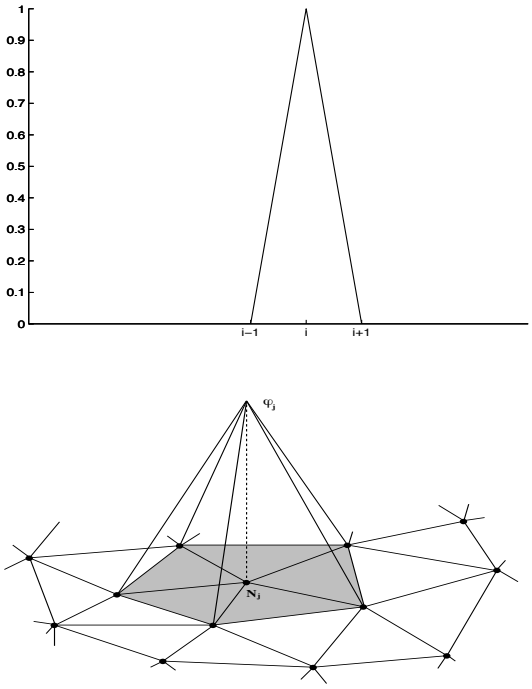

Fig. 6.5. Nodal basis functions in 1d and 2d

Since $\{\varphi_i, i = 1, \cdots n_h\}$ is a basis of V_h, therefore for any $v_h \in V_h$, we have the representation

$$v_h(x) = \sum_{i=1}^{n_h} v_h(x_i)\varphi_i(x).$$

Let us see how our construction of continuous linear finite space and the nodal basis looks like in one spatial dimension. Associated with the mesh

$$\mathcal{T}_h = \{0 = x_0 < x_1 < \ldots < x_{n_h} < x_{n_h+1} = 1\},$$

by the definition given in (6.7) and the definition $V_{h,0} = V_h \cap H_0^1(\Omega)$, we have

$$V_{h,0} = \{v : \ v \text{ is continuous and piecewise linear w. r. t. } \mathcal{T}_h,\ v(0) = v(1) = 0\}.$$

A plot of a typical element of $V_{h,0}$ is shown in Fig. 6.6.

It is easily calculated (as we already mentioned), that the dimension of $V_{h,0}$ is equal to the number of internal vertices, and the nodal basis functions spanning $V_{h,0}$ (for $i = 1, 2, \cdots, n_h$) are (see also Fig. 6.5):

$$\varphi_i(x) = \begin{cases} \dfrac{x - x_{i-1}}{h}, & x \in [x_{i-1}, x_i]; \\ \dfrac{x_{i+1} - x}{h}, & x \in [x_i, x_{i+1}]; \\ 0 & \text{elsewhere.} \end{cases} \tag{6.9}$$

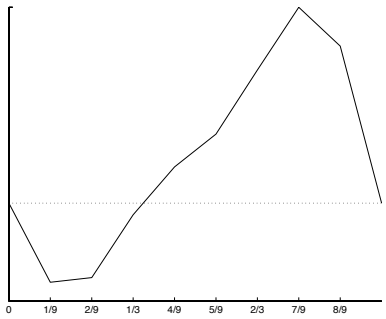

Fig. 6.6. Plot of a typical element from $V_{h,0}$.

Nodal value interpolant

For any continuous function u, we define its linear finite element interpolation, $(I_h u)(x) \in V_{h,0}$, as follows:

$$(I_h u)(x) = \sum_{i=1}^{n_h} u(x_i)\varphi_i(x). \tag{6.10}$$

Usually, we also denote $(I_h u)(x)$ as $u_I(x)$. Using interpolation, we can obtain the following approximation property of linear finite element space.

Theorem 9. *Assume that $\mathcal{T}_h$ is quasi-uniform and V_h is the linear finite element space associated with $\mathcal{T}_h$, then*

$$\inf_{v_h \in V_h} \|v - v_h\| + h|v - v_h|_1 \lesssim h^2 |v|_2 \quad \forall\ v \in H^2(\Omega). \tag{6.11}$$

Proof. Let us first prove Theorem 9 for $d = 1, 2, 3$. This proof presented here follows from Xu [**?**] (see also Xu [**?**]). Let $x = (x^1, \ldots, x^d)$ and $a_i = (a_i^1, \ldots, a_i^d)$. Introducing the auxiliary functions

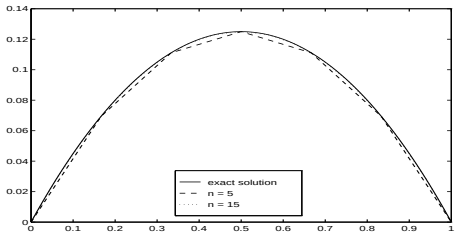

Fig. 6.7. Approximation of finite element space.

$$g_i(t) = v(a_i(t)), \text{ with } a_i(t) = a_i + t(x - a_i),$$

we have

$$g_i'(t) = (\nabla v)(a_i(t)) \cdot (x - a_i) = \sum_{l=1}^{d} (\partial_l v)(a_i(t))(x^l - a_i^l)$$

and

$$g_i''(t) = \sum_{k,l=1}^{d} \partial_{kl}^2 v)(a_i(t))(x^k - a_i^k)(x^l - a_i^l). \tag{6.12}$$

Note Taylor expansion

$$g_i(0) = g_i(1) - g_i'(1) + \int_0^1 t g_i''(t) dt,$$

namely

$$v(a_i) = v(x) - (\nabla v)(x) \cdot (x - a_i) + \int_0^1 t g_i''(t) dt, \tag{6.13}$$

and note that

$$(I_h v)(x) = \sum_{i=1}^{d+1} v(a_i)\lambda_i(x), \quad \sum_{i=1}^{d+1} \lambda_i(x) = 1,$$

and

$$\sum_{i=1}^{d+1} (x - a_i)\lambda_i(x) = 0.$$

It follows that

$$(I_h v - v)(x) = \sum_{i=1}^{d+1} \lambda_i(x) \int_0^1 t g_i''(t) dt. \tag{6.14}$$

Using (6.12) and the trivial fact that $|x^l - a_i^l| \le h$, we obtain

$$\|g_i''(t)\|_{L^2(\tau)} \le h^2 \sum_{k,l=1}^{d} \|(\partial_{kl}^2 v)(a_i(t))\|_{L^2(\tau_i^t)} \le h^2 t^{-d/2} \sum_{k,l=1}^{d} \|\partial_{kl}^2 v\|_{L^2(\tau)},$$

where we have used the following change of variable

$$y = a_i + t(x - a_i) : \tau \mapsto \tau_i^t \subset \tau \text{ with } dy = t^d dx.$$

Now taking the $L^2(\tau)$ norm on both hand of sides of (6.14), we get

$$\begin{aligned}
\|I_h v - v\|_{L^2(\tau)} &\le h^2 \sum_{i=1}^{d+1} \max_{x\in\tau} |\lambda_i(x)| \int_0^1 t \|g_i''(t)\|_{L^2(\tau)}\, dt \\
&\le (d+1) \int_0^1 t^{-d/2} dt\, h^2 \sum_{k,l=1}^{d} \|\partial_{kl}^2 v\|_{L^2(\tau)} \\
&\le \frac{2(d+1)}{4-d} h^2 \sum_{k,l=1}^{d} \|\partial_{kl}^2 v\|_{L^2(\tau)} \\
&\le \frac{4d(d+1)}{4-d} h^2 |v|_{H^2(\tau)}.
\end{aligned}$$

Now we prove the H^1 error estimate. Notice that

$$[\partial_j (I_h v - v)](x) = \sum_i (\partial_j \lambda_i)(x) \int_0^1 t g_i''(t) dt + \sum_i \lambda_i(x) \partial_j \int_0^1 t g_i''(t) dt.$$

By (6.13),

$$\int_0^1 t g_i''(t) dt = v(a_i) - v(x) + (\nabla v)(x) \cdot (x - a_i)$$

therefore,

$$\begin{aligned}
&\partial_j \int_0^1 t g_i''(t) dt \\
&= -\partial_j v + (\nabla \partial_j v)(x)(x - a_i) + \nabla v \cdot e_j \quad (e_j \text{ is the } j\text{-th standard basis}) \\
&= (\nabla \partial_j v)(x)(x - a_i).
\end{aligned}$$

Noting that $\sum_i \lambda_i (\nabla \partial_j v)(x)(x - a_i) = 0$, we have

$$[\partial_j (I_h v - v)](x) = \sum_i (\partial_j \lambda_i)(x) \int_0^1 t g_i''(t) dt.$$

Then the estimate for $|\nabla(I_h v - v)|_{L^2(\tau)}$ follows by a similar argument and the following obvious estimate

$$|(\nabla \lambda_i)(x)| \lesssim \frac{1}{h}.$$

On the proof of Theorem 10 for $d \geq 4$, the above proof does not apply for $d \geq 4$. This is because when $d \geq 4$, the embedding relation between $H^2(\Omega) \hookrightarrow C(\bar{\Omega})$ is no longer true. Only continuous functions can have interpolations. In this case, one approach is to use the so-called Scott-Zhang interpolation [**?**], the details can be found in [**?**]. □

As a result of Theorem 9, we have

Theorem 10. *Let V_N be linear finite element space on a quasi-uniform triangulation consisting of N element. Then*

$$\inf_{v_h \in V_N} \|v - v_h\| + N^{-\frac{1}{d}} |v - v_h|_1 \lesssim N^{-\frac{2}{d}} |v|_2 \quad \forall\, v \in H^2(\Omega). \tag{6.15}$$

7

Deep Neural Network Functions

7.1 Motivation: from finite element to neural network

In this section, we will introduce the so-called shallow neural network (deep neural network with one hidden layer) from the viewpoint of finite element method.

Let us recall the linear finite element functions on the unit interval $\bar{\Omega} = [0, 1]$ in Section 6.1.2. Consider a set of equidistant girds $\mathcal{T}_\ell$ of level ℓ and mesh length $h_\ell = 2^{-\ell}$. The grid points $x_{\ell,i}$ are given by

$$x_{\ell,i} := ih_\ell, \quad 0 \le i \le 2^\ell. \tag{7.1}$$

For $\ell = 1$, we denote the special hat function by $\varphi(x)$ and any nodal basis function in (6.9) on grid $\mathcal{T}_\ell$ by $\varphi_{\ell,i}$ as below

$$\varphi(x) = \begin{cases} 2x & x \in [0, \frac{1}{2}] \\ 2(1-x) & x \in [\frac{1}{2}, 1] \\ 0, & \text{others} \end{cases}, \qquad \varphi_{\ell,i} = \varphi(\frac{x - x_{\ell,i-1}}{2h_\ell}) = \varphi(w_\ell x + b_{\ell,i}). \tag{7.2}$$

That is to say, any $\varphi_{\ell,i}(x)$ can be obtained from $\varphi(x)$ by scaling (dilation) and translation with

$$w_\ell = 2^{\ell-1}, \quad b_{\ell,i} = \frac{-(i-1)}{2}, \tag{7.3}$$

in $\varphi_{\ell,i} = \varphi(w_\ell x + b_{\ell,i})$.

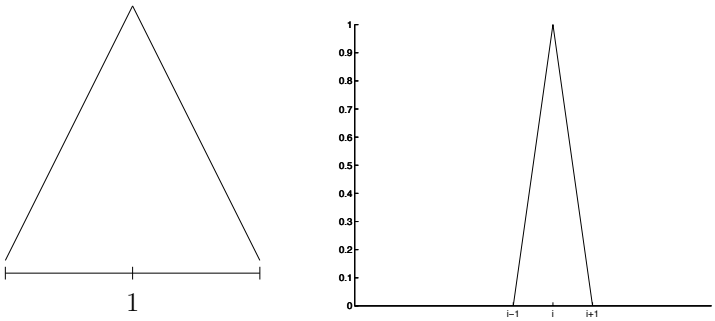

Fig. 7.1. Diagram of $\varphi(x)$ (left) and $\varphi_{\ell,i}(x)$ (right).

Let us recall the finite element interpolation in Section 6.1.2 as

$$u(x) \approx u_\ell(x) := \sum_{0\le i\le 2^\ell} u(x_{\ell,i})\varphi_{\ell,i}(x), \tag{7.4}$$

for any smooth function $u(x)$ on $(0,1)$. The above interpolation will converge as $\ell \to \infty$, which shows that

$$\text{span}\,\{\varphi(w_\ell x + b_{\ell,i})\} \quad \text{is dense in} \quad H^1(0,1). \tag{7.5}$$

Thus, we may have the next concise relation:

$$\begin{aligned} \text{FE space} =& \text{span}\left\{\varphi(w_\ell x + b_{\ell,i}) \mid 0 \le i \le 2^\ell, \ell = 1, 2, \cdots\right\} \\ \subset& \text{span}\,\{\varphi(wx+b) \mid w, b \in \mathbb{R}\}. \end{aligned} \tag{7.6}$$

In other words, the finite element space can be understood as the linear combination of $\varphi(wx+b)$ with certain special choice of w and b.

Here, we need to point out that this $\text{span}\,\{\varphi(wx+b) \mid w, b \in \mathbb{R}\}$ is exact the deep neural networks with one hidden layer (shallow neural networks) with activation function $\varphi(x)$. More precisely,

$$f \in \text{span}\,\{\varphi(wx+b) \mid w, b \in \mathbb{R}\}, \tag{7.7}$$

means there exist positive integer N and $w_j, b_j \in \mathbb{R}$ such that

$$f = \sum_{j=1}^{N} a_j \varphi(w_j x + b_j), \tag{7.8}$$

which is also called one hidden neural network function with N neurons.

Remark 3. 1. By making w_ℓ and $b_{\ell,i}$ in (7.2) arbitrary, we get a much larger class of function which is exact a special neural network with activation function $\varphi(x)$.

2. Generalizations:
   a) activation function φ can be different, such as $\mathrm{ReLU}(x) = \max\{0, x\}$.
   b) There is a natural extension for high dimension d as

$$\{\varphi(w \cdot x + b)\}, \tag{7.9}$$

where $w \in \mathbb{R}^d$, $b \in \mathbb{R}$ and $w \cdot x = \sum_{i=1}^{d} w_i x_i$. This is called "deep" neural network with one hidden layer.

7.2 Why we need deep neural networks via composition

7.2.1 FEM ans DNN_1 in 1D

Thanks to following connection between $\varphi(x)$ in (7.2) and $\mathrm{ReLU}(x) = \max(0, x) = x_+$

$$\varphi(x) = 2\mathrm{ReLU}(x) - 4\mathrm{ReLu}(x - \frac{1}{2}) + 2\mathrm{ReLU}(x - 1), \tag{7.10}$$

it suffices to show that each basis function $\varphi_{\ell,i}$ can be represented by a ReLU DNN. We first note that the basis function $\varphi_{\ell,i}$ has the support in $[x_{\ell,i-1}, x_{\ell,i+1}]$ can be easily written as

$$\varphi_{\ell,i}(x) = \frac{1}{h_\ell}\mathrm{ReLU}(x - x_{\ell,i-1}) - \frac{2}{h_\ell}\mathrm{ReLU}(x - x_{\ell,i}) + \frac{1}{h_\ell}\mathrm{ReLU}(x - x_{\ell,i+1}). \tag{7.11}$$

More generally, consider a general grid with vertex $\{x_i\}$, which is not necessarily uniform. The basis function φ_i of the linear element with support $[x_{i-1}, x_{i+1}]$ can be easily written as

$$\varphi_i(x) = \frac{1}{h_{i-1}}\mathrm{ReLU}(x - x_{i-1}) - (\frac{1}{h_{i-1}} + \frac{1}{h_i})\mathrm{ReLU}(x - x_i) + \frac{1}{h_i}\mathrm{ReLU}(x - x_{i+1}), \tag{7.12}$$

where $h_i = x_{i+1} - x_i$.

Thus is to say, we have the next theorem.

Theorem 11. *For $d = 1$, and $\Omega \subset \mathbb{R}^d$ is a bounded interval, then DNN_1 can be used to cover all linear finite element function in on Ω.*

7.2.2 Linear finite element cannot be recovered by DNN_1 for $d \geq 2$

In view of Theorem 11 and the fact that $\mathrm{DNN}_J \subseteq \mathrm{DNN}_{J+1}$, it is natural to ask that how many layers are needed at least to recover all linear finite element functions in $\mathbb{R}^d$ for $d \geq 2$. In this section, we will show that

$$J_d \geq 2, \quad \text{if} \quad d \geq 2, \tag{7.13}$$

where J_d is the minimal J such that all linear finite element functions in $\mathbb{R}^d$ can be recovered by DNN_J.

In particular, we will show the following theorem [**?**].

Theorem 12. *If $\Omega \subset \mathbb{R}^d$ is either a bounded domain or $\Omega = \mathbb{R}^d$, DNN_1 can not be used to recover all linear finite element functions on Ω.*

Proof. We prove it by contradiction. Let us assume that for any continuous piecewise linear function $f : \Omega \to \mathbb{R}$, we can find finite $N \in \mathbb{N}$, $w_i \in \mathbb{R}^{1,d}$ as row vector and $\alpha_i, b_i, \beta \in \mathbb{R}$ such that

$$f = \sum_{i=1}^{N} \alpha_i \mathrm{ReLU}(w_i \cdot x + b_i) + \beta,$$

with $f_i = \alpha_i \mathrm{ReLU}(w_i \cdot x + b_i)$, $\alpha_i \neq 0$ and $w_i \neq 0$. Consider the finite element functions, if this one hidden layer ReLU DNN can recover any basis function of FEM, then it can recover the finite element space. Thus let us assume f is a locally supported basis function for FEM. Furthermore, if Ω is a bounded domain, we assume that

$$d(\mathrm{supp}(f), \partial\Omega) > 0, \tag{7.14}$$

with

$$d(A, B) = \inf_{x \in A, y \in B} \|x - y\|,$$

as the distance of two closed sets.

A more important observation is that $\nabla f : \Omega \to \mathbb{R}^d$ is a piecewise constant vector function. The key point is to consider the discontinuous points for

$$g := \nabla f = \sum_{i=1}^{N} \nabla f_i.$$

For more general case, we can define the set of discontinuous points of a function by

$$D_g := \{x \in \Omega \mid x \text{ is a discontinuous point of } g\}.$$

Because of the property that

$$D_{f+g} \supseteq D_f \cup D_g \backslash (D_f \cap D_g), \tag{7.15}$$

we have

$$D_{\sum_{i=1}^N g_i} \supseteq \bigcup_{i=1}^{N} D_{g_i} \backslash \bigcup_{i \neq j} \left(D_{g_i} \cap D_{g_j} \right). \tag{7.16}$$

Note that

$$g_i = \nabla f_i(x) = \nabla \left(\alpha_i \mathrm{ReLU}(w_i \cdot x + b_i) \right) = \left(\alpha_i H(w_i \cdot x + b_i) \right) w_i \in \mathbb{R}^d, \tag{7.17}$$

for $i = 1 : N$ with H be the Heaviside function defined as:

$$H(x) = \begin{cases} 0 & \text{if } x \leq 0, \\ 1 & \text{if } x > 0. \end{cases}$$

This means that

$$D_{g_i} = \{x \mid w_i \cdot x + b_i = 0\} \tag{7.18}$$

is a $d-1$ dimensional affine space in $\mathbb{R}^d$.

Without loss of generality, we can assume that

$$D_{g_i} \neq D_{g_j}. \tag{7.19}$$

When the other case occurs, i.e. $D_{g_{\ell_1}} = D_{g_{\ell_2}} = \cdots = D_{g_{\ell_k}}$, by the definition of g_i in (7.17) and D_{g_i} in (7.18) , this happens if and only if there is a row vector (w, b) such that

$$c_{\ell_i}\begin{pmatrix} w & b \end{pmatrix} = \begin{pmatrix} w_{\ell_i} & b_{\ell_i} \end{pmatrix}, \tag{7.20}$$

with some $c_{\ell_i} \neq 0$ for $i = 1 : k$. We combine those g_{ℓ_i} as

$$\begin{aligned}
\tilde{g}_\ell &= \sum_{i=1}^{k} g_{\ell_i} = \sum_{i=1}^{k} \alpha_{\ell_i} H(w_{\ell_i} \cdot x + b_{\ell_i}) w_{\ell_i}, \\
&= \sum_{i=1}^{k} \left(c_{\ell_i}\alpha_{\ell_i} H\left(c_{\ell_i}(w \cdot x + b)\right)\right) w, \\
&= \begin{cases} \left(\left(\sum_{i=1}^{k} c_{\ell_i}\alpha_{\ell_i} H(c_{\ell_i})\right) w & \text{if} \quad wx + b > 0, \\ \left(\left(\sum_{i=1}^{k} c_{\ell_i}\alpha_{\ell_i} H(-c_{\ell_i})\right) w & \text{if} \quad wx + b \leq 0. \end{cases}
\end{aligned}$$

Thus, if

$$\left(\sum_{i=1}^{k} c_{\ell_i}\alpha_{\ell_i} H(c_{\ell_i})\right) = \left(\sum_{i=1}^{k} c_{\ell_i}\alpha_{\ell_i} H(-c_{\ell_i})\right),$$

$\tilde{g}_\ell$ is a constant vector function, that is to say $D_{\sum_{i=1}^{k} g_{\ell_i}} = D_{\tilde{g}_\ell} = \emptyset$. Otherwise, $\tilde{g}_\ell$ is a piecewise constant vector function with the property that

$$D_{\sum_{i=1}^{k} g_{\ell_i}} = D_{\tilde{g}_\ell} = D_{g_{\ell_i}} = \{x \mid w \cdot x + b = 0\}.$$

This means that we can use condition (7.20) as an equivalence relation and split $\{g_i\}_{i=1}^{N}$ into some groups, and we can combine those g_{ℓ_i} in each group as what we do above. After that, we have

$$\sum_{i=1}^{N} g_i = \sum_{\ell=1}^{\tilde{N}} \tilde{g}_\ell,$$

with $D_{\tilde{g}_s} \neq D_{\tilde{g}_t}$. Finally, we can have that $D_{\tilde{g}_s} \cap D_{\tilde{g}_t}$ is an empty set or a $d-2$ dimensional affine space in $\mathbb{R}^d$. Since $\tilde{N} \leq N$ is a finite number,

$$D := \bigcup_{i=1}^{N} D_{\tilde{g}_\ell} \setminus \bigcup_{s \neq t} \left(D_{\tilde{g}_s} \cap D_{\tilde{g}_t}\right)$$

is an unbounded set.

- If $\Omega = \mathbb{R}^d$,
$$\text{supp(f)} \supseteq D_g = D_{\sum_{i=1}^N g_i} = D_{\sum_{\ell=1}^{\tilde{N}} \tilde{g}_\ell} \supseteq D,$$
is contradictory to the assumption that f is locally supported.
- If Ω is a bounded domain,
$$d(D, \partial\Omega) = \begin{cases} s > 0 & \text{if} \quad D_{\tilde{g}_i} \cap \Omega = \emptyset, \forall i \\ 0 & \text{otherwise.} \end{cases}$$
Note again that all $D_{\tilde{g}_i}$'s are $d-1$ dimensional affine spaces, while $D_{\tilde{g}_i} \cap D_{\tilde{g}_j}$ is either an empty set or a d-2 dimensional affine space. If $d(D, \partial\Omega) > 0$, this implies that ∇f is continuous in Ω, which contradicts the assumption that f is a basis function in FEM. If $d(D, \partial\Omega) = 0$, this contradicts the previous assumption in (7.14).

Hence DNN_1 cannot recover any piecewise linear function in Ω for $d \geq 2$. □

Following the proof above, we have the following theorem [**?**].

Theorem 13. *$\{\text{ReLU}(w_i \cdot x + b_i)\}_{i=1}^m$ are linearly independent if (w_i, b_i) and (w_j, b_j) are linearly independent in $\mathbb{R}^{1\times(d+1)}$ for any $i \neq j$.*

7.3 Definition of deep neural networks (DNN)

In this section, we will give a brief introduction to a special function class related to deep neural networks (DNN) used in machine learning. We then explore the relationship between DNN (with ReLU as activation function) and linear finite element methods.

Given $n, m \geq 1$, the first ingredient in defining a deep neural network (DNN) is (vector) linear functions of the form

$$\theta : \mathbb{R}^n \to \mathbb{R}^m, \tag{7.21}$$

as $\theta(x) = Wx + b$ where $W = (w_{ij}) \in \mathbb{R}^{m\times n}$, $b \in \mathbb{R}^m$. The second main ingredient is a nonlinear activation function, usually denoted as

$$\sigma : \mathbb{R} \to \mathbb{R}. \tag{7.22}$$

By applying the function to each component, we can extend this naturally to

$$\sigma : \mathbb{R}^n \mapsto \mathbb{R}^n.$$

7.3.1 Definition of neurons

1. Primary variables $n_0 = d$
$$x^0 = x = \begin{pmatrix} x_1 \\ x_2 \\ \vdots \\ x_d \end{pmatrix}$$

2. n_1 hyperplanes $\theta^0(x^0) = W^0x + b^0$ where $W^0 : \mathbb{R}^d \mapsto \mathbb{R}^{n_1}$:

$$W^0x + b^0 = \begin{pmatrix} w_1^0x + b_1^0 \\ w_2^0x + b_2^0 \\ \vdots \\ w_{n_1}^0x + b_{n_1}^0 \end{pmatrix} \quad \text{with} \quad W^0 = \begin{pmatrix} w_1^0 \\ w_2^0 \\ \vdots \\ w_{n_1}^0 \end{pmatrix}, \quad b^0 = \begin{pmatrix} b_1^0 \\ b_2^0 \\ \vdots \\ b_{n_1}^0 \end{pmatrix}$$

3. n_1-neurons:

$$x^1 = \sigma(W^0x + b^0) = \begin{pmatrix} \sigma(w_1^0x + b_1^0) \\ \sigma(w_2^0x + b_2^0) \\ \vdots \\ \sigma(w_{n_1}^0x + b_{n_1}^0) \end{pmatrix}$$

4. n_2-hyperplanes $\theta^1(x^1) = W^1x + b^1$ where $W^1 : \mathbb{R}^{n_1} \mapsto \mathbb{R}^{n_2}$:

$$W^1x^1 + b^1 = \begin{pmatrix} w_1^1x^1 + b_1^1 \\ w_2^1x^1 + b_2^1 \\ \vdots \\ w_{n_2}^1x^1 + b_{n_2}^1 \end{pmatrix} \quad \text{with} \quad W^1 = \begin{pmatrix} w_1^1 \\ w_2^1 \\ \vdots \\ w_{n_2}^1 \end{pmatrix}, \; b^1 = \begin{pmatrix} b_1^1 \\ b_2^1 \\ \vdots \\ b_{n_2}^1 \end{pmatrix}$$

5. n_2-neurons:

$$x^2 = \sigma(W^1x + b^1) = \begin{pmatrix} \sigma(w_1^1x + b_1^1) \\ \sigma(w_2^1x + b_2^1) \\ \vdots \\ \sigma(w_{n_2}^1x + b_{n_2}^1) \end{pmatrix}$$

6. $\cdots$

7.3.2 Definition of deep neural network functions

Given $d, k \in \mathbb{N}^+$ and

$$n_1, \ldots, n_k \in \mathbb{N} \text{ with } n_0 = d, n_{k+1} = 1,$$

a general DNN function from $\mathbb{R}^d$ to $\mathbb{R}$ is given by

$$\begin{aligned} f^0(x) &= \theta^0(x) \\ f^\ell(x) &= [\theta^\ell \circ \sigma](f^{\ell-1}(x)) \quad \ell = 1 : k \\ f(x) &= f^k(x). \end{aligned}$$

The following more concise notation is often used in computer science literature:

$$f(x) = \theta^k \circ \sigma \circ \theta^{k-1} \circ \sigma \cdots \circ \theta^1 \circ \sigma \circ \theta^0(x), \tag{7.23}$$

here $\theta^i : \mathbb{R}^{n_i} \to \mathbb{R}^{n_{i+1}}$ are linear functions as defined in (7.21). Such a DNN is called a $(k+1)$-layer DNN, and is said to have k-hidden layers. The size of this DNN is $n_1 + \cdots + n_k$.

Thus, we have the following connection of neurons and DNN functions

$$f^k(x) = \theta^k(x^k) = \theta^k \circ \sigma \circ \theta^{k-1}(x^{k-1}) = [\theta^k \circ \sigma](f^{k-1}),$$

or we can see that

$$x^k = \sigma(f^{k-1}) = \sigma \circ \theta^{k-1} \circ \sigma(f^{k-2}) = [\sigma \circ \theta^{k-1}](x^{k-1}).$$

Based on these notation and connections, we have the following definition of general artificial neural network functions.

Shallow (one hidden layer) neural network functions:

(7.24)

$$_n\mathrm{N}(\sigma; n_1) = \left\{ f^1(x) = \theta^1(x^1), \text{ with } W^\ell \in \mathbb{R}^{n_{\ell+1}\times n_\ell}, b^\ell \in \mathbb{R}^{n_\ell}, \ell = 0, 1, n_0 = d, n_2 = 1 \right\}$$

Deep neural network functions:

(7.25)

$$_n\mathrm{N}(\sigma; n_1, n_2, \ldots, n_L) = \left\{ f^L(x) = \theta^L(x^L), \text{ with } W^\ell \in \mathbb{R}^{n_{\ell+1}\times n_\ell}, b^\ell \in \mathbb{R}^{n_\ell}, \ell = 0 : L, n_0 = d, n_{L+1} = 1 \right\}$$

If we ignore the width (number of neurons) of network functions, we may denote the general deep neural network functions with certain layers.

The 1-hidden layer (shallow) neural network is defined as:

$$_n\mathrm{N} = {}_n\mathrm{N}(\sigma) = {}_n\mathrm{N}^1(\sigma) = \bigcup_{n_1 \geq 1} {}_n\mathrm{N}(\sigma; n_1, 1) \tag{7.26}$$

Generally, we can define the L-hidden layer neural network as:

$$_n\mathrm{N}^L(\sigma) := \bigcup_{n_1, n_2, \cdots, n_L \geq 1} {}_n\mathrm{N}(\sigma; n_1, n_2, \cdots, n_L, 1). \tag{7.27}$$

7.3.3 ReLU DNN

In this section, we mainly consider a special activation function, known as the *rectified linear unit* (ReLU), and defined as $\mathrm{ReLU} : \mathbb{R} \mapsto \mathbb{R}$,

$$\mathrm{ReLU}(x) := \max(0, x), \quad x \in \mathbb{R}. \tag{7.28}$$

A ReLU DNN with k hidden layers might be written as:

$$f(x) = \theta^k \circ \mathrm{ReLU} \circ \theta^{k-1} \circ \mathrm{ReLU} \cdots \circ \theta^1 \circ \mathrm{ReLU} \circ \theta^0(x). \tag{7.29}$$

We note that ReLU is a continuous piecewise linear (CPWL) function. Since the composition of two CPWL functions is still a CPWL function, we have the following observation [**?**].

Lemma 20. *Every ReLU DNN: $\mathbb{R}^d \to \mathbb{R}^c$ is a continuous piecewise linear function. More specifically, given any ReLU DNN, there is a polyhedral decomposition of $\mathbb{R}^d$ such that this ReLU DNN is linear on each polyhedron in such a decomposition.*

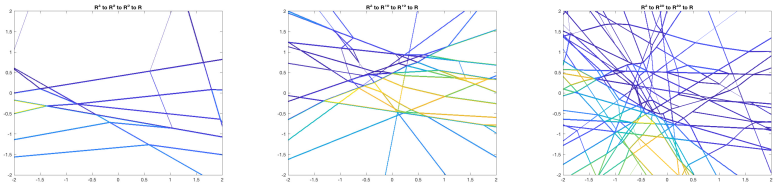

Fig. 7.2. Projections of the domain partitions formed by 2-layer ReLU DNNs with sizes $(n_0, n_1, n_2, n_3) = (2, 5, 5, 1), (2, 10, 10, 1)$and $(2, 20, 20, 1)$ with random parameters.

Here is a simple example for the "grid" created by some 2-layer ReLU DNNs in $\mathbb{R}^2$.

For convenience of exposition, we introduce the following notation: Namely ${}_n\mathrm{N}^L(\sigma)$ represents the DNN model with L hidden layers and ReLU activation function with arbitrary size, if $\sigma = \mathrm{ReLU}$.

7.3.4 Fourier transform of polynomials

We begin by noting that an activation function σ, which satisfies a polynomial growth condition $|\sigma(x)| \leq C(1 + |x|)^n$ for some constants C and n, is a tempered distribution. As a result, we make this assumption on our activation functions in the following theorems. We briefly note that this condition is sufficient, but not necessary (for instance an integrable function need not satisfy a pointwise polynomial growth bound) for σ to be represent a tempered distribution.

We begin by studying the convolution of σ with a Gaussian mollifier. Let η be a Gaussian mollifier

$$\eta(x) = \frac{1}{\sqrt{\pi}} e^{-x^2}. \tag{7.30}$$

Set $\eta_\epsilon = \frac{1}{\epsilon}\eta(\frac{x}{\epsilon})$. Then consider

$$\sigma_\epsilon(x) := \sigma * \eta_\epsilon(x) = \int_{\mathbb{R}} \sigma(x - y)\eta_\epsilon(y)dy \tag{7.31}$$

for a given activation function σ. It is clear that $\sigma_\epsilon \in C^\infty(\mathbb{R})$. Moreover, by considering the Fourier transform (as a tempered distribution) we see that

$$\hat{\sigma}_\epsilon = \hat{\sigma}\hat{\eta}_\epsilon = \hat{\sigma}\eta_{\epsilon^{-1}}. \tag{7.32}$$

We begin by stating a lemma which characterizes the set of polynomials in terms of their Fourier transform.

Lemma 21. *Given a tempered distribution σ, the following statements are equivalent:*

1. *σ is a polynomial*

2. σ_ϵ *given by* (7.31) *is a polynomial for any* $\epsilon > 0$.
3. $\text{supp}(\hat{\sigma}) \subset \{0\}$.

Proof. We begin by proving that (3) and (1) are equivalent. This follows from a characterization of distributions supported at a single point (see [**?**], section 6.3). In particular, a distribution supported at 0 must be a finite linear combination of Dirac masses and their derivatives. In particular, if $\hat{\sigma}$ is supported at 0, then

$$\hat{\sigma} = \sum_{i=1}^{n} a_i \delta^{(i)}. \tag{7.33}$$

Taking the inverse Fourier transform and noting that the inverse Fourier transform of $\delta^{(i)}$ is $c_i x^i$, we see that σ is a polynomial. This shows that (3) implies (1), for the converse we simply take the Fourier transform of a polynomial and note that it is a finite linear combination of Dirac masses and their derivatives.

Finally, we prove the equivalence of (2) and (3). For this it suffices to show that $\hat{\sigma}$ is supported at 0 iff $\hat{\sigma}_\epsilon$ is supported at 0. This follows from equation 7.32 and the fact that $\eta_{\epsilon^{-1}}$ is nowhere vanishing. □

As an application of Lemma 21, we give a simple proof of the result in the next section.

8

Convolutional Multigrid Method

8.1 Two-point boundary problems and finite element discretization

Denote the functional space

$$V := H_0^1(0,1) = \{v : [0,1] \to R,\ v \text{ is continuous and } v(0) = v(1) = 0\}.$$

Given any $f : [0,1] \to R$, consider

$$J(v) = \frac{1}{2}\int_0^1 |v'|^2 dx - \int_0^1 fv dx.$$

Find $u \in V$ such that

$$u = \arg\min_{v \in V} J(v) \tag{8.1}$$

Theorem 14. *Problem* (8.1) *is equivalent to: Find $u \in V$ such that*

$$\begin{cases} -u'' = f,\ 0 < x < 1, \\ u(0) = u(1) = 0. \end{cases} \tag{8.2}$$

Proof. For any $v \in V, t \in R$, let $g(t) = J(u + tv)$. Since $u = \arg\min_{v \in V} J(v)$ means $g(t) \geq g(0)$. Hence, for any $v \in V$, 0 is the global minimum of the function $g(t)$. Therefore $g'(0) = 0$ implies

$$\int_0^1 u'v' dx = \int_0^1 fv dx \quad \forall v \in V.$$

By integration by parts, which is equivalent to

$$\int_0^1 (-u'' - f)v dx = 0 \quad \forall v \in V.$$

It can be proved that the above identity holds if and only if $-u'' = f$ for all $x \in (0,1)$. Namely u satisfies (8.2). □

Let V_h be finite element space and $\{\varphi_1, \varphi_2, \cdots \varphi_n\}$ be a nodal basis of V_h.

$$J(v_h) = \frac{1}{2}\int_0^1 |v_h'|^2 dx - \int_0^1 f v_h dx. \tag{8.3}$$

Let

$$v_h = \sum_{i=1}^n v_i \varphi_i, \quad v = (v_i)_{i=1}^n$$

then using the convolution notation, we have

$$J(v_h) = I(v) = \frac{1}{2} v^T A * v - b^T v$$

and

$$\nabla I(v) = A * v - b,$$

where $A = \frac{1}{h}[-1, 2, -1]$.

At the same time, let $u_h = \sum_{i=1}^n \mu_i \varphi_i$,

$$u_h = \arg\min_{v_h \in V_h} J(v_h) \Leftrightarrow \mu = \arg\min_{v \in R^n} I(v) \tag{8.4}$$

And u_h solves the problem: Find $u_h \in V_h$

$$\frac{d}{dt} J(u_h + t v_h)|_{t=0} = a(u_h, v_h) - \langle f, v_h \rangle = 0 \quad \forall v_h \in V_h. \tag{8.5}$$

where

$$a(u_h, v_h) = \int_0^1 u_h' v_h' dx.$$

Theorem 15. *Let V be a Hilbert space, $a(\cdot,\cdot)$ be a continuous, symmetric, bilinear form defining an inner product on V. Let $f(\cdot)$ be a continuous linear form. If u is solution to the problem (8.1) and u_h is a solution to (8.4), then the following equality holds:*

$$\|u - u_h\|_a = \inf_{v \in V_h} \|u - v\|_a, \tag{8.6}$$

where $\|u - u_h\|_a^2 = a(u - u_h, u - u_h)$.

Proof. Frist, one sees that

$$a(u - u_h, v) = 0, \quad \forall v \in V_h.$$

Thus, for any $v \in V_h$ we have

$$\|u-u_h\|_a^2 = a(u-u_h, u-u_h)$$

$$= a(u-u_h, u-v)$$

$$\leq \|u-u_h\|_a \|u-v\|_a.$$

Taking the infimum on both sides of this equation then gives.

$$\|u-u_h\|_a \leq \inf_{v\in V_h} \|u-v\|_a.$$

The proof is complete, since

$$\|u-u_h\|_a \geq \inf_{v\in V_h} \|u-v\|_a,$$

by the definition of infimum. □

Combining Theorem 9 and Theorem 15, we obtain the error estimate for the finite element method.

Theorem 16. *If $u \in H^2(\Omega)$ is solution to the problem (8.2) and u_h is a solution to (8.4), then we have:*

$$\|u-u_h\| + h|u-u_h|_1 \lesssim h^2|u|_2. \tag{8.7}$$

8.1.1 Gradient descent method

Using the convolution notation (8.42), we consider

$$J(v_h) = I(v) = \frac{1}{2} v^T A * v - b^T v$$

and

$$\nabla I(v) = A * v - b,$$

where $A = \frac{1}{h}[-1, 2, -1]$.

At the same time, let $u_h = \sum_{i=1}^{n} \mu_i \varphi_i$,

$$u_h = \arg\min_{v_h\in V_h} J(v_h) \Leftrightarrow \mu = \arg\min_{v\in R^n} I(v) \tag{8.8}$$

Noting that $\nabla I(v) = A * v - b$ and applying the gradient descent method to solve problem (8.8), we obtain

$$\mu^{(m)} = \mu^{(m-1)} - \eta(A * \mu^{(m-1)} - b), \quad m = 1, \cdots, \nu.$$

After ν iterations of gradient descent method, we denote the solution as u_h^ν.

Consider the finite element discretization of Poisson equation in 1D: One very simple iterative method for (8.8) is the following gradient descent method

$$\mu^{(m)} = \mu^{(m-1)} + \eta(b - A * \mu^{(m-1)}),$$

or, for $j = 1 : N$,

$$\mu_j^{(m)} = \mu_j^{(m-1)} + \eta\Big(\beta_j - \frac{-\mu_{j-1}^{(m-1)} + 2\mu_j^{(m-1)} - \mu_{j+1}^{(m-1)}}{h}\Big),$$

where $\eta > 0$ is a positive parameter named learning rate.

It is not so difficult to properly choose η so that the above iterative scheme converges, namely for any initial guess μ^0, the sequence $(\mu^{(m)})$ generated by the above iteration converges to the exact solution μ of (8.8).

Note that

$$\mu = \mu + \eta(b - A * \mu),$$

we get

$$\mu - \mu^{(m)} = (I - \eta A*)(\mu - \mu^{(m-1)}),$$

or

$$\mu - \mu^{(m)} = (I - \eta A*)^m(\mu - \mu^0), m = 1, 2, 3, \cdots$$

As we known,

$$(I - \eta A*)^m \longrightarrow 0$$

if and only if $\rho(I - \eta A*) < 1$. Here $\rho(B)$ is the spectral radius of B. However, $\rho(I - \eta A*) < 1$ if and only if

$$0 < \text{all the eigenvalue of } A* < 2\eta^{-1}.$$

Thus, a necessary and sufficient condition for the convergence is the following

$$0 < \eta < \frac{2}{\rho(A*)}.$$

It is easy to see that (for example, $4/h$ is an upper bound of its row sums)

$$\frac{4}{h} > \rho(A*).$$

Therefore it is reasonable to make the following choice

$$\eta = \frac{h}{4}$$

and the resulting algorithm is

$$\mu^{(m)} = \mu^{(m-1)} + \frac{h}{4}(b - A * \mu^{(m-1)}). \tag{8.9}$$

In the rest of this section, unless otherwise noted, we shall choose η as above for simplicity.

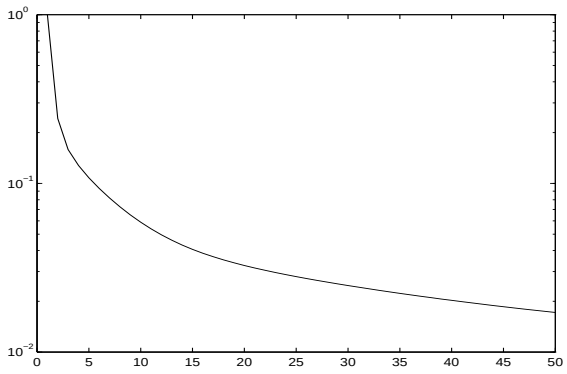

Fig. 8.1. A picture on the GD method convergence history

On Figure 8.1 the convergence history plot of the above gradient descent iterative method for typical application is shown. As we see, this iterative scheme converges very slowly.

Our main goal is to find a way to speed up such kind of rather slowly convergent iterative scheme. To do that, we need to study its convergent property in more microscopic level. First of all, let us now take a careful look at the convergence history picture and make the following observation:

> *Observation 1.* The scheme converges rather fast in the very beginning but then slows down after a few steps. Overall, the method converges very slowly.

To further understand this phenomenon, let us plot the detailed pictures of the error functions in the first few iterations. After a careful look at these pictures, we have the following observation:

> *Observation 2.* The scheme not only converges fast in the first few steps, but also smooth out the error function very quickly.

In other words, the error function becomes a much smoother function after a few such simple iterations. This property of the iterative scheme is naturally called *a smoothing property* and an iterative scheme having this smoothing property is called a *smoother*.

The above two observations, especially the second one, concern the most important property of the simple gradient descent method that we can take advantage to get a much faster algorithm.

The gradient descent method can be written in terms of $S_0 : \mathbb{R}^N \to \mathbb{R}^N$ satisfying

$$\mu^{(1)} = (S_0 b) = \frac{h}{4} b, \tag{8.10}$$

for equation (8.8) with initial guess zero. If we apply this method twice, then

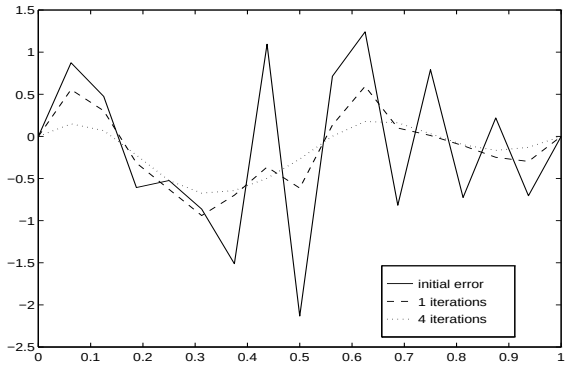

Fig. 8.2. The smoothing effect of the gradient descent method

$$\mu^{(2)} = S_1(b) = S_0 b + S_0(b - A * (S_0 b)),$$

with element-wise form

$$\mu_i^{(2)} = \frac{h}{16}(b_{i-1} + 6b_i + b_{i+1}). \tag{8.11}$$

Then by the definition of convolution (8.42), we have

$$\mu^{(1)} = S_0 * b \quad \mu^{(2)} = S_1 * b. \tag{8.12}$$

with

$$S_0 = \frac{h}{4}, \tag{8.13}$$

and

$$S_1 = \frac{h}{16}[1, 6, 1]. \tag{8.14}$$

Hence we denote S_0 or S_1 as S.
Now for any given $\mu^{(0)} = \tilde{\mu}^{(0)}$,

$$\begin{aligned} &m = 1, 2, \cdots, 2\nu \\ &\mu^{(m)} = \mu^{(m-1)} + S_0 * (b - A * \mu^{(m-1)}) \end{aligned} \tag{8.15}$$

$$\Leftrightarrow$$

$$\begin{aligned} &m = 1, 2, \cdots, \nu \\ &\tilde{\mu}^{(m)} = \tilde{\mu}^{(m-1)} + S_1 * (b - A * \tilde{\mu}^{(m-1)}) \end{aligned} \tag{8.16}$$

we obtain $\mu^{(2\nu)} = \tilde{\mu}^{(\nu)}$ which means one step S_1 is equivalent to two steps of S_0.

Convergence and smoothing properties of GD

Because of the extraordinary importance of this smoothing property, we shall now try to give some simple theoretical analysis. To do this, we make use of the eigenvalues and eigenvectors of the matrix A.

Fourier analysis for the gradient descent method

Our earlier numerical experiments indicate that the gradient descent method has a smoothing property. Based on our understanding of the relation between the smoothness and the size of Fourier coefficients, we can imagine that this smoothing property can be analyzed using the discrete Fourier expansion.

Let μ be the exact solution of (8.8) and $\mu^{(m)}$ the result of $m-th$ iteration from the gradient descent method (8.9). Then

$$\mu - \mu^{(m)} = (1 - \eta A*)(\mu - \mu^{(m-1)}) = \ldots = (1 - \eta A*)^m(\mu - \mu^{(0)}).$$

Consider the Fourier expansion of the initial error:

$$\mu - \mu^{(0)} = \sum_{k=1}^{N} \alpha_k \xi^k.$$

Then

$$\mu - \mu^{(m)} = \sum_{k=1}^{N} \alpha_k (I - \eta A*)^m \xi^k.$$

Note that $\eta = h/4$ and for any polynomial p

$$p(A*)\xi^k = p(\lambda_k)\xi^k,$$

we get

$$\mu - \mu^{(m)} = \sum_{k=1}^{N} \alpha_k (1 - \eta\lambda_k)^m \xi^k = \sum_{k=1}^{N} \alpha_k^{(m)} \xi^k$$

where

$$\alpha_k^{(m)} = \left(1 - \sin^2 \frac{k\pi}{2(N+1)}\right)^m \alpha_k.$$

For k close to N, for example $k = N$, note that

$$1 - \sin^2 \frac{N\pi}{2(N+1)} = \cos^2 \frac{N\pi}{2(N+1)} = \sin^2(\frac{\pi}{2} - \frac{N\pi}{2(N+1)})$$

implies

$$|\alpha_N^{(m)}| = |\alpha_N| \sin^{2m} \frac{N+1-N}{N+1}\frac{\pi}{2} \leq |\alpha_k| \left(\frac{1}{N+1}\frac{\pi}{2}\right)^{2m}$$

which approaches to 0 very rapidly when $m \to \infty$. This means that high frequency components get damped very quickly.

However, for k far away from N, for example $k = 1$, note that

$$\sin^2 \frac{\pi}{2(N+1)} \leq \left(\frac{\pi}{2(N+1)}\right)^2$$

implies

$$|\alpha_1^{(m)}| = |\alpha_1|\left(1 - \sin^2 \frac{\pi}{2(N+1)}\right)^m \geq |\alpha_1|\left(1 - \left(\frac{\pi}{2(N+1)}\right)^2\right)^m$$

which approaches to 0 very slowly when $m \to \infty$.

This simple analysis clearly justifies the smoothing property that has been observed by numerical experiments.

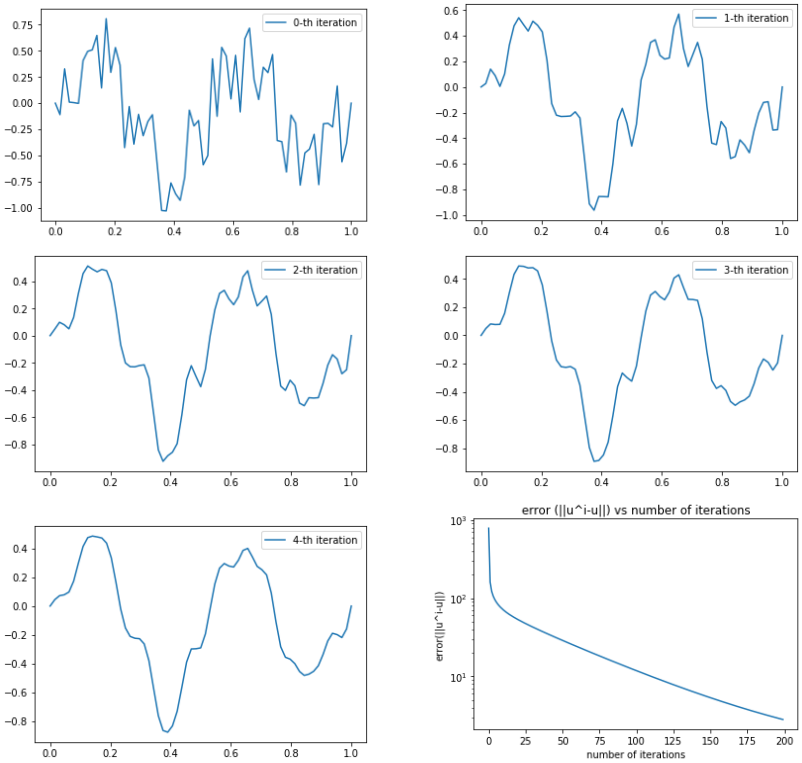

Fig. 8.3. $u - u^0$, $u - u^1$, $u - u^2$, $u - u^3$, $u - u^4$

An intuitive discussion

The gradient descent method is oftentimes called *local relaxation* methods. This name refers to the fact that what that algorithm does is just trying to correct the

residual vector locally at one nodal point at a time (recall that $\mu_j \approx u(x_j)$). This local relaxation procedure is then effective to the error components that are local in nature. Incidentally, the nonsmooth or high frequency component which oscillates across one or few grid points have a strong local feature. Therefore, it is not surprising the gradient descent iteration can damp out these nonsmooth components more easily. This method is very inefficient for relatively smoother components in the error since a smoother function is more globally related in nature.

8.1.2 Coarse grid correction and two grid method

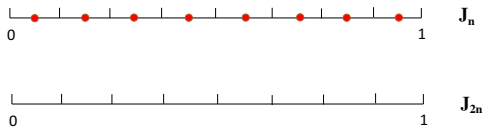

Fig. 8.4. Two level grids.

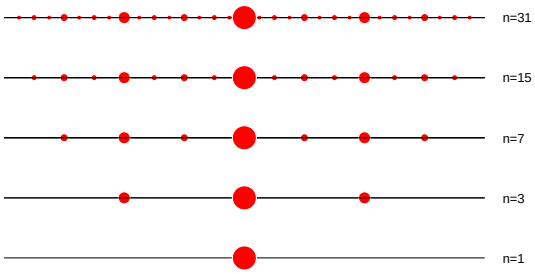

Fig. 8.5. Multiple grids in one dimension

As we discussed earlier, although gradient descent iteration usually converges very slowly, it does quickly smooth out the rough component in the error. In other words, the error becomes smooth after a few gradient descent iterations on a fine grid, but looks rough when viewed on a coarser grid. Hence, a few gradient descent iterations can further reduce the error on the coarse grid. The main idea of two grid method or multigrid method is to use the fact that a smooth function can be well approximated on a coarser grid.

In summery, we can write the two grid method in terms of finite element (FE) functions as follows:

Algorithm 7 A two grid method (in terms of FE functions)

Input u^0.

Step 1: Apply ν_1-times gradient descent iterations for

$$\min_{v^1 \in V_1} J(v^1)$$

with initial guess u^0 to obtain $u^1 \in V_1$.

Step 2: Apply ν_2-times gradient descent iterations for

$$\min_{v^2 \in V_2} J(u^1 + v^2)$$

with zero initial guess to obtain $u^2 \in V_2$.

Step 3: Update: $u = u^1 + u^2$.

Realization of step 1:

Step 1: Given $u^{1,0} \in V_1$, apply ν_1-times gradient descent method for

$$\min_{v^1 \in V_1} J(v^1)$$

with initial guess $u^{1,0}$ to obtain $u^1 \in V_1$.

Let $u^{1,0} = \sum_{i=1}^{n_1} \mu_i^0 \phi_i^1, \quad v^1 = \sum_{i=1}^{n_1} v_i^1 \phi_i^1, \quad \mu^0 = \{\mu_i^0\}_{i=1}^{n_1}, \quad v^1 = \{v_i^1\}_{i=1}^{n_1},$
where $\phi^1 = (\phi_1^1, \phi_2^1, \cdots, \phi_{n_1}^1)$ is the nodal basis of V_1.
Namely, $b^1 = b, \mu^1 \leftarrow \mu^0$, for $i = 1 : \nu_2$

$$\mu^1 \leftarrow \mu^1 - \eta_1(A_1 * \mu^1 - b^1).$$

After ν_1 iterations, we obtain updated μ^1 and $u^1 = \sum_{i=1}^{n_1} \mu_i^1 \phi_i^1$.

Realization of step 2:

Step 2: Apply ν_2-times gradient descent iterations for

$$\min_{v^2 \in V_2} J(u^1 + v^2)$$

with zero initial guess to obtain $u^2 \in V_2$.

Let

$$u^1 = \sum_{i=1}^{n_1} \mu_i^1 \phi_i^1, \; v^2 = \sum_{i}^{n_2} v_i^2 \phi_i^2, \; \mu^1 = \{\mu_i^1\}_{i=1}^{n_1}, \; v^2 = \{v_i^2\}_{i=1}^{n_2}.$$

We have

$$\begin{aligned} J(u^1 + v^2) &= \frac{1}{2}\int_0^1 |(u^1 + v^2)'|^2 dx - \int_0^1 f(u^1 + v^2) dx \\ &= J(u^1) + J(v^2) + \int_0^1 (u^1)'(v^2)' dx \\ &= \frac{1}{2}(\mu^1)^T A_1 * \mu^1 + \frac{1}{2}(v^2)^T A_2 * v^2 - (v^2)^T r^2 \end{aligned} \tag{8.17}$$

where

$$r_i^2 = \int_0^1 f\phi_i^2 - (u^1)'(\phi_i^2)' dx = (f, \phi_i^2) - a(u^1, \phi_i^2). \tag{8.18}$$

Now noting that

$$\phi_i^2 = \frac{1}{2}\phi_{2i-1}^1 + \phi_{2i}^1 + \frac{1}{2}\phi_{2i+1}^1, \tag{8.19}$$

Let $\phi^2 = \{\phi_i^2\}_{i=1}^{n_2}, \phi^1 = \{\phi_i^1\}_{i=1}^{n_1}$. Using the convolution with stride notation, we obtain

$$\phi^2 = R *_2 \phi^1 \tag{8.20}$$

with $R = [\frac{1}{2}, 1, \frac{1}{2}]$. Furthermore,

$$\begin{aligned} r_i^2 &= (f, \frac{1}{2}\phi_{2i-1}^1 + \phi_{2i}^1 + \frac{1}{2}\phi_{2i+1}^1) - a(u^1, \frac{1}{2}\phi_{2i-1}^1 + \phi_{2i}^1 + \frac{1}{2}\phi_{2i+1}^1) \\ &= \frac{1}{2}b_{2i-1}^1 + b_{2i}^1 + \frac{1}{2}b_{2i+1}^1 - \Big(\frac{1}{2}(A_1 * \mu^1)_{2i-1} + (A_1 * \mu^1)_{2i} + \frac{1}{2}(A_1 * \mu^1)_{2i+1}\Big) \\ &= \frac{1}{2}(b^1 - A_1 * \mu^1)_{2i-1} + (b^1 - A_1 * \mu^1)_{2i} + \frac{1}{2}(b^1 - A_1 * \mu^1)_{2i+1} \\ &= \frac{1}{2}r_{2i-1}^1 + r_{2i}^1 + \frac{1}{2}r_{2i+1}^1, \end{aligned} \tag{8.21}$$

where $r^1 = b^1 - A_1 * \mu^1$.

Lemma 22. *Using the convolution with stride notation, we have*

$$r^2 = R *_2 r^1$$

with $R = [\frac{1}{2}, 1, \frac{1}{2}]$.

Therefore applying gradient descent method ν_2-times for (8.17) reads:

$r^1 = b^1 - A_1 * \mu^1, r^2 = R *_2 r^1, \mu^2 \leftarrow 0$, for $i = 1 : \nu_2$

$$\mu^2 \leftarrow \mu^2 - \eta_2(A_2 * \mu^2 - r^2). \tag{8.22}$$

After ν_2 iterations, we obtain updated μ^2 and $u^2 = \sum_{i=1}^{n_2} \mu_i^2 \phi_i^2$.

Realization of step 3:

Step 3: $u = u^1 + u^2$.

Let $\mu^2 = \{\mu_i^2\}_{i=1}^{n_2}, \phi^2 = \{\phi_i^2\}_{i=1}^{n_2}$. Therefore $u^2 = \sum_{i=1}^{n_2} \mu_i^2 \phi_i^2 = (\mu^2, \phi^2)_{l^2}$ and by (8.20) we have

$$\begin{aligned} u^2 &= (\mu^2, \phi^2)_{l^2} = (\mu^2, R *_2 \phi^1)_{l^2} = (R *_2^\top \mu^2, \phi^1)_{l^2} \\ &= \sum_{i=1}^{n_1} \Big(R *_2^\top \mu^2\Big)_i \phi_i^1 \end{aligned} \tag{8.23}$$

with $R = [\frac{1}{2}, 1, \frac{1}{2}]$.

Lemma 23. *The prolongation can be written as* $R *_2^T : \mathbb{R}^{n_2} \to \mathbb{R}^{n_1}$, *for* $\mu^2 \in \mathbb{R}^{n_2}$, $(R *_2^T \mu^2) \in R^{n_1}$ *with*

$$(R *_2^T \mu^2)_{2i} = \mu_i^2 \quad (R *_2^T \mu^2)_{2i+1} = \frac{1}{2}(\mu_{i+1}^2 + \mu_i^2).$$

Noting that $u^1 = \sum_{i=1}^{n_1} \mu_i^1 \phi_i^1$, $\mu^1 = \{\mu_i^1\}_{i=1}^{n_1}$, we obtain

$$\mu = \mu^1 + R *_2^T \mu^2 \quad \text{and} \quad u = u^1 + u^2.$$

Next we show how to realize the Algorithm 7 in vector and convolution form.

Algorithm 8 A two grid algorithm $\mu = 2G1(b; \mu^0; 2, \nu_1, \nu_2)$

Set up

$$b^1 = b, \quad \mu^1 = \mu^0.$$

Step 1: Smoothing and restriction from fine to coarse level (nested)
for $i = 1 : \nu_1$ **do**

$$\mu^1 \leftarrow \mu^1 + S^1 * (b^1 - A_1 * \mu^1). \tag{8.24}$$

end for
Step 2: Form restricted residual and set initial guess:

$$\mu^2 \leftarrow 0, \quad b^2 \leftarrow R *_2 (b^1 - A_1 * \mu^1),$$

for $i = 1 : \nu_2$ **do**

$$\mu^2 \leftarrow \mu^2 + S^2 * (b^2 - A_2 * \mu^2). \tag{8.25}$$

end for
Step 3: Prolongation and restriction from coarse to fine level

$$\mu^1 \leftarrow \mu^1 + R *_2^\top \mu^2.$$

$$\mu \leftarrow \mu^1.$$

8.1.3 Multilevel coarse grid corrections and a multigrid method

To describe a multigrid algorithm, we first need to have a multiple level of grids, say $\mathcal{T}_\ell$ with $\ell = 1 : J$ and $\mathcal{T}_1 = \mathcal{T}_h$ being the finest mesh. There are many ways to obtain multiple level of grids and one simple definition of the grid points in $\mathcal{T}_\ell$ is as follows:

$$x_i^\ell = \frac{i}{2^{J+1-\ell}}, \quad i = 1, 2, \cdots, N_\ell, \ell = 1, 2, \cdots, J,$$

where $N_\ell = 2^{J+1-\ell} - 1$. Note that $\mathcal{T}_{\ell-1}$ can be viewed as being obtained by adding midpoints of the subintervals in $\mathcal{T}_\ell$. For each ℓ the set of above nodes will be denoted by $\mathcal{N}_\ell$.

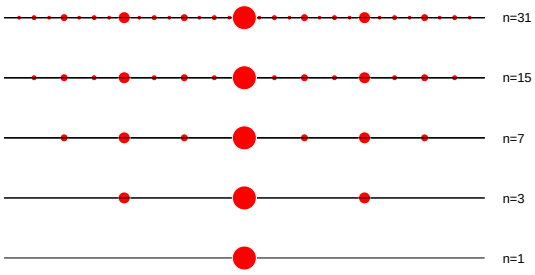

Fig. 8.6. Multiple grids in one dimension

With our previous experiences in two-grid method, the description of a multigrid method is not very difficult. In fact, the multiple level grids are treated by treating each two consecutive grids, say $\mathcal{T}_{\ell-1}$ versus $\mathcal{T}_\ell$. If we think $\mathcal{T}_{\ell-1}$ versus $\mathcal{T}_\ell$ like $\mathcal{T}_h$ and $\mathcal{T}_{2h}$, then there is not much new in the multigrid setting.

Let us give some on details the definition of the restriction and prolongation matrices. The restriction matrix $R^\ell_{\ell-1} : R^{N_{\ell-1}} \mapsto R^{N_\ell}$ can be defined by

$$\gamma^\ell = R^\ell_{\ell-1}\gamma^{\ell-1} : \ \gamma^\ell_i = \frac{1}{2}\gamma^{\ell-1}_{2i-1} + \gamma^{\ell-1}_{2i} + \frac{1}{2}\gamma^{\ell-1}_{2i+1}. \tag{8.26}$$

In matrix form

$$R^\ell_{\ell-1} = \begin{pmatrix} \frac{1}{2} & 1 & \frac{1}{2} & & & & \\ & \frac{1}{2} & 1 & \frac{1}{2} & & & \\ & & \frac{1}{2} & 1 & \frac{1}{2} & & \\ & & & \ddots & & & \\ & & & & \frac{1}{2} & 1 & \frac{1}{2} \end{pmatrix} \tag{8.27}$$

For a special case, when $N_1 = 7, N_2 = 3$, we have

$$R^2_1 = \begin{pmatrix} \frac{1}{2} & 1 & \frac{1}{2} & 0 & 0 & 0 & 0 \\ 0 & 0 & \frac{1}{2} & 1 & \frac{1}{2} & 0 & 0 \\ 0 & 0 & 0 & 0 & \frac{1}{2} & 1 & \frac{1}{2} \end{pmatrix}. \tag{8.28}$$

The prolongation matrix $P^{\ell-1}_\ell : R^{N_\ell} \mapsto R^{N_{\ell-1}}$ can be defined as

$$\epsilon^{\ell-1} = P^{\ell-1}_\ell \epsilon^\ell : \ \epsilon^{\ell-1}_{2i} = \epsilon^\ell_i, \epsilon^{\ell-1}_{2i+1} = \frac{1}{2}(\epsilon^\ell_i + \epsilon^\ell_{i+1}), \ i = 1 : N_\ell. \tag{8.29}$$

With the restriction and prolongation matrices in hands, we can now present a multilevel version of the earlier two-grid algorithm. As mentioned before, the idea is to repeat this two grid process for the coarse grid by using an even coarser grid. The resulting algorithm is just a desired multigrid algorithm.

Using the convolution with stride notation, the restriction subprocess can also be written as $R*_2 : \mathbb{R}^{N_\ell} \to \mathbb{R}^{N_{\ell+1}}$, for any $v \in \mathbb{R}^{N_\ell}$, $u = (R *_2 v) \in R^{N_{\ell+1}}$ with

$$(R *_2 v)_i = \frac{1}{2} v_{2i-1} + v_{2i} + \frac{1}{2} v_{2i+1}, \quad \text{namely} \quad R *_2 v = R^\ell_{\ell-1} v$$

where $R = [\frac{1}{2}, 1, \frac{1}{2}]$ and $R^\ell_{\ell-1}$ is defined by (8.27).

Next let $u^{\ell+1} = \sum_{j=1}^{n_{\ell+1}} \mu_j^{\ell+1} \phi_j^{\ell+1} = (\mu^{\ell+1}, \phi^{\ell+1})_{l^2}$, then we have

$$\begin{aligned} u^{\ell+1} &= (\mu^{\ell+1}, \phi^{\ell+1})_{l^2} = (\mu^{\ell+1}, R *_2 \phi^\ell)_{l^2} = (R *_2^\top \mu^{\ell+1}, \phi^\ell)_{l^2} \\ &= \sum_{j=1}^{n_\ell} \left(R *_2^\top \mu^{\ell+1}\right)_j \phi_j^\ell. \end{aligned} \tag{8.30}$$

The prolongation subprocess can be written as $R*_2^T : \mathbb{R}^{N_{\ell+1}} \to \mathbb{R}^{N_\ell}$, for any $v \in \mathbb{R}^{N_{\ell+1}}$, $u = (R *_2^T v) \in R^{N_\ell}$ with

$$(R *_2^T v)_{2i} = v_i, \quad (R *_2^T v)_{2i+1} = \frac{1}{2}(v_{i+1} + v_i), \quad \text{namely} \quad R *_2^T v = P_\ell^{\ell-1} v$$

where $R = [\frac{1}{2}, 1, \frac{1}{2}]$.

Using the convolution notation, the subprocess to apply A_ℓ to a vector $v \in \mathbb{R}^{N_\ell}$ can be written as $A_\ell* : \mathbb{R}^{N_\ell} \to \mathbb{R}^{N_\ell}$, for any $v \in \mathbb{R}^{N_\ell}$, $r = (A_\ell * v) \in R^{N_\ell}$ with

$$(A_\ell * v)_i = \frac{1}{h_\ell}(-v_{i-1} + 2v_i - v_{i+1})$$

where $A_\ell = \frac{1}{h_\ell}[-1, 2, -1]$.

Algorithm 9 A multigrid algorithm $\mu = \text{MG1}(b; \mu^0; J, \nu_1, \cdots, \nu_J)$

Set up

$$b^1 = b, \quad \mu^1 = \mu^0.$$

Smoothing and restriction from fine to coarse level (nested)
for $\ell = 1 : J$ **do**
  for $i = 1 : \nu_\ell$ **do**

$$\mu^\ell \leftarrow \mu^\ell + S^\ell * (b^\ell - A_\ell * \mu^\ell). \tag{8.31}$$

  end for
  Form restricted residual and set initial guess:

$$\mu^{\ell+1} \leftarrow 0, \quad b^{\ell+1} \leftarrow R *_2 (b^\ell - A_\ell * \mu^\ell), A_{\ell+1} = R *_2 A_\ell * (R *_2^\top).$$

end for
Prolongation and restriction from coarse to fine level
for $\ell = J - 1 : 1$ **do**

$$\mu^\ell \leftarrow \mu^\ell + R *_2^\top \mu^{\ell+1}.$$

end for

$$\mu \leftarrow \mu^1.$$

Application of Multigrid: Given $\mu^{(0)}$, for $m = 1, 2, \cdots$ till convergence

$$\mu^{(m)} = \text{MG1}(b; \mu^{(m-1)}; J, \nu_1, \cdots, \nu_J).$$

Example 4. Let $f(x) = 1$. Consider

$$\begin{cases} -u'' = f, \ 0 < x < 1, \\ u(0) = u(1) = 0. \end{cases} \tag{8.32}$$

The true solution $u = \frac{1}{2}x(1-x)$. Given the partition with the grid points $x_i = \frac{i}{n+1}, i = 0, 1, \cdots, n+1$, then by finite element discretization, we obtain

$$A * \mu = b, A = \frac{1}{h}[-1, 2, -1]. \tag{8.33}$$

Use gradient descent method and multigrid to solve (8.33) with random initial guess μ^0.

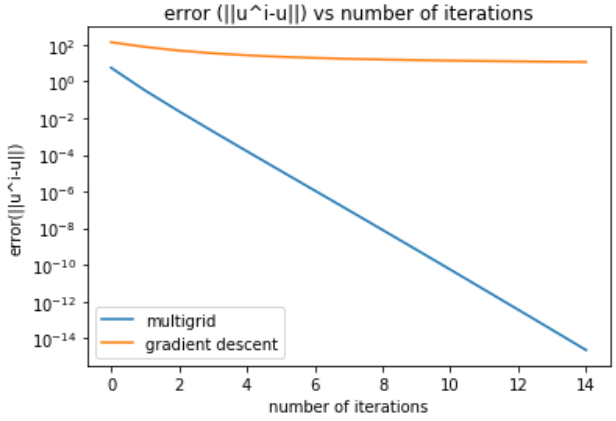

Fig. 8.7. Comparison GD with Multigrid

8.1.4 Comparison between 1D and 2D finite element discretization

1D and 2D Comparison for Finite Element and Multigrid

$1D : \Omega = (0,1)$	$2D : \Omega = (0,1) \times (0,1)$
$\begin{cases} -u'' = f & x \in \Omega \\ u(0) = u(1) = 0 \end{cases}$	$\begin{cases} -\triangle u = f & x \in \Omega \\ u = 0 & x \in \partial\Omega \end{cases}$
$u = \arg\min_{v \in V} J(v)$	
$J(v) = \frac{1}{2}\int_0^1 \lvert v' \rvert^2 dx - \int_0^1 fv dx$	$J(v) = \frac{1}{2}\int_\Omega \lvert \nabla v \rvert^2 dx - \int_\Omega fv dx$
$V = \{v : \Omega \to \mathbb{R}$ is continuous and piecewise smooth, $v\lvert_{\partial\Omega} = 0\}$	
FE space: $V_h = \{v_h \in V, v_h$ is piecewise linear w.r.t. $\mathcal{T}_h\}$	
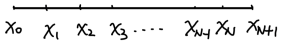	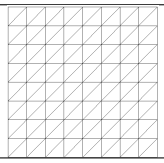
$\phi_i(x)$	$\phi_{ij}(x,y)$
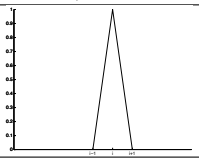	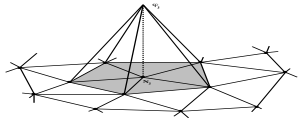
Find $u_h \in V_h$ s.t. $J(u_h) = \min_{v_h \in V_h} J(v_h)$	
$u_h = \sum_{i=1}^{n} \mu_i \phi_i(x)$	$u_h = \sum_{i,j=1}^{n} \mu_{ij} \phi_{ij}(x,y)$
Find $\mu \in \mathbb{R}^n$ s.t. $I(\mu) = \min_{\nu \in \mathbb{R}^n} I(\nu)$	Find $\mu \in \mathbb{R}^{n \times n}$ s.t. $I(\mu) = \min_{\nu \in \mathbb{R}^{n \times n}} I(\nu)$
$I(\nu) = \frac{1}{2}(A * \nu, \nu)_{l^2} - (b, \nu)_{l^2}$	
$A = \frac{1}{h}(-1, 2, -1)$	$A = \begin{pmatrix} 0 & -1 & 0 \\ -1 & 4 & -1 \\ 0 & -1 & 0 \end{pmatrix}$
$\mu = \arg\min I(\nu) \Longleftrightarrow \nabla J(\mu) = A * \mu - b = 0$	
GD Method: $\mu^{(m+1)} = \mu^{(m)} - \eta(A * \mu^{(m)} - b)$	
$\eta = \frac{h}{4}$	$\eta = \frac{1}{8}$

Basic multigrid components

<table>
<tr><td> 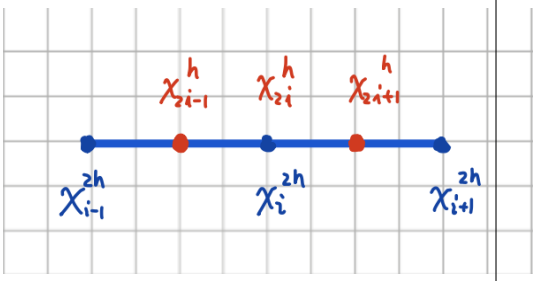
</td><td> 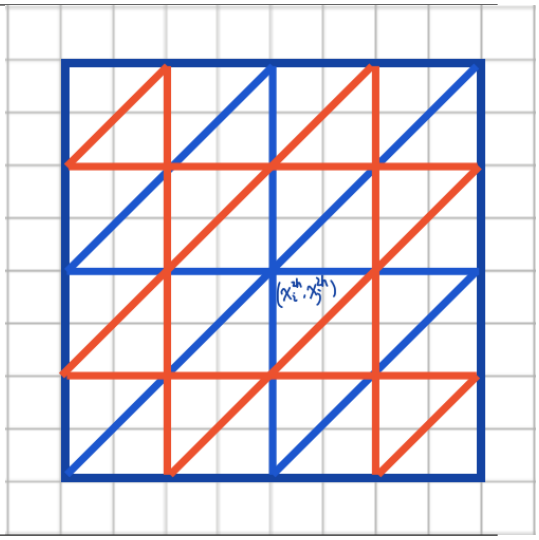
</td></tr>
<tr><td>$\phi^{2h}_i = \frac{1}{2}\phi^h_{2i-1} + \phi^h_{2i} + \frac{1}{2}\phi^h_{2i+1}$</td><td>$\phi^{2h}_{i,j} = \phi^h_{2i,2j} + \frac{1}{2}\left(\phi^h_{2i-1,2j-1} + \phi^h_{2i+1,2j+1}\right) + \frac{1}{2}\left(\phi^h_{2i-1,2j} + \phi^h_{2i,2j-1} + \phi^h_{2i+1,2j} + \phi^{2h}_{2i,2j+1}\right)$</td></tr>
<tr><td colspan="2">$\Phi^{2h} = R *_2 \Phi^h$</td></tr>
<tr><td>$R = (\frac{1}{2}, 1, \frac{1}{2})$</td><td>$R = \begin{pmatrix} 0 & \frac{1}{2} & \frac{1}{2} \\ \frac{1}{2} & 1 & \frac{1}{2} \\ \frac{1}{2} & \frac{1}{2} & 0 \end{pmatrix}$</td></tr>
</table>

8.2 Finite element method and convolution

Let us first briefly describe finite element methods for the numerical solution of the following boundary value problem

$$-\Delta u = f, \text{ in } \Omega, \quad u = 0 \text{ on } \partial\Omega, \quad \Omega = (0,1)^2. \tag{8.34}$$

For the x direction and the y direction, we consider the partition:

$$0 = x_0 < x_1 < \cdots < x_{n+1} = 1, \quad x_i = \frac{i}{m+1}, \quad (i = 0, \cdots, m+1); \tag{8.35}$$

$$0 = y_0 < y_1 < \cdots < y_{n+1} = 1, \quad y_j = \frac{j}{n+1}, \quad (j = 0, \cdots, n+1). \tag{8.36}$$

For $\Omega = (0,1)^2$, we just choose $m = n$. Such a uniform partition in the x and y directions leads us to a special example in two dimensions, a uniform square mesh $\mathbb{R}^2_h = \{(ih, jh); i, j \in \mathbb{Z}\}$ (Figure 8.2).

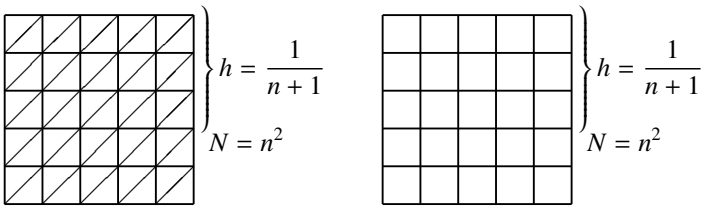

Fig. 8.8. Two-dimensional uniform grids for finite element

We consider two finite elements: continuous linear element and bilinear element. These two finite element methods find $u_h \in V_h$ such that

$$(\nabla u_h, \nabla v_h) = (f, v_h), \ \forall v_h \in V_h. \tag{8.37}$$

Basis functions ϕ_{ij} satisfy

$$\phi_{ij}(x_k, y_l) = \delta_{(i,j),(k,l)}. \tag{8.38}$$

Consider continuous linear finite element discretization of (8.34) on the left triangulation in Fig 8.2. The discrete space for linear finite element is

$$\mathcal{V}_h = \{v_h : v_h|_K \in P_1(K) \text{ and } v_h \text{ is globally continuous}\}.$$

By simple computation, we have

$$(\nabla\phi_{i,j}, \nabla\phi_{k,l}) = \begin{cases} -1 & \text{if } |k-i| + |j-l| = 1, \\ 4 & \text{if } (k,l) = (i,j), \\ 0 & \text{elsewhere.} \end{cases} \tag{8.39}$$

It is easy to verify that the formulation for the linear element method is

$$A*u = 4u_{i,j}-(u_{i+1,j}+u_{i-1,j}+u_{i,j+1}+u_{i,j-1}) = f_{i,j},\ \ u_{i,j} = 0 \text{ if } i \text{ or } j \in \{0, n+1\}, \tag{8.40}$$

where

$$f_{i,j} = \int_\Omega f(x,y)\phi_{i,j}(x,y)\mathrm{d}x\mathrm{d}y \approx h^2 f(x_i, y_j). \tag{8.41}$$

Definition 11. *A convolution defined on $\mathbb{R}^{m\times n}$ is a linear mapping $K* : \mathbb{R}^{m\times n} \mapsto \mathbb{R}^{m\times n}$ defined with padding, for any $g \in \mathbb{R}^{m\times n}$ by:*

$$[K * g]_{i,j} = \sum_{p,q=-k}^{k} K_{p,q} g_{i+p,j+q}, \quad i = 1:m, j = 1:n. \tag{8.42}$$

The coefficients in (8.42) constitute a kernel matrix

$$K \in \mathbb{R}^{(2k+1)\times(2k+1)}, \tag{8.43}$$

where k is often taken as a small integer. Here we note that the indices for the entries in K are given in a special way. For example, if $k = 1, K \in \mathbb{R}^{3\times 3}$, and

$$K = \begin{pmatrix} K_{-1,-1} & K_{-1,0} & K_{-1,1} \\ K_{0,-1} & K_{0,0} & K_{0,1} \\ K_{1,-1} & K_{1,0} & K_{1,1} \end{pmatrix},$$

for we may have the following 2D Laplacian kernel

$$K = \begin{pmatrix} 0 & -1 & 0 \\ -1 & 4 & -1 \\ 0 & -1 & 0 \end{pmatrix}. \tag{8.44}$$

Here padding means how $g_{i+p,j+q}$ is defined when $(i+p, j+q)$ is out of $1:m$ or $1:n$. The following three choices are often used

$$g_{i+p,j+q} = \begin{cases} 0, & \text{zero padding,} \\ f_{(i+p) \pmod m,(s+q) \pmod n}, & \text{periodic padding,} \\ f_{|i-1+p|,|j-1+q|}, & \text{reflected padding,} \end{cases} \tag{8.45}$$

if

$$i + p \notin \{1, 2, \ldots, m\} \text{ or } j + q \notin \{1, 2, \ldots, n\}. \tag{8.46}$$

Here $d \pmod m \in \{1, \cdots, m\}$ means the remainder when d is divided by m.

Definition 12. *For $g \in \mathbb{R}^{m\times n}$, convolution with stride 2 is defined as*

$$[K *_2 g]_{i,j} = \sum_{p,q=-k}^{k} K_{p,q} g_{2i+p-1,2j+q-1}, \quad i = 1 : \lfloor \frac{m+1}{2} \rfloor, j = 1 : \lfloor \frac{n+1}{2} \rfloor. \tag{8.47}$$

Using the convolutional notation (8.42), (8.40) can be written as

$$A * u = f \tag{8.48}$$

with

$$A = \begin{pmatrix} 0 & -1 & 0 \\ -1 & 4 & -1 \\ 0 & -1 & 0 \end{pmatrix}. \tag{8.49}$$

Proposition 1. *The mapping $A*$ has following properties*

1. *A is symmetric, namely*

$$(A * u, v)_{l^2} = (u, A * v)_{l^2}.$$

2. $(A * v, v)_F > 0, \quad if \quad v \neq 0.$
3. *$A * u = f$ if and only if*

$$u \in \arg\min_{v\in\mathcal{V}_h} J(v) = \frac{1}{2}(A * v, v) - (f, v). \tag{8.50}$$

4. *The eigenvalues λ_{kl} and eigenvectors u^{kl} of A are given by*

$$\lambda_{kl} = 4(\sin^2 \frac{k\pi}{2(n+1)} + \sin^2 \frac{l\pi}{2(n+1)}),$$

$$u^{kl}_{ij} = \sin \frac{ki\pi}{n+1} \sin \frac{lj\pi}{n+1}, \ 1 \le i \le n, \ 1 \le j \le n,$$

and $\rho(A) < 8$. Furthermore,

$$\lambda_{n,n} = 8\cos^2 \frac{\pi}{2(n+1)} \approx 8(1 - (\frac{\pi}{2(n+1)})^2) \approx 8 - \frac{2\pi^2}{(n+1)^2}$$

Continuous bilinear finite element discretization of (8.34) on the right mesh in Fig. 8.2. The discrete space for linear finite element is

$$\mathcal{V}_h = \{v_h : v_h|_K \in \{1, \ x, \ y, \ xy\} \text{ and } v_h \text{ is globally continuous}\}.$$

For bilinear element case, we have

(8.51)

$$
\begin{aligned}
(\nabla \mathbf{u}_h, \nabla \mathbf{v}_h) &= \sum_{i,j=1}^{n} \int_{E_{i,j}} \nabla \mathbf{u}_h, \nabla \mathbf{v}_h dxdy \\
&= \sum_{i,j=1}^{n} \int_{E_{i,j}} \left(\frac{(u_{i+1,j} - u_{i,j})(y_{j+1} - y)}{h^2} + \frac{(u_{i,j+1} - u_{i+1,j+1})(y - y_j)}{h^2} \right) \\
&\qquad \left(\frac{(v_{i+1,j} - v_{i,j})(y_{j+1} - y)}{h^2} + \frac{(v_{i,j+1} - v_{i+1,j+1})(y - y_j)}{h^2} \right) \\
&\qquad + \left(\frac{(u_{i,j+1} - u_{i,j})(x_{i+1} - x)}{h^2} + \frac{(u_{i+1,j} - u_{i+1,j+1})(x - x_i)}{h^2} \right) \\
&\qquad \left(\frac{(v_{i,j+1} - v_{i,j})(x_{i+1} - x)}{h^2} + \frac{(v_{i+1,j} - v_{i+1,j+1})(x - x_i)}{h^2} \right) dxdy \\
&= (A * u, v)_{l^2}.
\end{aligned}
$$

where $A = \begin{pmatrix} -1 & -1 & -1 \\ -1 & 8 & -1 \\ -1 & -1 & -1 \end{pmatrix}$ and $A * u$ is given by (8.52).

And we have

(8.52)

$$A * u = 8u_{ij} - (u_{i+1,j} + u_{i-1,j} + u_{i,j+1} + u_{i,j-1} + u_{i+1,j+1} + u_{i-1,j-1} + u_{i-1,j+1} + u_{i+1,j-1}) = f_{i,j},$$

and $u_{i,j} = 0$ if i or $j \in \{0, n+1\}$.

8.3 Piecewise linear functions on multilevel grids in 2D

An image can be viewed as a function on a grid. Images with different resolutions can then be viewed as functions on grids of different sizes. The use of such multiple-grids is a main technique used in the standard multigrid method for solving discretized partial differential equations, and it can also be interpreted as a main ingredient used in convolutional neural networks (CNN) for image calssification.

An image can be viewed as a function on a grid [**?**] on a rectangle domain $\Omega \in \mathcal{R}^2$. Without loss of generality, we assume that the grid, $\mathcal{T}$, is of size

$$m = 2^s + 1 \quad n = 2^t + 1$$

for some integers $s, t \geq 1$. Starting from $\mathcal{T}_1 = \mathcal{T}$, we consider a sequence of coarse grids with $J = \min(s, t)$ (as depicted in Fig. 8.3 with $J = 4$):

(8.53) $$\mathcal{T}_1, \mathcal{T}_2, \ldots, \mathcal{T}_J$$

such that $\mathcal{T}_\ell$ consist of $m_\ell \times n_\ell$ grid points, with

$$m_\ell = 2^{s-\ell+1} + 1, \quad n_\ell = 2^{t-\ell+1} + 1. \tag{8.54}$$

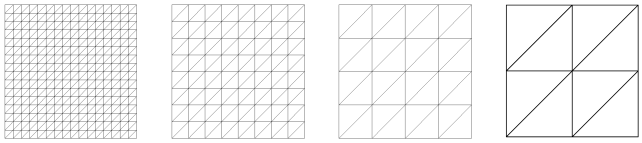

$\mathcal{T}_1$ $\mathcal{T}_2$ $\mathcal{T}_3$ $\mathcal{T}_4$

Fig. 8.9. multilevel grids for piecewise linear functions

The grid points of these grids can be given by

$$x_i^\ell = ih_\ell, y_j^\ell = jh_\ell, i = 0, \ldots, m_\ell - 1, j = 0, \ldots, n_\ell - 1.$$

Here $h_\ell = 2^{-s+\ell-1}a$ for some $a > 0$. The above geometric coordinates (x_i^ℓ, y_j^ℓ) are usually not used in image precess literatures, but they are relevant in the context of multigrid method for numerical solution of PDEs. We now consider piecewise bilinear (or linear) functions on the sequence of grids (9.12) and we obtain a nested sequence of linear vector spaces

$$\mathcal{V}_1 \supset \mathcal{V}_2 \supset \ldots \supset \mathcal{V}_J. \tag{8.55}$$

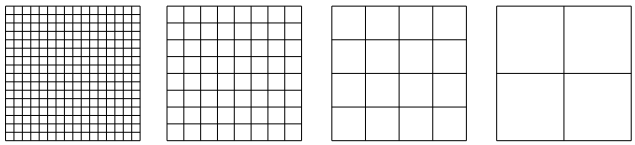

$\mathcal{T}_1$ $\mathcal{T}_2$ $\mathcal{T}_3$ $\mathcal{T}_4$

Fig. 8.10. multilevel grids for piecewise bilinear functions

Here each $\mathcal{V}_\ell$ consists of all piecewise linear (or bilinear) functions with respect to the grid (9.12) and (9.13). Each $\mathcal{V}_\ell$ has a set of basis functions: $\phi_{i,j}^\ell \in \mathcal{V}_\ell$ satisfying:

$$\phi_{i,j}^\ell(x_p^\ell, y_q^\ell) = \delta_{(i,j),(p,q)} = \begin{cases} 1 & \text{if} \quad (p,q) = (i,j), \\ 0 & \text{if} \quad (p,q) \neq (i,j). \end{cases} \tag{8.56}$$

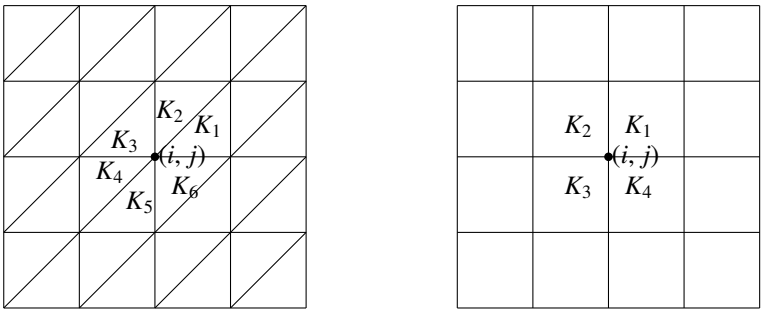

For the piecewise linear finite element space, the nodal basis function $\phi^\ell_{i,j}$ associate with each (x^ℓ_i, y^ℓ_j) (satisfying (8.56)) is given by

$$\phi^\ell_{i,j}(x,y) = \begin{cases} \frac{x^\ell_{i+1}-x}{h}, & (x,y)\in K_1, \\ \frac{y^\ell_{j+1}-y}{h}, & (x,y)\in K_2, \\ \frac{x-x^\ell_{i-1}-(y-y^\ell_j)}{h}, & (x,y)\in K_3, \\ \frac{x-x^\ell_{i-1}}{h}, & (x,y)\in K_4, \\ \frac{y-y^\ell_{j-1}}{h}, & (x,y)\in K_5, \\ \frac{x^\ell_{i+1}-x+y-y^\ell_j}{h}, & (x,y)\in K_6 \\ 0, & \text{elsewhere.} \end{cases} \tag{8.57}$$

shown in Fig. 8.11.

For bilinear element, it is easy to see that the nodal basis function $\phi^\ell_{i,j}$ associated with each (x^ℓ_i, y^ℓ_j) (satisfying (8.56)) is given by

$$\phi^\ell_{i,j}(x,y) = \begin{cases} \frac{(x^\ell_{i+1}-x)(y^\ell_{j+1}-y)}{h^2}, & (x,y)\in K_1, \\ \frac{(x-x^\ell_{i-1})(y^\ell_{j+1}-y)}{h^2}, & (x,y)\in K_2, \\ \frac{(x-x^\ell_{i-1})(y-y^\ell_{j-1})}{h^2}, & (x,y)\in K_3, \\ \frac{(x^\ell_{i+1}-x)(y-y^\ell_{j-1})}{h^2}, & (x,y)\in K_4, \\ 0 & \text{elsewhere.} \end{cases} \tag{8.58}$$

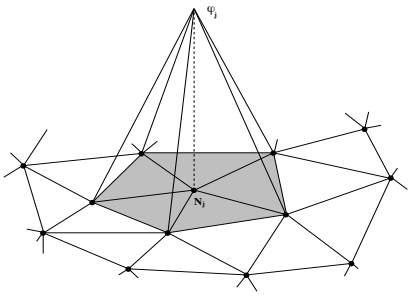

Fig. 8.11. Nodal basis for linear element.

Associated with the above nodal basis functions $\phi^\ell_{i,j}(x,y) \subset \mathcal{V}_\ell$, we define the corresponding dual basis functions $\psi^\ell_{i,j}(x,y) \subset \mathcal{V}_\ell$ satisfying

$$(\psi^\ell_{i,j}(x,y), \phi^\ell_{p,q}(x,y))_{L^2(\Omega)} = \delta_{(i,j),(p,q)}. \tag{8.59}$$

The existence of dual basis functions is obvious, but the exact expression of the dual basis functions are in general difficult to obtain. In fact, (8.59) is the only property that is needed in the application of dual basis.

We write $\mathbf{u}_h(x,y) = \sum_{i,j=1}^{n} u_{i,j}\phi_{i,j}(x,y), \mathbf{v}_h(x,y) = \sum_{i,j=1}^{n} v_{i,j}\phi_{i,j}(x,y)$.

Lemma 24. *For bilinear functions, we have*

(8.60)
$$\begin{aligned}\phi^{\ell+1}_{i,j}(x,y) = \phi^\ell_{2i,2j}(x,y) &+ \frac{1}{2}\left(\phi^\ell_{2i-1,2j}(x,y) + \phi^\ell_{2i,2j-1}(x,y) + \phi^\ell_{2i+1,2j}(x,y) + \phi^\ell_{2i,2j+1}(x,y)\right)\\ &+ \frac{1}{4}\left(\phi^\ell_{2i-1,2j-1}(x,y) + \phi^\ell_{2i+1,2j-1}(x,y) + \phi^\ell_{2i+1,2j+1}(x,y) + \phi^\ell_{2i-1,2j+1}(x,y)\right).\end{aligned}$$

For linear functions, we have

$$\begin{aligned}\phi^{\ell+1}_{i,j}(x,y) = \phi^\ell_{2i,2j}(x,y) &+ \frac{1}{2}\left(\phi^\ell_{2i-1,2j-1}(x,y) + \phi^\ell_{2i+1,2j+1}(x,y)\right)\\ &+ \frac{1}{2}\left(\phi^\ell_{2i-1,2j}(x,y) + \phi^\ell_{2i,2j-1}(x,y) + \phi^\ell_{2i+1,2j}(x,y) + \phi^\ell_{2i,2j+1}(x,y)\right).\end{aligned} \tag{8.61}$$

Thus, for each $\mathbf{v}^{\boldsymbol{\ell}} \in \mathcal{V}_\ell, \mathbf{f}^{\boldsymbol{\ell}} \in \mathcal{V}'_\ell = \mathcal{V}_\ell$, we have

$$\mathbf{v}^{\boldsymbol{\ell}}(x,y) = \sum_{i=1}^{m_\ell}\sum_{j=1}^{n_\ell} v^\ell_{i,j}\phi^\ell_{i,j}(x,y), \quad \mathbf{f}^{\boldsymbol{\ell}}(x,y) = \sum_{i=1}^{m_\ell}\sum_{j=1}^{n_\ell} f^\ell_{i,j}\psi^\ell_{i,j}(x,y), \tag{8.62}$$

where

$$v_{i,j}^{\ell} = \mathbf{v}^{\ell}(x_i^{\ell}, y_j^{\ell}), \quad f_{i,j}^{\ell} = (\mathbf{f}^{\ell}, \phi_{i,j}^{\ell})_{L^2(\Omega)}. \tag{8.63}$$

Let us introduce the following tensors:

$$v^{\ell} = (v_{i,j}^{\ell}), \quad f^{\ell} = (f_{i,j}^{\ell}), \quad \phi^{\ell} = (\phi_{i,j}^{\ell}), \quad \psi^{\ell} = (\psi_{i,j}^{\ell}). \tag{8.64}$$

The following identities obviously hold:

$$\mathbf{v}^{\ell} = (v^{\ell}, \phi^{\ell})_{l^2}, \quad \mathbf{f}^{\ell} = (f^{\ell}, \psi^{\ell})_{l^2}, \quad (\mathbf{f}^{\ell}, \mathbf{v}^{\ell})_{L^2(\Omega)} = (f^{\ell}, v^{\ell})_{l^2}.$$

Denote $\phi^{\ell} = (\phi_{i,j}^{\ell}) \in \mathbb{R}^{m_\ell \times n_\ell}$, by the definitions of convolution (9.27) and stride (9.25), (8.60) means that

$$\phi^{\ell+1} = R *_2 \phi^{\ell},$$

where

$$R = \begin{cases} \begin{pmatrix} \frac{1}{4} & \frac{1}{2} & \frac{1}{4} \\ \frac{1}{2} & 1 & \frac{1}{2} \\ \frac{1}{4} & \frac{1}{2} & \frac{1}{4} \end{pmatrix} & \text{for bilinear functions;} \\ \begin{pmatrix} 0 & \frac{1}{2} & \frac{1}{2} \\ \frac{1}{2} & 1 & \frac{1}{2} \\ \frac{1}{2} & \frac{1}{2} & 0 \end{pmatrix} & \text{for linear functions.} \end{cases} \tag{8.65}$$

8.4 Deconvolution

For any linear mapping $C : \mathbb{R}^{m\times n} \mapsto \mathbb{R}^{m'\times n'}$, its transpose is the unique linear mapping $C^{\top} : \mathbb{R}^{m'\times n'} \mapsto \mathbb{R}^{m\times n}$ satisfying

$$(C^{\top}u, v)_{l^2} = (u, Cv)_{l^2} \quad \forall\, u \in \mathbb{R}^{m'\times n'}, v \in \mathbb{R}^{m\times n}$$

Associated with any kernel K, a deconvolution is defined as the transpose of convolution with stride 2 with respect to the l^2-inner product as:

$$(u, K *_2^{\top} v)_{l^2} = (K *_2 u, v)_{l^2}, \tag{8.66}$$

with

$$u \in \mathbb{R}^{m\times n} \quad \text{and} \quad v \in \mathbb{R}^{\frac{m+1}{2}\times\frac{m+1}{2}}. \tag{8.67}$$

Lemma 25. *For any $K \in \mathbb{R}^{(2k+1)\times(2k+1)}$,*

$$K*_2^{\top} = \tilde{K} * \mathcal{S}^{\top}, \tag{8.68}$$

where $\tilde{K}$ is defined as

$$\tilde{K}_{p,q} = K_{-p,-q}, \quad p, q = -k : k. \tag{8.69}$$

Intuitively, if we take $K_{0,0}$ as the center for the convolutional kernel K, then $\tilde{K}$ is the central symmetry of K. In 2D case, it can also be understood as the rotation of π with respect to the center $K_{0,0}$.

Recalling the definition of deconvolution in (8.66), we have

$$(u, K *_2^\top v)_{l^2} = (K *_2 u, v)_{l^2} = (\mathcal{S}C_K u, v)_{l^2} = (u, C_K^\top \mathcal{S}^\top v)_{l^2}, \tag{8.70}$$

with definition

$$\mathcal{S}^\top : \mathbb{R}^{\frac{m+1}{2}\times\frac{n+1}{2}} \mapsto \mathbb{R}^{m\times n}, \tag{8.71}$$

and

$$[\mathcal{S}^\top(f)]_{i,j} = \begin{cases} 0 & \text{if i or j is even,} \\ f_{i/2,j/2}, & \text{else.} \end{cases} \tag{8.72}$$

Thus to say, we have the simple version of the deconvolution for $K*$ as

$$K *_2^\top v = C_K^\top \circ \mathcal{S}^\top(v) = C_{\tilde{K}} \circ \mathcal{S}^\top(v) = \tilde{K} * \mathcal{S}^\top(v), \tag{8.73}$$

thus to say

$$K*_2^\top = \tilde{K} * \mathcal{S}^\top. \tag{8.74}$$

In short, we have the next decomposition

- convolution with stride = stride ∘ convolution,
- deconvolution with stride = transposed convolution ∘ transposed stride = convolution with the central symmetry of original kernel ∘ transposed stride.

Theorem 17. *Let us consider*

$$K = (K_{p,q}), \quad p, q = -1, 0, 1. \tag{8.75}$$

Then we have

$$K *_2^\top v = \tilde{K} * \mathcal{S}^\top(v).$$

As in (8.72) and the Lemma 25, we have the final version is

$$[K *_2^\top v]_{2i,2j} = K_{0,0} v_{i,j}, \tag{8.76}$$

with

$$[K *_2^\top v]_{2i-1,2j} = K_{0,1} v_{i-1,j} + K_{0,-1} v_{i,j}, \quad [K *_2^\top v]_{2i,2j-1} = K_{1,0} v_{i,j} + K_{-1,0} v_{i,j-1}, \tag{8.77}$$

and

$$[K *_2^\top v]_{2i-1,2j-1} = K_{1,1} v_{i,j} + K_{-1,1} v_{i-1,j} + K_{1,-1} v_{i,j-1} + K_{-1,-1} v_{i-1,j-1}. \tag{8.78}$$

Remark 4. Deconvolution can obviously be also defined for general stride s, but we believe it is sufficient to use $s = 2$ in most applications.

8.5 Linear feature mappings

We consider the following linear mapping

$$\mathbf{Au} = \mathbf{f} \tag{8.79}$$

where

$$\mathbf{A} : \mathcal{V} \mapsto \mathcal{V}'. \tag{8.80}$$

For example, for the elliptic problem (8.34), $(\mathbf{Au}, \mathbf{v}) = (\nabla u_h, \nabla v_h)$. We consider the restriction of the mapping $\mathbf{A}_1 \equiv \mathbf{A}$ on the coarser multilevel spaces:

$$\mathbf{A}_\ell : \mathcal{V}_\ell \mapsto \mathcal{V}'_\ell \tag{8.81}$$

and the corresponding equation read as:

$$\mathbf{A}_\ell \mathbf{u}^\ell = \mathbf{f}^\ell. \tag{8.82}$$

In image process, we can view $\mathbf{f}$ as the input images and $\mathbf{u}$ as the extracted features of the original image $\mathbf{f}$. We then view $\mathbf{f}^\ell$ as the projection of images on a coarser resolution and $\mathbf{u}^\ell$ as the extracted features of the coarsened image $\mathbf{f}^\ell$.

One main question is how to obtain coarser images and features defined by (8.82) from the original equation (8.79). We now consider a special technique.

We define $\mathbf{u}^\ell \in \mathcal{V}_\ell$ by

$$(\mathbf{Au}^\ell, \mathbf{v}^\ell) = (\mathbf{f}, \mathbf{v}^\ell), \quad \forall \mathbf{v}^\ell \in \mathcal{V}_\ell \tag{8.83}$$

Lemma 26. *The restricted $\mathbf{u}^\ell \in \mathcal{V}_\ell$ defined by (8.83) satisfies (8.82) if $\mathbf{A}_\ell : \mathcal{V}_\ell \mapsto \mathcal{V}'_\ell$ and $\mathbf{f}_\ell \in \mathcal{V}'_\ell$ are defined by*

$$(\mathbf{A}_\ell \mathbf{u}^\ell, \mathbf{v}^\ell) = (\mathbf{Au}^\ell, \mathbf{v}^\ell), \quad \forall \mathbf{v}^\ell \in \mathcal{V}_\ell \tag{8.84}$$

$$(\mathbf{f}^\ell, \mathbf{v}^\ell) = (\mathbf{f}, \mathbf{v}^\ell), \quad \forall \mathbf{v}^\ell \in \mathcal{V}_\ell \tag{8.85}$$

8.6 Restriction and prolongation under the convolution notation

Now we derive the restriction and prolongation as follows. We show the details for the case of bilinear functions here. The case of linear function can be shown similarly. Let $f^{\ell+1}_{i,j} = (\mathbf{f}^\ell, \phi^{\ell+1}_{i,j})_{L^2(\Omega)}$, then we have

$$\begin{aligned} f^{\ell+1} &= \int_\Omega \mathbf{f}^\ell \phi^{\ell+1} = \sum_{i=1}^{m_\ell} \sum_{j=1}^{n_\ell} \int_\Omega f^\ell_{i,j} \psi^\ell_{i,j} \left[(R *_2) \phi^\ell \right] = \sum_{i=1}^{m_\ell} \sum_{j=1}^{n_\ell} f^\ell_{i,j} (R *_2) \int_\Omega \psi^\ell_{i,j} \phi^\ell \\ &= \sum_{i=1}^{m_\ell} \sum_{j=1}^{n_\ell} (R *_2) f^\ell_{i,j} e_i e_j^T = R *_2 f^\ell. \end{aligned} \tag{8.86}$$

Hence the restriction

$$R_\ell^{\ell+1} : \mathbb{R}^{m_\ell \times n_\ell} \mapsto \mathbb{R}^{m_{\ell+1}\times n_{\ell+1}}$$

is obtain by $R_\ell^{\ell+1} f^\ell = R *_2 f^\ell$ with $R \in \mathbb{R}^{3\times 3}$ given by (8.65), namely

$$\begin{aligned} f_{i,j}^{\ell+1} &= f_{2i,2j}^\ell + \frac{1}{2}(f_{2i-1,2j}^\ell + f_{2i,2j-1}^\ell + f_{2i+1,2j}^\ell + f_{2i,2j+1}^\ell) \\ &\quad + \frac{1}{4}\left(f_{2i-1,2j-1}^\ell + f_{2i+1,2j-1}^\ell + f_{2i+1,2j+1}^\ell + f_{2i-1,2j+1}^\ell\right). \end{aligned} \tag{8.87}$$

Next let $\mathbf{u}^{\ell+1} = \sum_{i=1}^{m_{\ell+1}} \sum_{j=1}^{n_{\ell+1}} u_{i,j}^{\ell+1} \phi_{i,j}^{\ell+1} = (\mathbf{u}^{\ell+1}, \phi^{\ell+1})_{l^2}$, then we have

$$\begin{aligned} \mathbf{u}^{\ell+1} &= (u^{\ell+1}, \phi^{\ell+1})_{l^2} = (u^{\ell+1}, R *_2 \phi^\ell)_{l^2} = (R *_2^\top u^{\ell+1}, \phi^\ell)_{l^2} \\ &= \sum_{i=1}^{m_\ell} \sum_{j=1}^{n_\ell} \left(R *_2^\top u^{\ell+1}\right)_{i,j} \phi_{i,j}^\ell. \end{aligned} \tag{8.88}$$

Namely

$$\mathbf{u}^{\ell+1}(x_i^\ell, y_j^\ell) = \left(R *_2^\top u^{\ell+1}\right)_{i,j}.$$

And we obtain the prolongation

$$P_{\ell+1}^\ell = R *_2^\top : \mathbb{R}^{m_{\ell+1}\times n_{\ell+1}} \mapsto \mathbb{R}^{m_\ell \times n_\ell}$$

is defined by

$$u_{2i,2j}^\ell = u_{i,j}^{\ell+1},$$

$$u_{2i-1,2j}^\ell = \frac{1}{2}(u_{i,j}^\ell + u_{i-1,j}^\ell), \quad u_{2i,2j-1}^\ell = \frac{1}{2}(u_{i,j}^{\ell+1} + u_{i,j-1}^{\ell+1})$$

and

$$u_{2i-1,2j-1}^\ell = \frac{1}{4}(u_{i,j}^{\ell+1} + u_{i-1,j}^{\ell+1} + u_{i-1,j-1}^{\ell+1} + u_{i,j-1}^{\ell+1}).$$

In summery, we have the restriction and prolongation as follows:

Lemma 27. *The restriction*

$$R_\ell^{\ell+1} : \mathbb{R}^{m_\ell \times n_\ell} \mapsto \mathbb{R}^{m_{\ell+1}\times n_{\ell+1}} \ \ is \ \ R_\ell^{\ell+1} = R *_2$$

and the prolongation

$$P_{\ell+1}^\ell : \mathbb{R}^{m_{\ell+1}\times n_{\ell+1}} \mapsto \mathbb{R}^{m_\ell \times n_\ell} \ \ is \ \ P_{\ell+1}^\ell = R *_2^\top$$

where

$$R = \begin{cases} \begin{pmatrix} \frac{1}{4} & \frac{1}{2} & \frac{1}{4} \\ \frac{1}{2} & 1 & \frac{1}{2} \\ \frac{1}{4} & \frac{1}{2} & \frac{1}{4} \end{pmatrix} & \textit{for bilinear functions;} \\ \begin{pmatrix} 0 & \frac{1}{2} & \frac{1}{2} \\ \frac{1}{2} & 1 & \frac{1}{2} \\ \frac{1}{2} & \frac{1}{2} & 0 \end{pmatrix} & \textit{for linear functions.} \end{cases} \tag{8.89}$$

Let $(\phi^\ell_{i,j})$ is a basis of $\mathcal{V}_\ell$, for any $\mathbf{u}^\ell \in \mathcal{V}_\ell$, then $\mathbf{u}^\ell = \sum_{i=1}^{m_\ell}\sum_{j=1}^{n_\ell} u^\ell_{i,j}\phi^\ell_{i,j}$, and we denote $u^\ell = (u^\ell_{i,j}) \in \mathbb{R}^{m_\ell \times n_\ell}$ the matrix representation of $\mathbf{u}^\ell$ under the basis $(\phi^\ell_{i,j})$. Let $(\psi^\ell_{s,t})$ is a basis of $\mathcal{V}'_\ell$ which is dual to $(\phi^\ell_{i,j})$. Denote $A_\ell = (a^\ell_{stij})$ the tensor representation of $\mathbf{A}_\ell : \mathcal{V}_\ell \mapsto \mathcal{V}'_\ell$ and defined as

$$\mathbf{A}_\ell \phi^\ell_{i,j} = \sum_{s=1}^{m_\ell}\sum_{t=1}^{n_\ell} a^\ell_{stij}\psi^\ell_{s,t}.$$

Hence $a^\ell_{stij} = (\mathbf{A}_\ell \phi^\ell_{i,j}, \phi^\ell_{s,t})$. From $(\mathbf{A}_{\ell+1}\phi^{\ell+1}_{i,j}, \phi^{\ell+1}_{s,t}) = (\mathbf{A}_\ell \phi^{\ell+1}_{i,j}, \phi^{\ell+1}_{s,t})$, we have

$$a^{\ell+1}_{stij} = \sum_{r=1}^{m_\ell}\sum_{q=1}^{n_\ell}\left(\sum_{k=1}^{m_\ell}\sum_{m=1}^{n_\ell} P^{\ell,\ell+1}_{kmij} a^\ell_{rqkm}\right) P^{\ell,\ell+1}_{rqst}$$

Where $P^{\ell,\ell+1} = (P^{\ell,\ell+1}_{rqst})$ is the tensor representation of the prolongation $P^\ell_{\ell+1}$.

Consider the finite element method on two different grids $\mathcal{T}_\ell$, $\mathcal{T}_{\ell+1}$, $h_{\ell+1} = 2h_\ell, \mathcal{V}_{\ell+1} \subset \mathcal{V}_\ell$. With the restriction $R^{\ell+1}_\ell$ and prolongation $P^\ell_{\ell+1}$ obtained in Lemma 27, we have the following relationship to define coarse operation

$$\begin{aligned} A_{\ell+1} &= R^{\ell+1}_\ell A_\ell P^\ell_{\ell+1}. \\ &= R *_2 A_\ell * (R*_2^\top), \quad (\ell = 1 : J-1), \end{aligned} \tag{8.90}$$

with $A_1 = A$.

Theorem 18. *If R is consistent with A_ℓ which means that R should be linear or bi-linear as A_ℓ, then we have the $A_{\ell+1}$ operation in coarse grid defined in (8.90) is the same with A_ℓ.*

Proof. For any $u_{\ell+1}$ and $v_{\ell+1}$ in $\mathcal{V}_{\ell+1}$, it remains to prove that

$$(A_\ell P^\ell_{\ell+1} u_{\ell+1}, P^\ell_{\ell+1} v_{\ell+1}) = (A_{\ell+1} u_{\ell+1}, v_{\ell+1})$$

where A_ℓ and $A_{\ell+1}$ are the tensor representation of $\mathbf{A}_\ell$ and $\mathbf{A}_{\ell+1}$.

We can also view them as convolutions. By the definition of operators $R^{\ell+1}_\ell$ and $P^\ell_{\ell+1}$, a direct computation gives the above result. □

Proof. By the definition above, we have that

$$A_{\ell+1}(v) = \mathcal{S}\Big((R * A_\ell * R) * \mathcal{S}^\top(v)\Big), \tag{8.91}$$

because of the properties of convolution we know that

$$(R * A_\ell * R)* = K*, \tag{8.92}$$

for some

$$K \in \mathbb{R}^{7\times 7}.$$

Then we have the next computation for $A_{\ell+1}(v)$

$$
\begin{aligned}
[A_{\ell+1}(v)]_{i,j} &= [\mathcal{S}\Big((R * A_\ell * R) * \mathcal{S}^\top(v)\Big)]_{i,j}, \\
&= [K * \mathcal{S}^\top(v)]_{2i,2j}, \\
&= \sum_{p,q=-3}^{3} [\mathcal{S}^\top(v)]_{2i+p,2j+q} K_{p,q}, \\
&= \sum_{p,q=-1}^{1} [\mathcal{S}^\top(v)]_{2(i+p),2(j+q)} K_{2p,2q}, \\
&= \sum_{p,q=-1}^{1} v_{i+p,j+q} \hat{K}_{p,q},
\end{aligned}
\tag{8.93}
$$

Thus to say, we have

$$
A_{\ell+1}(v) = \hat{K} * v, \tag{8.94}
$$

with

$$
\hat{K}_{p,q} = K_{2p,2q}, \quad p, q = -1, 0, 1,
$$

with K is defined in (8.92).

Then by the direct computation of (8.92) as

$$
(R * A_\ell * R)* = K*
$$

and take the even index we have that

$$
A_{\ell+1} = \hat{K} = A_\ell, \tag{8.95}
$$

if R is consistent with A_ℓ which means that R should be linear or bi-linear as A_ℓ. □

8.7 Multigrid for finite element methods

By the definition of convolution (9.27), we can rewrite (8.40) and (8.52) as follows:

(8.96)

$$
A* : \mathbb{R}^{m\times n} \to \mathbb{R}^{m\times n}, \quad A*u = f, \quad \Leftrightarrow \quad u = \arg\min J(v) = \arg\min \left(\frac{1}{2}(A * v, v) - (f, v)_{l^2} \right)
$$

where $u = (u_{ij})$, $f = (f_{ij})$,

$$A = \begin{cases} \begin{pmatrix} 0 & -1 & 0 \\ -1 & 4 & -1 \\ 0 & -1 & 0 \end{pmatrix} & \text{for linear finite element,} \\ \begin{pmatrix} -1 & -1 & -1 \\ -1 & 8 & -1 \\ -1 & -1 & -1 \end{pmatrix} & \text{for bilinear finite element.} \end{cases} \tag{8.97}$$

It is easy to see that

$$\nabla J(v) = A * v - f := -r, \quad r = f - A * v.$$

Applying the gradient descent method to (8.50), we obtain the following iterative method:

$$u^{k+1} = u^k + \eta r^k, \quad r^k = f - A * u^k. \tag{8.98}$$

Here we can clearly see that gradient descent method is equivalent to damped Jacobi method. Usually, we call this as smoother.

Lemma 28. *The gradient descent method (8.98) for linear finite element converges if $\eta = \frac{1}{8}$, and the one for bilinear finite element converges if $\eta = \frac{1}{16}$. Furthermore, the high frequence in $u - u^k$ are damped very rapidly.*

Proof. According to (8.98) ,

$$u^{k+1} - u = (I - \eta A) * (u^k - u).$$

The gradient descent method (8.98) converges if $\rho((I - \eta A)*) < 1$, namely $\eta\rho(A*) < 2$. For linear finite element, if $\eta = \frac{1}{8}$, $\rho(A*) < 8$, thus the gradient descent method (8.98) converges. For bilinear finite element, if $\eta = \frac{1}{16}$, $\rho(A*) < 16$, thus the gradient descent method (8.98) converges.

For linear finite element, let (λ_i, v_i) satisfy $A * v_i = \lambda_i v_i$ and $0 < \lambda_1 \leq \lambda_2 \leq \cdots \lambda_N$ with $N = n^2$. Expand the error $u^k - u$ in terms of eigenvectors v_i, namely,

$$u^k - u = \sum_{i=1}^{N} a_i^k v_i.$$

Then

$$u^k - u = \sum_{i=1}^{N} a_i^k (1 - \eta\lambda_i) v_i = \sum_{i=1}^{N} a_i^0 (1 - \eta\lambda_i)^k v_i.$$

According to Proposition 1, it is easy to see that

$$1 - \frac{1}{8}\lambda_N \approx \frac{\pi^2}{4(n+1)^2} \ll 1.$$

For $\eta = \frac{1}{8}$, the coefficient $a_N^0(1 - \frac{1}{8}\lambda_N)^k$ of v_N approximates to zero much faster. This means that high frequency in the error will damp rapidly. □

For an initial guess u^0, the left picture in Fig 8.12 plots the error $u - u^0$ and the the right one plots the error $u - u^1$. Fig 8.12 shows that the high frequency in the error of the initial guess u^0 is damped after one step of smoothing and results in a smoother error $u - u^1$. Next, we make the following particular choice:

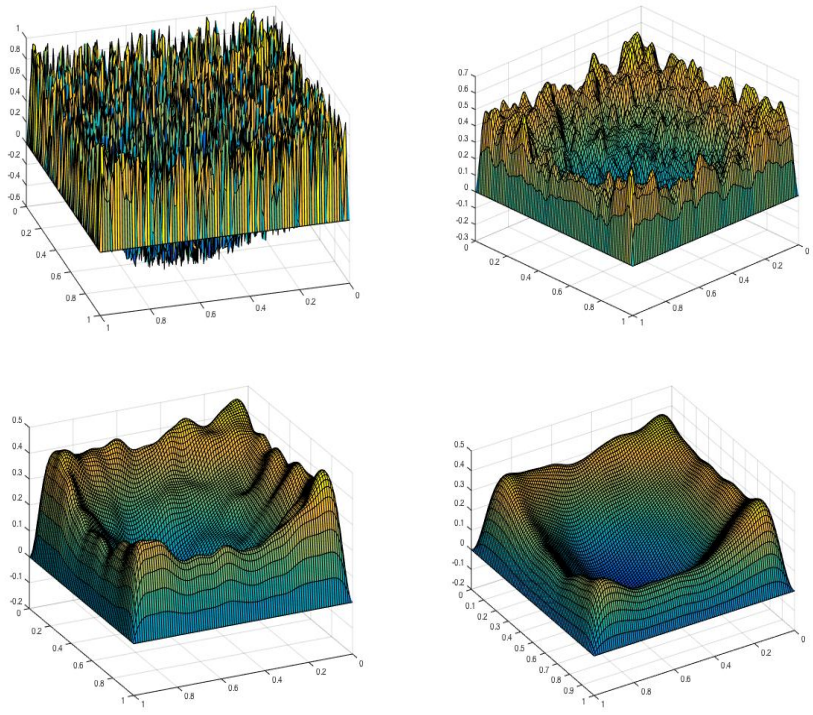

Fig. 8.12. The errors of an random initial guess u^0, u^{10}, u^{50} and u^{100}.

$$\eta = \frac{1}{8}. \tag{8.99}$$

The gradient descent method can be written in terms of $S_0 : \mathbb{R}^{m\times n} \mapsto \mathbb{R}^{m\times n}$ satisfying

$$u^1 = (S_0 f) = \frac{1}{8} f, \tag{8.100}$$

for equation (8.40) with initial guess zero. If we apply this method twice, then

$$u^2 = S_1(f) = S_0 f + S_0(f - A * (S_0 f)),$$

with element-wise form

$$u^2_{i,j} = \frac{3}{16} f_{i,j} + \frac{1}{64}(f_{i+1,j} + f_{i-1,j} + f_{i,j+1} + f_{i,j-1}). \tag{8.101}$$

Then by the definition of convolution (9.27), we have

$$u^1 = S_0 * f \quad u^2 = S_1 * f. \tag{8.102}$$

with

$$S_0 = \frac{1}{8}, \tag{8.103}$$

and

$$S_1 = \frac{1}{64}\begin{pmatrix} 0 & 1 & 0 \\ 1 & 12 & 1 \\ 0 & 1 & 0 \end{pmatrix}. \tag{8.104}$$

Next, we make the following particular choice for the bilinear case:

$$\eta = \frac{1}{16}. \tag{8.105}$$

The gradient descent method can be written in terms of $S_0 : \mathbb{R}^{m\times n} \mapsto \mathbb{R}^{m\times n}$ satisfying

$$u^1 = (S_0 f)_{i,j} = \frac{1}{16} f_{i,j}, \tag{8.106}$$

for equation (8.52) with initial guess zero. If we apply this method twice, then

$$u^2 = S_1(f) = S_0 f + S_0(f - A * (S_0 f)),$$

with element-wise form

$$u^2_{i,j} = \frac{3}{32} f_{i,j} + \frac{1}{256}(f_{i+1,j} + f_{i-1,j} + f_{i,j+1} + f_{i,j-1} + f_{i+1,j+1} + f_{i-1,j-1} + f_{i-1,j+1} + f_{i+1,j-1}). \tag{8.107}$$

Then by the definition of convolution (9.27), we have

$$u^1 = S_0 * f \quad u^2 = S_1 * f. \tag{8.108}$$

with

$$S_0 = \frac{1}{16}, \tag{8.109}$$

and

$$S_1 = \frac{1}{256}\begin{pmatrix} 1 & 1 & 1 \\ 1 & 24 & 1 \\ 1 & 1 & 1 \end{pmatrix}. \tag{8.110}$$

We note the gradient descent method (8.98) can be written as

$$u^k = u^{k-1} + S_0 * (f - A * u^{k-1}). \tag{8.111}$$

$$u^{2k} = u^{2(k-1)} + S_1 * (f - A * u^{2(k-1)}). \tag{8.112}$$

We can sometimes use S_1 and the above identity to define a smoother directly, namely

$$u^k = u^{k-1} + S_1 * (f - A * u^{k-1}). \tag{8.113}$$

Similarly, with the smoother obtained by (8.108), we can define $S^\ell : \mathbb{R}^{m_\ell \times n_\ell} \mapsto \mathbb{R}^{m_\ell \times n_\ell}$.

First solve the problem on the fine grid $\mathcal{T}_\ell$, denote the solution by u^ℓ,

$$u^\ell \leftarrow u^\ell + S^\ell * (f^\ell - A_\ell * u^\ell). \tag{8.114}$$

Denote the error by $e^\ell = u - u^\ell$ and the residual

$$r^\ell = f - A_\ell * u^\ell. \tag{8.115}$$

It is obvious that $A_\ell * e^\ell = r^\ell$. We need to solve the residual equation

$$A_\ell * e^\ell = r^\ell. \tag{8.116}$$

The idea of multigrid method is to solve this residual equation on the coarse grid space $\mathcal{V}_{\ell+1}$ and repeat the process until coarsest grid.

We note that the restriction of (8.116) to the coarse level $\ell + 1$ is

$$A_{\ell+1} * e^{\ell+1} = r^{\ell+1} \tag{8.117}$$

with $r^{\ell+1} = R_\ell^{\ell+1} r^\ell = R * r^\ell$.

Denote the finite element approximation to e_ℓ on the coarse grid $\mathcal{T}_{\ell+1}$ by $e_{\ell+1}$. Interpolate the error $e_{\ell+1}$ back to the fine space $\mathcal{V}_\ell$ and add the resulting residual to $u_{\ell+1}$, that is

$$u^\ell \leftarrow u^\ell + P_{\ell+1}^\ell e^{\ell+1} \tag{8.118}$$

Now using the smoother S^ℓ, prolongation $P_{\ell+1}^\ell$, restriction $R_\ell^{\ell+1}$ and mapping A^ℓ as given in (8.90), we can formulate the following algorithm as a major component of a multigrid algorithm.

Algorithm 10 $(u^1, u^2, \cdots, u^J) = \text{MG0}(f; u^0; J, \nu_1, \cdots, \nu_J)$

Set up

$$f^1 = f, \quad u^1 = u^0.$$

Smoothing and restriction from fine to coarse level (nested)
for $\ell = 1 : J$ **do**
for $i = 1 : \nu_\ell$ **do**

$$u^\ell \leftarrow u^\ell + S^\ell * (f^\ell - A_\ell * u^\ell). \tag{8.119}$$

end for
Form restricted residual and set initial guess:

$$u^{\ell+1,0} \leftarrow 0, \quad f^{\ell+1} \leftarrow R *_2 (f^\ell - A_\ell * u^\ell), A_{\ell+1} = R *_2 A_\ell * (R *_2^\top).$$

end for

Here S^ℓ can be chosen as S_0 or S_1 as definition in (8.109) and (8.110).

Using the above algorithm, there are different multigrid algorithms such as: \-cycle, V-cycle and W-cycle. Let us now only give one special form of multigrid algorithm for solving (8.34) as follows.

Algorithm 11 $u = \text{MG1}(f; u^0; J, \nu_1, \cdots, \nu_J)$

$$u \leftarrow u^0.$$

$$(u^1, u^2, \cdots, u^J) = \text{MG0}(f; u; J, \nu_1, \cdots, \nu_J).$$

Prolongation and restriction from coarse to fine level
for $\ell = J - 1 : 1$ **do**

$$u^\ell \leftarrow u^\ell + R *_2^\top u^{\ell+1}.$$

end for

$$u \leftarrow u^1.$$

If we add the post-smoothing with a symmetric form which means we use $[S^\ell *]^\top$ as the smoother, then we can get the V-cycle version multigrid algorithm.

Algorithm 12 $u = \text{MG2}(f; u^0; J, \nu_1, \cdots, \nu_J; \nu'_1, \cdots, \nu'_J)$

$$(u^1, u^2, \cdots, u^J) = \text{MG0}(f; u^0; J, \nu_1, \cdots, \nu_J).$$

Prolongation and restriction from coarse to fine level
for $\ell = J - 1 : 1$ **do**

$$u^\ell \leftarrow u^\ell + R *_2^\top u^{\ell+1}.$$

for $i = 1 : \nu'_\ell$ **do**

$$u^\ell \leftarrow u^\ell + S^\ell * (f^\ell - A_\ell * u^\ell)$$

end for
end for

$$u = u^1.$$

Here S^ℓ means the central symmetry of kernel for smoother S^ℓ as in the definition of (8.69) in Lemma 25.

We note that

$$\text{MG1}(f; u^0; J, \nu_1, \cdots, \nu_J) = \text{MG2}(f; u^0; J, \nu_1, \cdots, \nu_J; 0, \cdots, 0).$$

Either MG1 or MG2 only represents one cycle in a multigrid process. There many different ways to use this basis multigrid cycle. For a given iterate u, we need to define a metric to measure the accuracy of u. One way to define it is:

$$\text{error}(u) = \|f - A * u\|/\|f - A * u^0\|.$$

Sometimes, when we debug a code, we can first try to find the exact solution. u_{exact}, and then define

$$\text{error}(u) = \|u_{\text{exact}} - u\|_A.$$

Below is one example fo algorithm for application of the basic multigrid cycle, say MG1:

Algorithm 13 $u = \text{multigrid1}(f; u^0; J, \nu_1, \cdots, \nu_J; \text{tol})$;

$$u \leftarrow u^0.$$

while $\text{error}(u) \geq tol$ **do**

$$u \leftarrow u + \text{MG1}(f - Au; 0; \nu_1, \cdots, \nu_J).$$

end while

A slightly more general multigrid method.

---

1. Initialization of inputs

$$g_1 \leftarrow g, \quad u_1 \leftarrow \text{random}.$$

2. Smoothing and restriction
   - For $\ell = 1 : J$

– For $i = 1 : \nu_\ell$

$$u_\ell \leftarrow u_\ell + S_\ell * (g_\ell - A_\ell * u_\ell). \tag{8.120}$$

– Form restricted residual and set initial guess:

$$u_{\ell+1,0} \leftarrow \Pi_\ell^{\ell+1} u_\ell, \quad g_{\ell+1} \leftarrow R_\ell *_2 (g_\ell - A_\ell * u_\ell) + A_{\ell+1} * u_{\ell+1}^0,$$

3. Prolongation with post-smoothing

- For $\ell = J - 1 : 1$

$$u_\ell \leftarrow u_\ell + R_\ell *_2^\top (u_{\ell+1} - u_{\ell+1}^0).$$

– For $i = 1 : \nu'_\ell$

$$u_\ell \leftarrow u_\ell + S'_\ell * (g_\ell - A_\ell * u_\ell)$$

4. Output

$$u_1$$

8.8 Numerical examples

We consider to solve

$$-\Delta u = f, \text{ in } \Omega, \quad u = 0 \text{ on } \partial\Omega, \quad \Omega = (0,1)^2. \tag{8.121}$$

For the x direction and the y direction, we consider the partition:

$$0 = x_0 < x_1 < \cdots < x_{n+1} = 1, \quad x_i = \frac{i}{n+1}, \quad (i = 0, \cdots, n+1); \tag{8.122}$$

$$0 = y_0 < y_1 < \cdots < y_{n+1} = 1, \quad y_j = \frac{j}{n+1}, \quad (j = 0, \cdots, n+1). \tag{8.123}$$

We use linear finite to discretize the 2D Laplacian equation (8.121). The size of unknowns is n^2. We use gradient descent method as smoother in the multigrid method.

From the Table 8.8 and Figure 8.13, we can see that the multigrid method is much faster than Gauss-Seidel method and is uniform with respect to the size of unknowns.

8.9 ReLU multigrid method for nonnegative solution

Considering $f = (1, 1, ..., 1)^\top$,

Algorithm 15 $(u^1, u^2, \cdots, u^J) = \text{MG0}(f; u^0; J, \nu_1, \cdots, \nu_J)$

Set up

$$f^1 = f, \quad u^1 = u^0.$$

Smoothing and restriction from fine to coarse level (nested)

for $\ell = 1 : J$ **do**

for $i = 1 : \nu_\ell$ **do**

Size of Unkowns	Gauss-Seidel for A	Multigrid for A
225	226/0.04s	13/0.004s
961	910/0.26s	13/0.007s
3969	3,044/2.40s	13/0.021s
16,129	9,869/31.45s	13/0.08s
65,025	30,226/347.38s	13/0.3s

Table 8.1. Number of iterations for $\|Ax - b\|/\|b\| \leq 10^{-6}$.

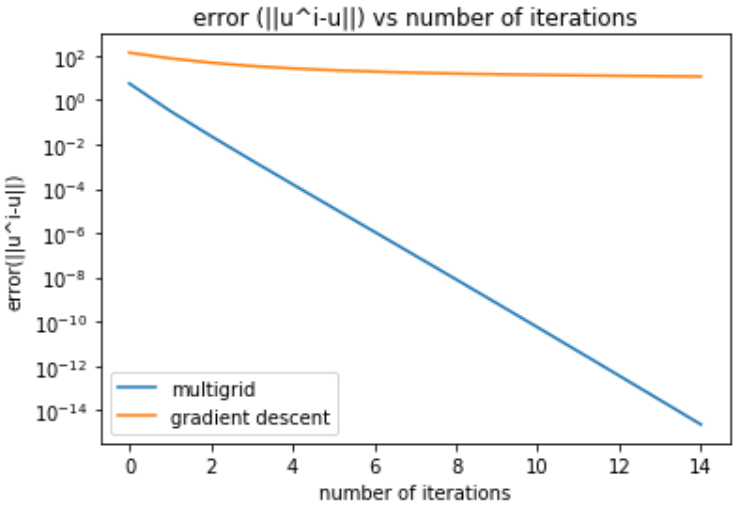

Fig. 8.13. Comparison GD with Multigrid.

(8.124) $$u^\ell \leftarrow u^\ell + S^\ell * \text{Relu}((f^\ell - A_\ell * u^\ell)).$$

end for

Form restricted residual and set initial guess:

$$u^{\ell+1,0} \leftarrow 0, \quad f^{\ell+1} \leftarrow R *_2 (f^\ell - A_\ell * u^\ell), A_{\ell+1} = R *_2 A_\ell * (R *_2^\top).$$

end for

Algorithm 5 is not convergent.

Algorithm 16 $(u^1, u^2, \cdots, u^J) = \text{MG0}(f; u^0; J, \nu_1, \cdots, \nu_J)$

Set up

$$f^1 = f, \quad u^1 = u^0.$$

Smoothing and restriction from fine to coarse level (nested)
for $\ell = 1 : J$ **do**
  for $i = 1 : \nu_\ell$ **do**

$$u^\ell \leftarrow u^\ell + \text{Relu}(S^\ell * (f^\ell - A_\ell * u^\ell)). \tag{8.125}$$

  end for
  Form restricted residual and set initial guess:

$$u^{\ell+1,0} \leftarrow 0, \quad f^{\ell+1} \leftarrow R *_2 (f^\ell - A_\ell * u^\ell), A_{\ell+1} = R *_2 A_\ell * (R*_2^\top).$$

end for

Algorithm 6 is convergent, the iterative steps is list below. $l = 2$

J	MG	Algorithm 6
2	15	27
3	16	35
4	17	38

8.9.1 Π is interpolation

Not Convergent

$$u^{\ell,i} \leftarrow u^{\ell,i-1} + \text{Relu} \circ B_{\ell,i}(f^\ell - A^\ell(u^{\ell,i-1})). \tag{8.126}$$

$$u^{\ell,i} \leftarrow u^{\ell,i-1} + B_{\ell,i} \circ \text{Relu}(f^\ell - A^\ell(u^{\ell,i-1})). \tag{8.127}$$

Almost the same as without Relu

$$u^{\ell,i} \leftarrow u^{\ell,i-1} + B_{\ell,i}(f^\ell - \text{Relu} \circ A^\ell(u^{\ell,i-1})). \tag{8.128}$$

$$u^{\ell,i} \leftarrow u^{\ell,i-1} + B_{\ell,i}(f^\ell - A^\ell \circ \text{Relu}(u^{\ell,i-1})). \tag{8.129}$$

8.10 Multigrid methods for nonlinear problem

In classification, the key problem can be reduced to find the representation (feature) for high dimension image for classifying. Here we propose to solve the next unbalanced nonlinear system

$$L(u) = f, \tag{8.130}$$

for finding the suitable feature representation $u \in \mathbb{R}^c$ for image $f \in \mathbb{R}^n$. The rationality of system can be traced back to the low-dimension assumption that natural image need to be concentrated on a low-dimension manifold with respect to the pixel space.

In order to motivate how to deal with the nonlinear system (8.130), we consider a simple nonlinear model problem

$$\begin{cases} -\nabla \cdot (a(u)\nabla u) + c(u) = f, & x \in \Omega, \\ u = 0 \quad \text{on} \quad \partial\Omega. \end{cases} \tag{8.131}$$

The weak formulation of (8.131) reads: Find $u \in H_0^1(\Omega)$, such that

$$(a(u)\nabla u, \nabla v) + (c(u), v) = (f, v), \quad \forall v \in H_0^1(\Omega).$$

Define

$$(L(u), v) = (a(u)\nabla u, \nabla v) + (c(u), v). \tag{8.132}$$

Then we have

$$L(u) = f. \tag{8.133}$$

Now the discretization problem reads: Find $u_h \in V_h$ such that

$$(a(u_h)\nabla u_h, \nabla v_h) + (c(u_h), v_h) = (f, v_h) \quad \forall v_h \in V_h. \tag{8.134}$$

Again define

$$(L_h(u_h), v_h) = (a(u_h)\nabla u_h, \nabla v_h) + (c(u_h), v_h).$$

Then we obtain

$$L_h(u_h) = f_h. \tag{8.135}$$

If $a(u_h)$ is a constant, then (8.135) reduces to a linear system and we denote the linear system as $A_h u_h = f_h$.

Recall the two grid method described in (8.114), (8.115), (8.116), (8.117) and (8.118) for linear problem

$$A_h u_h = f_h, \tag{8.136}$$

reads as following three steps:

1. Fine grid smoothing:
$$u_h \leftarrow u_h + S_h(f_h - A_h u_h)$$
such as gradient descent method.
2. Coarse grid correction: solving the residual equation restricted on the coarse grid $\mathcal{T}_{2h}$ to obtain
$$A_{2h} e_{2h} = Q_{2h} r^h$$
with $r^h = f_h - A_h u_h$.
3. Update: $u_h \leftarrow u_h + e_{2h}$.

Coarse grid correction for the linear case can be rewritten as:

$$A_{2h} e_{2h} = Q_{2h}(f_h - A_h u_h).$$

For any u_h^0, we write the above equation as

$$Q_{2h}(A_h(u_h^0 + e_{2h}) - A_h u_h^0) = Q_{2h}(f_h - A_h u_h). \tag{8.137}$$

Noting that $Q_{2h}A_h = A_{2h}P_{2h}$, where P_{2h} is the energy projection into V_{2h}. Therefore (8.137) can be written as

$$A_{2h}(P_{2h}u_h^0 + e_{2h}) = Q_{2h}(f_h - A_h u_h) + A_{2h}(P_{2h}u_h^0). \tag{8.138}$$

Now let

$$u_{2h,0} = P_{2h}u_h^0 \quad \text{and} \quad u_{2h} = P_{2h}u_h^0 + e_{2h},$$

then solving e_{2h} in (8.138) is equivalent to solve u_{2h} in the following equation

$$A_{2h}u_{2h} = Q_{2h}(f_h - A_h u_h) + A_{2h}(u_{2h,0}). \tag{8.139}$$

In this case, noting that $e_{2h} = u_{2h} - P_{2h}u_h^0 = u_{2h} - u_{2h,0}$, hence the step 3 means

$$\text{Update: } u_h \leftarrow u_h + u_{2h} - u_{2h,0}.$$

In summery, the two grid method for the linear system (8.136) can be rewritten as following three steps:

1. Fine grid smoothing:
$$u_h \leftarrow u_h + S_h(f_h - A_h u_h)$$
such as gradient descent method.
2. Coarse grid correction: for any u_h^0, solving the residual equation restricted on the coarse grid $\mathcal{T}_{2h}$ to obtain
$$u_{2h,0} = P_{2h}u_h^0, \quad A_{2h}u_{2h} = Q_{2h}(f_h - A_h u_h) + A_{2h}(u_{2h,0}).$$
where P_{2h} is the energy projection into V_{2h}.
3. Update: $u_h \leftarrow u_h + u_{2h} - u_{2h,0}$.

Usually, after the fine grid smoothing, we choose u_h^0 as the solution updated from the fine grid smoothing. And for nonlinear problems, we replace $P_{2h}u_h^0$ by $\Pi_h^{2h}u_h^0$, where Π_h^{2h} is an interpolation or projection from V_h to V_{2h}. Now we apply the above two grid method to the nonlinear system (8.135), namely $L_h(u_h) = f_h$, we obtain the two grid method for nonlinear system

1. Fine grid smoothing:
$$u_h \leftarrow u_h + S_h(f_h - L_h(u_h))$$
such as gradient descent method.
2. Coarse grid correction: solving the residual equation restricted on the coarse grid $\mathcal{T}_{2h}$ to obtain
$$u_{2h,0} = \Pi_h^{2h}u_h, \quad L_{2h}(u_{2h}) = Q_{2h}(f_h - L_h(u_h)) + L_{2h}(u_{2h,0}).$$
where Π_h^{2h} is an interpolation or projection from V_h to V_{2h}.
3. Update: $u_h \leftarrow u_h + u_{2h} - u_{2h,0}$.

To solve the nonlinear system, we can try the multilevel ideas with smoothing in fine level, and truncated it into coarse level by recursion. One strategy to involve the multi-scale idea is to "smoothing" in the fine level, and restrict it as a good approximation in the coarse level, this idea can be found in many literatures especially for multigrid methods in optimization [**? ?**]. So, there is a more general nonlinear multigrid named scheme-fully approximation scheme (FAS) [**? ?**], which can be considered as the generalization of linear multigrid Algorithm 11. Here we show a FAS algorithm with V-cycle as

Algorithm 17 $u =$ Bslash-FAS$(u^{1,0}, f, J, m_1, \cdots, m_J)$

Initialization
$$f^1 = f.$$
Smoothing and restriction from fine to coarse level (nested)
for $\ell = 1 : J$ **do**
Nonlinear relaxation on level ℓ:
for $i = 1 : m_j$ **do**
$$u^{\ell,i} = u^{\ell,i-1} + S_\ell^i(f^\ell - L^\ell(u^{\ell,i-1})).$$
end for
Form the initial guess and right side term for level $\ell + 1$:
$$u^{\ell+1,0} = \Pi_\ell^{\ell+1}u^{\ell,m_\ell}, \quad f^{\ell+1} = R_\ell^{\ell+1}(f^\ell - L^\ell(u^{\ell,m_\ell})) + L^{\ell+1}(u^{\ell+1,0}).$$
end for
Prolongation and correction from coarse to fine level
for $\ell = J - 1 : 1$ **do**
Form error in coarse level
$$e^{\ell+1} = u^{\ell+1,m_{\ell+1}} - u^{\ell+1,0}.$$

Correction by using error in coarse level

$$u^{\ell,m_\ell} \leftarrow u^{\ell,m_\ell} + P_{\ell+1}^{\ell} e^{\ell+1}.$$

end for

If the problem in (8.130) is linear, then we have the next theorem to show that this FAS scheme is consist with the classical multigrid methods for linear systems.

Theorem 19. *If $L(u)$ in (8.130) is a linear operation. Then Algorithm 17 is equivalent to Algorithm 11 with any choice of $\Pi_\ell^{\ell+1}$.*

8.11 A nonlinear BVP example

Consider the following boundary value problem

$$-u'' + 2u^3 = 0 \quad (0 < x < 1), \quad u(0) = \frac{1}{3} \text{ and } u(1) = \frac{1}{4}.$$

The analytical solution is $u = \frac{1}{x+3}$. The weak formulation becomes

$$(u', v') + (2u^3, v) = 0. \tag{8.140}$$

By choosing $u_h = \sum \alpha_i \phi_i$, we have

$$L_h(\boldsymbol{\alpha}) := A\boldsymbol{\alpha} + 2h\boldsymbol{\alpha}^3 - b, \tag{8.141}$$

where $A = \frac{1}{h}\begin{pmatrix} 2 & -1 & & & \\ -1 & 2 & -1 & & \\ & \vdots & \vdots & \vdots & \\ & & -1 & 2 & -1 \\ & & & -1 & 2 \end{pmatrix}$ and $b = \frac{1}{h}\begin{pmatrix} \frac{1}{3} \\ \vdots \\ \frac{1}{4} \end{pmatrix}$. We use gradient descent method and nonlinear multigrid method to solve (8.141). The smoother used in the nonlinear multigrid method is two steps of gradient descent method:

$$\boldsymbol{\alpha}^{n+1} = \boldsymbol{\alpha}^n - \eta L_h(\boldsymbol{\alpha}^n) - \eta L_h(\boldsymbol{\alpha}^n - \eta L_h(\boldsymbol{\alpha}^n))$$

where L_h is defined by (8.141) and η is the learning rate.

From the above numerical results shown in Table 8.11, the nonlinear multigrid method is uniform with respect to the size of unknowns and much faster than the gradient descent method.

Size of Unkowns	Nonlinear Multigrid ethod	Gradient Descent method
15	13 steps	61.6 k steps
31	14 steps	976.6 k steps
63	15 steps	> 1000 k steps
127	16 steps	> 1000 k steps
255	16 steps	> 1000 k steps
511	17 steps	> 1000 k steps
1023	18 steps	> 1000 k steps

Table 8.2. Number of iterations for $\|L_h(\boldsymbol{\alpha})\|/\|b\| \leq 10^{-6}$

9

Convolutional Neural Networks

9.1 Nonlinear classifiable sets

In the section, we will extend the linearly separable sets to the nonlinear case. A natural extension is like what the kernel method does in SVM for binary case. We will introduce the so-called feature mapping.

Definition 13 (nonlinearly separable sets). *These data sets $A_1, A_2, \cdots, A_k \subset \mathbb{R}^d$ are called nonlinearly separable, if there exist a feature space $\mathbb{R}^{\tilde{d}}$ and a smooth (if it has derivatives of all orders) feature mapping*

$$\varphi : \mathbb{R}^d \mapsto \mathbb{R}^{\tilde{d}} \tag{9.1}$$

such that

$$\tilde{A}_i := \varphi(A_i) = \{\tilde{x} \mid \tilde{x} = \varphi(x), x \in A_i\}, \quad i = 1, 2, \ldots, k, \tag{9.2}$$

are linearly separable.

Remark 5.

1. This definition is consistent with the definition of linearly separable as we can just take $\tilde{d} = d$ and $\varphi = \mathrm{id}$ if $A_1, A_2, \cdots, A_k$ are already linearly separable.
2. The kernel method in SVM is mainly based on this idea for binary case (k=2) where they use kernel functions to approximate $\varphi(x)$.
3. Most commonly used deep learning models are related to softmax mappings which means we can interpret these deep learning models as the approximation for feature mapping φ.

Theorem 20. *$A_1, A_2, \cdots, A_k \subset \mathbb{R}^d$ are nonlinearly separable is equivalent to that there exists a smooth classification function*

$$\psi : \mathbb{R}^d \mapsto \mathbb{R}^k \tag{9.3}$$

such that for all $1 \leq i \leq k$ and $j \neq i$

$$\psi_i(x) > \psi_j(x), \quad \forall x \in A_i. \tag{9.4}$$

Proof. On the one hand, it is easy to see that if $A_1, A_2, \cdots, A_k \subset \mathbb{R}^d$ are nonlinearly separable, we can take

$$\psi(x) = \boldsymbol{p}(\varphi(x); \theta), \tag{9.5}$$

where $\boldsymbol{p}(\varphi(x); \theta)$ is the softmax function for linearly separable sets $\varphi(A_i)$ for $i = 1, 2, \cdots, k$.

On the other hand, let assume that ψ is the smooth classification functions for $A_1, A_2, \cdots, A_k \subset \mathbb{R}^d$. We can take $\varphi(x) = \psi(x)$ and then

$$\varphi(A_1), \varphi(A_2), \cdots, \varphi(A_k) \subset \mathbb{R}^k \quad (\tilde{d} = k), \tag{9.6}$$

will be linearly separable. Recall the definition of softmax mapping in Definition 5, if we take $\theta = (I, 0)$ in softmax mapping $\boldsymbol{p}(x; \theta)$, then the monotonicity of e^x shows that for all $i = 1 : k$ and $j \neq i$

$$\boldsymbol{p}_i(\varphi(x); \theta) = \frac{e^{\psi_i(x)}}{\sum_{i=1}^k e^{\psi_i(x)}} > \frac{e^{\psi_j(x)}}{\sum_{i=1}^k e^{\psi_i(x)}} = \boldsymbol{p}_j(\varphi(x); \theta), \quad \forall x \in A_i. \tag{9.7}$$

□

Similar to linearly separable sets, we have the next lemma for $k = 2$.

Lemma 29. *A_1 and $A_2 \subset \mathbb{R}^d$ are nonlinearly separable is equivalent that there exists a function $\varphi : \mathbb{R}^d \mapsto \mathbb{R}$ such that*

$$\varphi(x) > 0 \quad \forall x \in A_1 \quad \textit{and} \quad \varphi(x) < 0 \quad \forall x \in A_2. \tag{9.8}$$

Proof. On the one hand, based the equivalence of nonlinearly separable sets, there exists $\psi_1(x)$ and $\psi_2(x)$ such that for all $i = 1 : 2$ and $j \neq i$

$$\psi_i(x) > \psi_j(x), \quad \forall x \in A_i. \tag{9.9}$$

Then, we can just take

$$\varphi(x) = \psi_1(x) - \psi_2(x). \tag{9.10}$$

On the other hand, if there exist $\varphi(x)$ satisfies (9.8), then we can construct $\psi_1(x)$ and $\psi_2(x)$ as

$$\psi_1(x) = \frac{1}{2}\varphi(x) \quad \text{and} \quad \psi_2(x) = -\frac{1}{2}\varphi(x). \tag{9.11}$$

□

Remark 6. Here the only assumption is that for all $i = 1 : k$ and $j \neq i$, we have $\psi_i(x) > \psi_j(x)$, $\forall x \in A_i$ for nonlinearly separable. We do not assume that $\psi_i(x) \geq 0$ or $\sum_{i=1}^k \psi_i(x) = 1$, which means that

$$\psi(x) = \Big(\psi_1(x), \psi_2(x), \cdots, \psi_k(x)\Big)^T$$

is not a discrete probability distribution over all k classes.

The previous theorem shows that the softmax function is not so crucial in nonlinearly separable case. Combined with deep learning models, we have the following understanding about what deep learning models.

1. If the classification model is followed with a softmax, then it is approximating the feature mapping $\varphi : \mathbb{R}^d \mapsto \mathbb{R}^{\tilde{d}}$.
2. If the classification model dose not followed by a softmax, then it is approximating $\psi : \mathbb{R}^d \mapsto \mathbb{R}^k$ directly.

Example 5. Consider $k = 2$ and

$$A_1 \subset \{(x_1, x_2) | x_1^2 + x_2^2 < 1\}, \quad A_2 \subset \{(x_1, x_2) | x_1^2 + x_2^2 > 1\},$$

then we have the following nonlinear feature mapping:

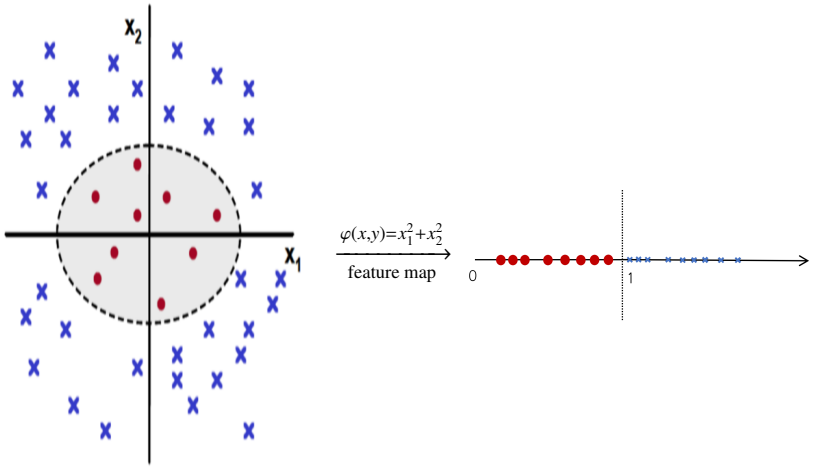

Here we have the following comparison between linear and nonlinear models from the viewpoint of loss functions:

Linear case (Logistic regression):

$$L_\lambda(\theta) = \sum_{j=1}^{N} \ell(y_j, p(x_j; \theta)) + \lambda R(\|\theta\|),$$

as defined in (2.38).

Nonlinear case:

$$L_\lambda(\theta) = \sum_{j=1}^{N} \ell(y_j, p(\varphi(x_j; \theta_1); \theta_2)) + \lambda R(\|\theta\|).$$

Here $p(x;\theta) = \text{softmax}(Wx+b)$ where $\theta = (W,b)$, and $\theta = (\theta_1,\theta_2)$ for the nonlinear case. For both cases, $\ell(q,p) = \sum_{i=1}^{k} -q_i \log p_i$ represents the cross-entropy, and $\lambda R(\|\theta\|)$ is the regularization term.

In general, we have the following popular nonlinear models for $\varphi(x;\theta)$:

1. Polynomials.
2. Piecewise polynomials (finite element method).
3. Kernel functions in SVM, see in Section 2.4.1.
4. Deep neural networks.

In this chapter, we first introduce some widely used convolutional operations, some examples of convolution filters and their performance, and then some popular convolutional neural network (CNN) models.

9.2 Convolutional operations

9.2.1 Images as matrix

An image can be viewed as a piecewise constant function on a grid. Images with different resolutions can then be viewed as functions on grids of different sizes. The use of such multiple-grids is a main technique used in the standard multigrid method for solving discretized partial differential equations, and it can also be interpreted as a main ingredient used in convolutional neural networks (CNN) for image calssification.

An image can be viewed as a function on a grid [**?**] on a rectangular domain $\Omega \in \mathcal{R}^2$. Without loss of generality, we assume that the grid, $\mathcal{T}$, is of size

$$m = 2^s, \quad n = 2^t$$

for some integers $s,t \geq 1$. Starting from $\mathcal{T}_1 = \mathcal{T}$, we consider a sequence of coarse grids with $J = \min(s,t)$ (as depicted in Fig. 9.2.1 with $J = 4$):

$$\mathcal{T}_1, \mathcal{T}_2, \ldots, \mathcal{T}_J \tag{9.12}$$

such that $\mathcal{T}_\ell$ consist of $m_\ell \times n_\ell$ grid points, with

$$m_\ell = 2^{s-\ell+1}, \quad n_\ell = 2^{t-\ell+1}. \tag{9.13}$$

Here, please note that each element in this grid can be viewed as a pixel or an image or an element in a matrix.

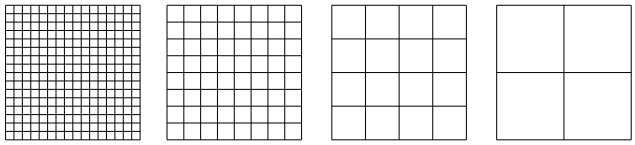

Fig. 9.1. multilevel grids for piecewise constant functions (images)

9.2.2 Convolution operation with one channel

For simplicity of exposition, we denote

$$m = m_1 = 2^s, \quad n = n_1 = 2^t. \tag{9.14}$$

Recall the definition of convolution in Definition 11. In image processing, a kernel, convolution matrix, or mask is a small matrix, denoted by K below. It is used for blurring, sharpening, embossing, edge detection, and more. This is accomplished by doing a convolution between a kernel and an image, denoted by g below. Convolution is the process of adding each element of the image to its local neighbors, weighted by the kernel.

Definition 14. *A convolution defined on $\mathbb{R}^{m\times n}$ is a linear mapping $K* : \mathbb{R}^{m\times n} \mapsto \mathbb{R}^{m\times n}$ defined with padding, for any $g \in \mathbb{R}^{m\times n}$ by:*

$$[K * g]_{i,j} = \sum_{p,q=-k}^{k} K_{p,q} g_{i+p,j+q}, \quad i = 1:m, j = 1:n. \tag{9.15}$$

The convolution maps the original image g to a modified one $K * g$ with the same size, and each element $[K * g]_{i,j}$ in the resulting image $K * g$ is a weighted average of elements in the original image g with weights $K_{p,q}$. The weights in (9.15) constitute a kernel matrix

$$K \in \mathbb{R}^{(2k+1)\times(2k+1)}, \tag{9.16}$$

where k is often taken as a small integer. Here we note that the indices for the entries in K are given in a special way. For example, if $k = 1$, $K \in \mathbb{R}^{3\times 3}$, and

$$K = \begin{pmatrix} K_{-1,-1} & K_{-1,0} & K_{-1,1} \\ K_{0,-1} & K_{0,0} & K_{0,1} \\ K_{1,-1} & K_{1,0} & K_{1,1} \end{pmatrix},$$

for we may have the following 2D Laplacian kernel

$$K = \begin{pmatrix} 0 & -1 & 0 \\ -1 & 4 & -1 \\ 0 & -1 & 0 \end{pmatrix}. \tag{9.17}$$

Here padding means how $g_{i+p,j+q}$ is defined when $(i+p, j+q)$ is out of $1:m$ or $1:n$. The following three choices are often used

$$g_{i+p,j+q} = \begin{cases} 0, & \text{zero padding,} \\ f_{(i+p) \pmod m,(s+q) \pmod n}, & \text{periodic padding,} \\ f_{|i-1+p|,|j-1+q|}, & \text{reflected padding,} \end{cases} \tag{9.18}$$

if

$$i + p \notin \{1, 2, \ldots, m\} \text{ or } j + q \notin \{1, 2, \ldots, n\}. \tag{9.19}$$

Here $d \pmod m \in \{1, \cdots, m\}$ means the remainder when d is divided by m.

Here is a diagram for convolution with one channel (and also stride one).

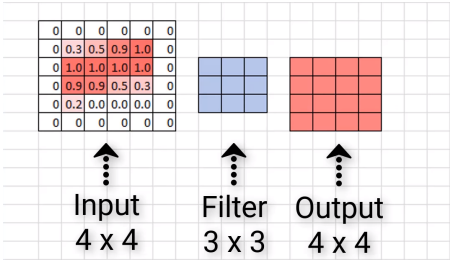

In [**?**], the authors show that by "averaging" the values of the finite element solution u_h of elliptic problem using convolution in the neighborhood of a point x they may construct an approximation to the true solution $u(x)$ which is often a better approximation than $u_h(x)$ itself. The "averaging" operator showed in [**?**] is just the convolution operator defined here and does not depend on the specific elliptic operator involved.

9.2.3 Convolution with stride (one channel)

Recall the definition of convolution with stride 2 in Definition 12, namely, for $g \in \mathbb{R}^{m\times n}$, convolution with stride 2 is defined as

$$[K *_2 g]_{i,j} = \sum_{p,q=-k}^{k} K_{p,q} g_{2i+p-1,2j+q-1}, \quad i = 1 : \lfloor \frac{m+1}{2} \rfloor, j = 1 : \lfloor \frac{n+1}{2} \rfloor. \tag{9.20}$$

Note that the convolution with stride 2 maps the original image with size $2m \times 2n$ to a new one with smaller size $m \times n$, namely lower resolution.

Lemma 30. *The convolution with stride* 2 *can be written as:*

$$K *_2 g = \mathcal{S}(K * g), \tag{9.21}$$

where $\mathcal{S}$ *is a stride operator defined by:*

$$\mathcal{S} : \mathbb{R}^{m\times n} \mapsto \mathbb{R}^{\frac{m+1}{2}\times\frac{n+1}{2}}, \tag{9.22}$$

with

$$[\mathcal{S}(g)]_{i,j} = g_{2i-1,2j-1}, \quad i = 1 : \lfloor\frac{m+1}{2}\rfloor, j = 1 : \lfloor\frac{n+1}{2}\rfloor. \tag{9.23}$$

Example 6. The so-called average pooling with kernel size 3×3 and stride 2 means

$$K *_2 \quad \text{with} \quad K = \frac{1}{9}\begin{pmatrix} 1 & 1 & 1 \\ 1 & 1 & 1 \\ 1 & 1 & 1 \end{pmatrix}. \tag{9.24}$$

We note that, in general, for any given integer $s \geq 1$, a convolution with stride s for $g \in \mathbb{R}^{m\times n}$ can be defined as:

$$[K *_s g]_{i,j} = \sum_{p,q=-k}^{k} K_{p,q} g_{s(i-1)+p+1,s(j-1)+q+1}, \quad i = 1 : \lfloor\frac{m+1}{s}\rfloor, j = 1 : \lfloor\frac{n+1}{s}\rfloor. \tag{9.25}$$

Here $\lfloor\frac{m}{s}\rfloor$ denotes the biggest integer that less than $\frac{m}{s}$. Similarly, the convolution with stride s maps the original image with size $sm \times sn$ to a new one with smaller size $m \times n$. The following is a diagram for stride 2.

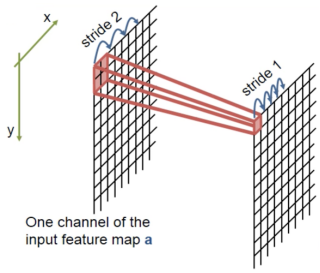

9.2.4 Convolutional operations with multi-channel

In many applications, we need to deal with images with multiple channels. A typical example is the RGB image, where each RGB channel emphasizes different aspects of the original images. Then the inputs become a three-dimensional tensor with size $3 \times m \times n$. We refer to this axis, with a size of 3, as the channel dimension.

When the input data contain multiple channels, we need to construct a convolution kernel with the same number of input channels as the input data, so that it can perform cross-correlation with the input data. One important class of linear mapping is the so-called convolution:

$$\theta : \mathbb{R}^{c\times m\times n} \mapsto \mathbb{R}^{h\times m\times n},$$

where $m \times n$ is called the spatial dimension or resolution, c and h are corresponding to input and output channels. Let $f \in \mathbb{R}^{c\times m\times n}$ and the t-th channel $[f]_t \in \mathbb{R}^{m\times n}$. The operation is defined by

$$[\theta(f)]_s = \sum_{t=1}^{c} \mathbf{K}_{s,t} * [f]_t + b_s \mathbf{1} \in \mathbb{R}^{m\times n}, \quad s = 1 : h, \tag{9.26}$$

where $\mathbf{1} \in \mathbb{R}^{m\times n}$ is a $m \times n$ matrix with all elements being 1, and $\mathbf{K}_{s,t}$ is a convolution operator which maps $[f]_t \in \mathbb{R}^{m\times n}$ to $[\theta(f)]_s \in \mathbb{R}^{m\times n}$.

$$[\mathbf{K}_{s,t} * [f]_t]_{i,j} = \sum_{p,q=-k}^{k} K_{s,t;p,q} f_{t;i+p,j+q}, \quad i = 1 : m, j = 1 : n. \tag{9.27}$$

The coefficients kernel $\mathbf{K}_{s,t}$ in (9.27) constitute a kernel matrix

$$\mathbf{K}_{s,t} \in \mathbb{R}^{(2k+1)\times(2k+1)}, \tag{9.28}$$

where k is often taken as small integers.

Here a more compact notation for multi-channel convolution can be written as

$$\theta(f) = \mathbf{K} * f + \mathbf{b} \tag{9.29}$$

where

$$f = \begin{pmatrix} [f]_1 \\ [f]_2 \\ \vdots \\ [f]_c \end{pmatrix}, \quad \mathbf{K} = \begin{pmatrix} K_{1,1} & K_{1,2} & \cdots & K_{1,c} \\ K_{2,1} & K_{2,2} & \cdots & K_{2,c} \\ \vdots & \vdots & \ddots & \vdots \\ K_{h,1} & K_{h,2} & \cdots & K_{h,c} \end{pmatrix}, \quad \mathbf{b} = \begin{pmatrix} b_1\mathbf{1} \\ b_2\mathbf{1} \\ \vdots \\ b_h\mathbf{1} \end{pmatrix} = b \otimes \mathbf{1}. \tag{9.30}$$

Furthermore, we have the following natural extension of convolution with stride for multi-channel by

$$[\theta(f)]_s = \sum_{t=1}^{c} \mathbf{K}_{s,t} *_2 [f]_t + b_s \mathbf{1} \in \mathbb{R}^{\tilde{m}\times\tilde{n}}, \quad s = 1:h, \tag{9.31}$$

where

$$\tilde{m} = \lfloor \frac{m+1}{2} \rfloor, \quad \tilde{n} = \lfloor \frac{n+1}{2} \rfloor, \tag{9.32}$$

9.2.5 Pooling operation in CNNs

When processing images, we want to gradually reduce the spatial resolution of our hidden representations, aggregating information so that the higher up we go in the network, the larger the receptive field (in the input) to which each hidden node is sensitive.

Finally, we introduce another type of important operation in CNNs – pooling. The key purpose for pooling operator is to reduce the spatial resolution of images (features) in a typical CNN models. Basically, pooling is an operator

$$T : \mathbb{R}^{c_1\times m_1\times n_1} \mapsto \mathbb{R}^{c_2\times m_2\times n_2}. \tag{9.33}$$

where

$$m_2 = \lfloor \frac{m+1}{s} \rfloor, \quad n_2 = \lfloor \frac{n+1}{s} \rfloor, \tag{9.34}$$

for any choice of $c_2 \geq 1$. Here s is also called the stride in pooling operations. There are generally two types of pooling:

Convolution with stride s as pooling

In this case, it often happens that

$$T = R*_s, \quad (s = 2 \text{ for the main case }). \tag{9.35}$$

Here R can be learned or fixed such as average pooling as we discussed before.

Nonlinear pooling

The most commonly used nonlinear pooling is called max-pooling, a max pooling with kernel size $(2k+1)\times(2k+1)$ and stride s is is defined as

$$[R_{\max}(f)]_{t;i,j} = \max\{f_{t;s(i-1)+p+1,s(j-1)+q+1} \mid -k \leq p,q \leq k\}, \tag{9.36}$$

here t means channel and $c_2 = c_1$ in this case.

Here is an example for max-pooling with kernel size 3×3 and stride 3.

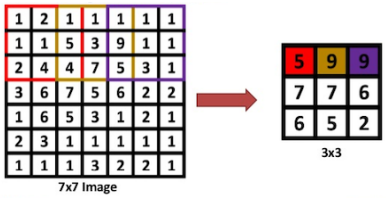

9.3 Examples of convolution filters and performance

In this section, we will give a brief description how convolution operations are used for image processing. One useful description can be found in the following link:

http://aishack.in/tutorials/image-convolution-examples/

Convolutions is a technique for general signal processing. People studying electrical/electronics will tell you the near-infinite sleepless nights these convolutions have given them. Entire books have been written on this topic. And the questions and theorems that need to be proved are insurmountable. But for computer vision, we'll just deal with some simple things.

A convolution lets you do a very wide variety of things, like calculating derivatives, detecting edges, apply ing blurs, etc. And all of this is done with a "convolution kernel".

9.3.1 Calculation with convolutions

The most direct way to compute a convolution would be to use multiple for loops. But that causes a lot of repeated calculations. And as the size of the image and kernel increases, the time to compute the convolution increases quite drastically.

Techniques haves been developed to calculate convolutions rapidly. One such technique is using the Discrete Fourier Transform. It converts the entire convolution operation into a simple multiplication. Fortunately, you don't need to know the math to do this in OpenCV. It automatically decides whether to do it in frequency domain (after the DFT) or not.

9.3.2 Image convolution examples

A convolution is very useful for signal processing in general. There is a lot of complex mathematical theory available for convolutions. For digital image processing, you don't have to understand all of that. You can use a simple matrix as an image convolution kernel and do some interesting things!

9.3.3 Line detection by 1D Laplacian

With image convolutions, you can easily detect lines. Figure 9.2 represents the four convolutions to detect horizontal, vertical and lines at 45 and 135 degrees: Figure 9.3, 9.4, 9.5 and 9.6 plot the 0,90,45,135 lines detection that I got on an image.

In Figure 9.4, the black background is the original result, the white background is obtained by subtracting the original result from 255, the same below.

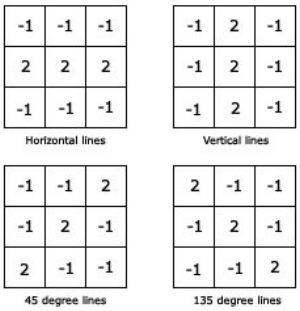

Fig. 9.2. Four convolutions to detect horizontal, vertical and lines at degrees 0,90,45,135.

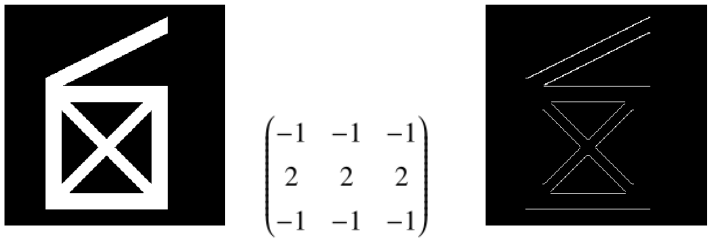

$$\begin{pmatrix} -1 & -1 & -1 \\ 2 & 2 & 2 \\ -1 & -1 & -1 \end{pmatrix}$$

(a) image (b) filter (c) result

Fig. 9.3. A horizontal line detection done with convolutions.

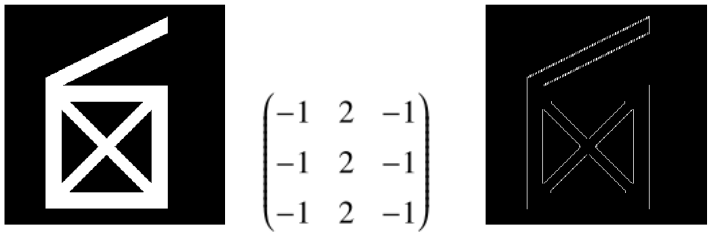

$$\begin{pmatrix} -1 & 2 & -1 \\ -1 & 2 & -1 \\ -1 & 2 & -1 \end{pmatrix}$$

(a) image (b) filter (c) result

Fig. 9.4. A vertical line detection done with convolutions.

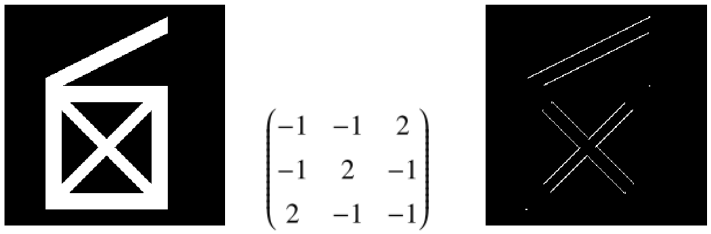

$$\begin{pmatrix} -1 & -1 & 2 \\ -1 & 2 & -1 \\ 2 & -1 & -1 \end{pmatrix}$$

(a) image (b) filter (c) result

Fig. 9.5. A 45 degree line detection done with convolutions.

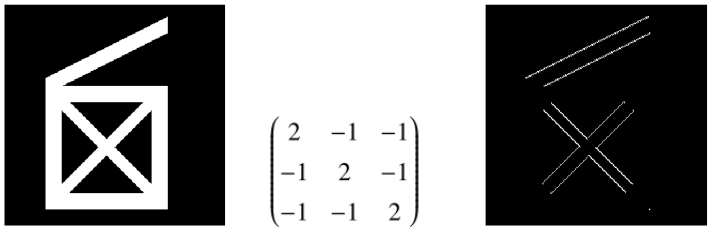

$$\begin{pmatrix} 2 & -1 & -1 \\ -1 & 2 & -1 \\ -1 & -1 & 2 \end{pmatrix}$$

(a) image (b) filter (c) result

Fig. 9.6. A 135 degree line detection done with convolutions.

9.3.4 Edge detection by 2D Laplacian operator

The laplacian is the second derivative of the image. It is extremely sensitive to noise, so it isn't used as much as other operators. Unless, of course you have specific requirements.

0	-1	0
-1	4	-1
0	-1	0

The laplacian operator

-1	-1	-1
-1	8	-1
-1	-1	-1

The laplacian operator (include diagonals)

Here's the result of the convolution kernel without diagonals:

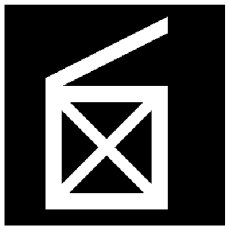

(a) image

$$\begin{pmatrix} 0 & -1 & 0 \\ -1 & 4 & -1 \\ 0 & -1 & 0 \end{pmatrix}$$

(b) filter

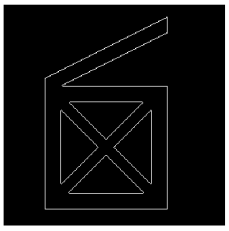

(c) result

(d) image

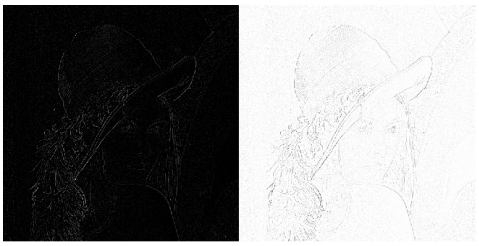

(e) result

Fig. 9.7. A laplace operator done with convolutions

Below is the result of the convolution kernel with diagonals.

(a) image

$$\begin{pmatrix} -1 & -1 & -1 \\ -1 & 8 & -1 \\ -1 & -1 & -1 \end{pmatrix}$$

(b) filter

(c) result

(d) image (e) result

Fig. 9.8. A laplace operator including diagonals are done with convolutions

9.3.5 The Laplacian of Gaussian

The laplacian alone has the disadvantage of being extremely sensitive to noise. So, smoothing the image before a laplacian improves the results we get. This is done with a 5x5 image convolution kernel.

0	0	-1	0	0
0	-1	-2	-1	0
-1	-2	16	-2	-1
0	-1	-2	-1	0
0	0	-1	0	0

Below is the result by applying this image convolution.

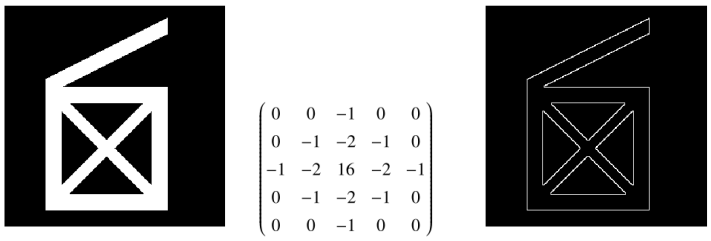

$$\begin{pmatrix} 0 & 0 & -1 & 0 & 0 \\ 0 & -1 & -2 & -1 & 0 \\ -1 & -2 & 16 & -2 & -1 \\ 0 & -1 & -2 & -1 & 0 \\ 0 & 0 & -1 & 0 & 0 \end{pmatrix}$$

(a) image (b) filter (c) result

(d) image

(e) result

Fig. 9.9. A Laplacian of Gaussian operator done with convolutions

9.3.6 Other examples with ReLU activation

(a) input image

$$\begin{pmatrix} 0 & 0 & -1 & 0 & 0 \\ 0 & -1 & -2 & -1 & 0 \\ -1 & -2 & 16 & -2 & -1 \\ 0 & -1 & -2 & -1 & 0 \\ 0 & 0 & -1 & 0 & 0 \end{pmatrix}$$

(b) filter

(c) convolution result

(d) result after ReLU

$$\begin{pmatrix} \frac{1}{9} & \frac{1}{9} & \frac{1}{9} \\ \frac{1}{9} & \frac{1}{9} & \frac{1}{9} \\ \frac{1}{9} & \frac{1}{9} & \frac{1}{9} \end{pmatrix}$$

(e) filter

(f) result after average

9.3.7 Summary

These examples show how different convolution kernels modify an image in different ways. Note that the filter plays an important role in detecting edges on an image.

9.4 Some popular CNN models

In this section, we will use these convolutional operations introduced above to give a brief description of some classic convolutional neural network (CNN) models. Firstly, CNNs are actually a class of special DNN models. Let us recall the DNN structure as:

$$\begin{cases} f^0(x) &= x \\ f^\ell(x) &= \sigma(\theta^\ell(f^{\ell-1})) \quad \ell = 1:L\,, \\ f(x) &= W^L f^L + b^L \end{cases} \tag{9.37}$$

where f^0 is the original image, θ^ℓ is a linear mapping and σ is the activation function

$$\theta^\ell(f^{\ell-1}) = W^\ell f^{\ell-1}(x) + b^\ell. \tag{9.38}$$

The key features of CNNs are

1. Replace the general linear mapping θ^ℓ by convolution operations with multi-channel.
2. Use multi-resolution of images as shown in the next diagram.

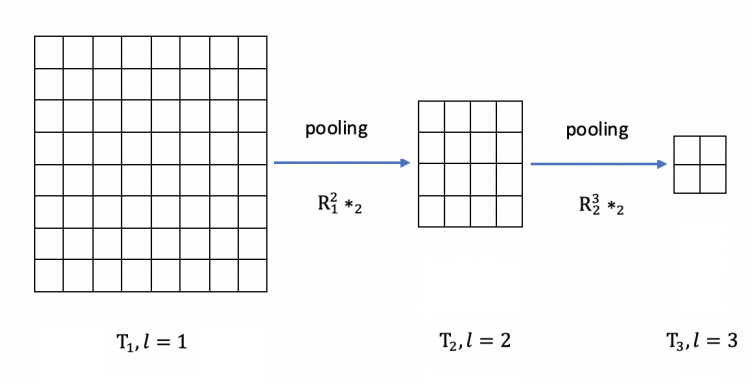

Then we will introduce some classical architectures in convolution neural networks.

9.4.1 LeNet-5, AlexNet and VGG

LeNet-5 [**?**] is aconvolutional network designed for handwritten and machine-printed character recognition. AlexNet [**?**] showed, for the first time, that the features obtained by learning can transcend manually-designed features, breaking the previous paradigm in computer vision. While previous derivatives of AlexNet focused on

smaller window sizes and strides in the first convolutional layer, VGG [**?**] addresses another very important aspect of CNNs: depth.

The LeNet-5, AlexNet and VGG can be written as:

Algorithm 18 h = Classic CNN$(f; J, \nu_1, \cdots, \nu_J)$

1: Initialization: $f^{1,0} = f_{\text{in}}(f)$.
2: **for** $\ell = 1 : J$ **do**
3: **for** $i = 1 : \nu_\ell$ **do**
4: Basic Block:

$$f^{\ell,i} = \sigma\left(\theta^{\ell,i} * f^{\ell,i-1}\right) \tag{9.39}$$

5: **end for**
6: Pooling(Restriction):

$$f^{\ell+1,0} = R_\ell^{\ell+1} *_2 f^{\ell,\nu_\ell} \tag{9.40}$$

7: **end for**
8: Final average pooling layer: $h = R_{\text{ave}}(f^{L,\nu_\ell})$.

Here $R_\ell^{\ell+1}*_2$ represents for the pooling operation to sub-sampling these tensors into coarse spatial level (lower resolution). Here we use $R_\ell^{\ell+1}*_2$ to stand for the pooling operation. In general we can also have

- average pooling: fixed kernels such as

$$R_\ell^{\ell+1} = \frac{1}{9}\begin{pmatrix} 1 & 1 & 1 \\ 1 & 1 & 1 \\ 1 & 1 & 1 \end{pmatrix} \tag{9.41}$$

- Max pooling $R_{\max}$ as discussed before.

In these classic CNN models, they still need some extra fully connected layers after h as the output of CNNs. After few layers of fully connected layers, the model is completed by following a multi-class logistic regression model.

These fully connected layers are removed in ResNet to be described below.

9.4.2 ResNet

The original ResNet developed in [**?**] is one of the most popular CNN architectures in image classification problems.

Algorithm 19 h = ResNet$(f; J, \nu_1, \cdots, \nu_J)$

1: Initialization: $r^{1,0} = f_{\text{in}}(f)$.
2: **for** $\ell = 1 : J$ **do**
3: **for** $i = 1 : \nu_\ell$ **do**

4: Basic Block:

$$r^{\ell,i} = \sigma\left(r^{\ell,i-1} + A^{\ell,i} * \sigma \circ B^{\ell,i} * r^{\ell,i-1}\right). \tag{9.42}$$

5: **end for**
6: Pooling(Restriction):

$$r^{\ell+1,0} = \sigma\left(R_\ell^{\ell+1} *_2 r^{\ell,\nu_\ell} + A^{\ell+1,0} \circ \sigma \circ B^{\ell+1,0} *_2 r^{\ell,\nu_\ell}\right). \tag{9.43}$$

7: **end for**
8: Final average pooling layer: $h = R_{\text{ave}}(r^{L,\nu_\ell})$.

Here $f_{\text{in}}(\cdot)$ may depend on different data set and problems such as $f_{\text{in}}(f) = \sigma \circ \theta^0 * f$ for CIFAR [**?**] and $f_{\text{in}}(f) = R_{\max} \circ \sigma \circ \theta^0 * f$ for ImageNet [**?**] as in [**?**]. In addition $r^{\ell,i} = r^{\ell,i-1} + A^{\ell,i} * \sigma \circ B^{\ell,i} * \sigma(r^{i-1})$ is often called the basic ResNet block. Here, $A^{\ell,i}$ with $i \geq 0$ and $B^{\ell,i}$ with $i \geq 1$ are general 3×3 convolutions with zero padding and stride 1. In pooling block, $*_2$ means convolution with stride 2 and $B^{\ell,0}$ is taken as the 3×3 kernel with same output channel dimension of $R_\ell^{\ell+1}$ which is taken as 1×1 kernel and called as projection operator in [**?**]. During two consecutive pooling blocks, index ℓ means the fixed resolution or we ℓ-th grid level as in multigrid methods. Finally, R_{ave} ($R_{\max}$) means average (max) pooling with different strides which is also dependent on datasets and problems.

9.4.3 pre-act ResNet

The pre-act ResNet [**?**] shares a similar structure with ResNet.

Algorithm 20 h = pre-act ResNet(f; $J, \nu_1, \cdots, \nu_J$)

1: Initialization: $r^{1,0} = f_{\text{in}}(f)$.
2: **for** $\ell = 1 : J$ **do**
3: **for** $i = 1 : \nu_\ell$ **do**
4: Basic Block:

$$r^{\ell,i} = r^{\ell,i-1} + A^{\ell,i} * \sigma \circ B^{\ell,i} * \sigma(r^{\ell,i-1}). \tag{9.44}$$

5: **end for**
6: Pooling(Restriction):

$$r^{\ell+1,0} = R_\ell^{\ell+1} *_2 r^{\ell,\nu_\ell} + A^{\ell+1,0} \circ \sigma \circ B^{\ell+1,0} *_2 \sigma(r^{\ell,\nu_\ell}). \tag{9.45}$$

7: **end for**
8: Final average pooling layer: $h = R_{\text{ave}}(r^{L,\nu_\ell})$.

Here pre-act ResNet share almost the same setup with ResNet.

The only difference between ResNet and pre-act ResNet can be viewed as putting a σ in different places. The connection of those three models are often shown with next diagrams:

Without loss of generality, we extract the key feedforward steps on the same grid in different CNN models as follows.

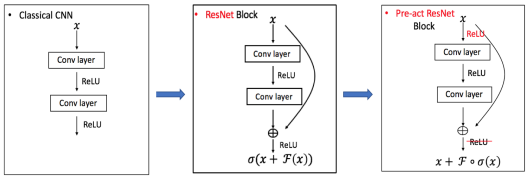

Fig. 9.10. Comparison of CNN Structures

Classic CNN

$$f^{\ell,i} = \xi^i \circ \sigma(f^{\ell,i-1}) \quad \text{or} \quad f^{\ell,i} = \sigma \circ \xi^i(f^{\ell,i-1}). \tag{9.46}$$

ResNet

$$r^{\ell,i} = \sigma(r^{\ell,i-1} + A^{\ell,i} \circ \sigma \circ B^{\ell,i}(r^{\ell,i-1})). \tag{9.47}$$

pre-act ResNet

$$r^{\ell,i} = r^{\ell,i-1} + A^{\ell,i} \circ \sigma \circ B^{\ell,i} \circ \sigma(r^{\ell,i-1}). \tag{9.48}$$

10

MgNet: a Unified Framework for CNN and MG

In this chapter, motivated by the multigrid method, we design a unified framework for convolutional neural network and multigrid method named MgNet. We first propose the framework and discuss some features of the new network structure. Then we discuss the relation between MgNet and ResNet. We will establish some new understandings of ResNet from the point view of MgNet.

10.1 MgNet: a new network structure

In this section, we introduce a new neural network structure, named as MgNet [**?**], motivated by the multigrid algorithm, Algorithm 10, as discussed in the previous section.

Here we recall the most important two structures in multigrid

1. iterative scheme (for linear system)

$$u^{\ell,i} = u^{\ell,i-1} + B^{\ell,i}(f^\ell - A^\ell * u^{\ell,i-1}). \tag{10.1}$$

2. interpolation and restriction

$$u^{\ell+1,0} = \Pi_\ell^{\ell+1} *_2 u^\ell, \quad f^{\ell+1} = R_\ell^{\ell+1} *_2 (f^\ell - A^\ell(u^\ell)) + A^{\ell+1} * u^{\ell+1,0}. \tag{10.2}$$

Considering the fine to coarse process of multigrid with the aforementioned two structures in (10.1) and (10.2). We are now in a position to state the main algorithm, namely MgNet by just putting some nonlinear activation function σ in some places.

Algorithm 21 $u^J = \text{MgNet}(f; J, \nu_1, \cdots, \nu_J)$

Initialization: $f^1 = \theta(f)$, $u^{1,0} = 0$
for $\ell = 1 : J$ **do**
  for $i = 1 : \nu_\ell$ **do**

$$u^{\ell,i} = u^{\ell,i-1} + \sigma \circ B^{\ell,i} * \sigma(f^\ell - A^\ell * u^{\ell,i-1}). \tag{10.3}$$

end for
Note $u^\ell = u^{\ell,\nu_\ell}$

$$u^{\ell+1,0} = \Pi_\ell^{\ell+1} *_2 u^\ell \tag{10.4}$$

$$f^{\ell+1} = R_\ell^{\ell+1} *_2 (f^\ell - A^\ell(u^\ell)) + A^{\ell+1} * u^{\ell+1,0}. \tag{10.5}$$

end for

Theorem 21. *If A^ℓ, $R_\ell^{\ell+1}$ and $B^{\ell,i} = S^\ell$ are all linear operations as described in multigrid method in §8.2 and all $\sigma = id$ in Algorithm 21. Then Algorithm 10 is equivalent to Algorithm 21 with any choice of $\Pi_\ell^{\ell+1}$.*

Proof. Here we replace $u^{\ell,i}$ and f^ℓ by $\tilde{u}^{\ell,i}$ and $\tilde{f}^\ell$ in MgNet. What we want to prove are

$$\tilde{f}^\ell = f^\ell + A_\ell \tilde{u}^{\ell,0} \quad \text{and} \quad u^{\ell,i} = \tilde{u}^{\ell,i} - \tilde{u}^{\ell,0}, \tag{10.6}$$

with $u^{\ell,i}$, f^ℓ in Algorithm 10 and $\tilde{u}^{\ell,i}$, $\tilde{f}^\ell$ in Algorithm 21 for any choice of $\Pi_\ell^{\ell+1}$. We prove this result by induction.

- It is easy to check that $\ell = 1$ is right by taking $\theta = \text{id}$.
- Once the above equation (10.6) is right for ℓ, let us prove the corresponded result for $\ell + 1$.
  - For $\tilde{f}^{\ell+1}$, as the definition in Algorithm 21, we have

$$\begin{aligned}
\tilde{f}^{\ell+1} &= R_\ell^{\ell+1}(\tilde{f}^\ell - A^\ell \tilde{u}^{\ell,\nu_\ell}) + A^{\ell+1}\tilde{u}^{\ell+1,0}, \\
&= R_\ell^{\ell+1}(f^\ell + A^\ell \tilde{u}^{\ell,0} - A^\ell \tilde{u}^{\ell,\nu_\ell}) + A^{\ell+1}\tilde{u}^{\ell+1,0} \\
&= R_\ell^{\ell+1}(f^\ell - A^\ell(\tilde{u}^{\ell,\nu_\ell} - u^{\ell,0})) + A^{\ell+1}\tilde{u}^{\ell+1,0} \\
&= R_\ell^{\ell+1}(f^\ell - A^\ell u^{\ell,\nu_\ell}) + A^{\ell+1}\tilde{u}^{\ell+1,0}, \\
&= f^{\ell+1} + A^{\ell+1}\tilde{u}^{\ell+1,0}.
\end{aligned}$$

  - For $u^{\ell+1,i}$, first we have

$$u^{\ell+1,0} = 0 = \tilde{u}^{\ell+1,0} - \tilde{u}^{\ell+1,0},$$

    then we prove

$$u^{\ell+1,i} = \tilde{u}^{\ell+1,i} - \tilde{u}^{\ell+1,0} \tag{10.7}$$

    by induction for i.
    We assume (10.7) holds for $0, 1, \cdots, i-1$. Let us miner $\tilde{u}^{\ell+1,0}$ in both sides of the smoothing process (10.3) in Algorithm 21. Then we have

$$\begin{aligned}
\tilde{u}^{\ell+1,i} - \tilde{u}^{\ell+1,0} &= \tilde{u}^{\ell+1,i-1} - \tilde{u}^{\ell+1,0} + B^{\ell+1,i}(\tilde{f}^{\ell+1} - A^{\ell+1}\tilde{u}^{\ell+1,i-1}), \\
&= \tilde{u}^{\ell+1,i-1} - \tilde{u}^{\ell+1,0} + B^{\ell+1,i}(f^{\ell+1} + A^{\ell+1}\tilde{u}^{\ell+1,0} - A^{\ell+1}\tilde{u}^{\ell+1,i-1}), \\
&= u^{\ell+1,i-1} + B^{\ell+1,i}(f^{\ell+1} - A^{\ell+1}u^{\ell+1,i-1}).
\end{aligned}$$

    This is exact the smoothing process in Algorithm 10 as we take $B^{\ell+1,i} = S^{\ell+1}$.

The main steps in MgNet can be understood as solving the following data-feature mappings in each grid ℓ:

$$A^\ell * u^\ell = f^\ell, \quad \ell = 1 : J, \tag{10.8}$$

where

$$f^\ell \in \mathbb{R}^{c_\ell \times m_\ell \times n_\ell}, \tag{10.9}$$

and

$$u^\ell \in \mathbb{R}^{h_\ell \times m_\ell \times n_\ell}, \tag{10.10}$$

with constrain

$$u \geq 0. \tag{10.11}$$

More details about this basic assumption in image classification can be found in [**?**].

Here, the next diagram gives a brief illustration for the above structure.

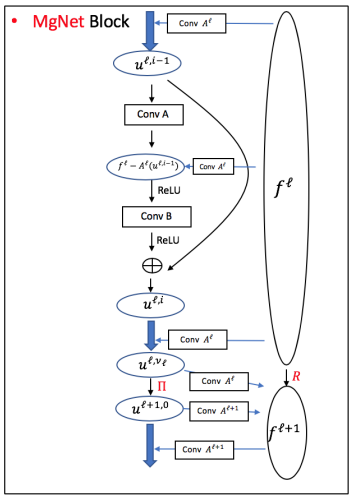

Fig. 10.1. Structure of MgNet

The first property of MgNet is that it recovers the multigrid methods. Despite of the simplicity look of Algorithm 21, there are rich mathematical structures and variants which we will briefly discuss below.

10.1.1 Initialization: feature space channels

Initially for $\ell = 1$, we take $m_1 = m$ and $n_1 = n$ and we may define the linear mapping

$$\theta : \mathbb{R}^{c\times m\times n} \mapsto \mathbb{R}^{c_1\times m_1\times n_1}, \tag{10.12}$$

to obtain $f^1 = \theta(f)$ with c changed to the channel of the initial data space to c_1. Usually

$$c_1 \geq c. \tag{10.13}$$

One possibility is that we choose $c_1 = c$. In this case, we choose θ to be identity. But in general, we may need to choose $c_1 \gg c$. One possible advantage of preprocessing the RGB ($c = 3$) to different color spaces is that we can better choose what kind of features the CNN can detect, and under what conditions those detections will be invariant.

One possibility of understanding and modifying this step is to decompose the data f into a number of more specialized data

$$f = \sum_{k=1}^{c_1} \xi_k f_k^1 = \xi^T f^1. \tag{10.14}$$

We may use some knowledge from image processing or physics to design a procedure to obtain the right decomposition of (10.14), or we can just train it. Conceivably, we may view $f^1 = \theta(f)$ as a special approximation solution of (10.14) with the same sparsity pattern to ξ.

10.1.2 Extracted units: u^ℓ and channels

The first new feature and the main new ingredient in the proposed neural network is the introduction of feature variables u^ℓ in (10.10), which will be known as the extracted units.

We emphasize that the extracted-units u^ℓ and the data f^ℓ can have different numbers of channels:

$$u^\ell \in \mathbb{R}^{c_{u,\ell}\times m_\ell\times n_\ell}, \quad f^\ell \in \mathbb{R}^{c_{f,\ell}\times m_\ell\times n_\ell} \tag{10.15}$$

One possibility is that the number of channels for both u and f remain unchanged in different grids:

$$c_{f,\ell} = c_f, \quad \ell = 1 : J, \tag{10.16}$$

and

$$c_{u,\ell} = c_u, \quad \ell = 1 : J. \tag{10.17}$$

Both c_f and c_u are two super-parameters that need to be tuned, and we may even take $c_u = c_f$.

10.1.3 Poolings: $\Pi^{\ell}_{\ell+1}$ and $R^{\ell}_{\ell+1}$

The pooling $\Pi^{\ell}_{\ell+1}$ in (10.4) and $R^{\ell}_{\ell+1}$ in (10.5) are in general different. They can be trained in general, but they may be a priori chosen.

There are many different possibilities to choose $\Pi^{\ell}_{\ell+1}$. The simplest choice of $\Pi^{\ell}_{\ell+1}$ is

$$\Pi^{\ell}_{\ell+1} = 0. \tag{10.18}$$

A more sophisticated choice can be obtained by considering an interpolation from fine grid to coarse (that, for example preserves linear function locally). Namely

$$\Pi^{\ell}_{\ell+1} = \bar{\Pi}^{\ell}_{\ell+1} \otimes I_{c_\ell \times c_\ell} \tag{10.19}$$

with $\bar{\Pi}^{\ell}_{\ell+1}$ given in finite element methods.

10.1.4 Data-feature mapping: A^{ℓ}

The second new feature of MgNet is that this data-feature mapping only depends on the grid $\mathcal{T}_\ell$, and it does not depend on layers within the same grid. This amounts to a significant saving of the number of parameters. In comparison, the existing CNN, such as pre-act ResNet, can be interpreted as a network related to the case that A^{ℓ} is replaced by $A^{\ell,i}$, namely

$$u^{\ell,i} = u^{\ell,i-1} + \sigma \circ B^{\ell,i} * \sigma(f^{\ell} - A^{\ell,i} * u^{\ell,i-1}). \tag{10.20}$$

The underlying convolution kernels can be different on different grids and they can all be trained.

10.1.5 Feature extractors: $\sigma \circ B^{\ell,i} * \sigma$

Here we adopt the feature extractor as:

$$\sigma \circ B^{\ell,i} * \sigma. \tag{10.21}$$

Other than the level dependent extractors, the following different strategies can be used

Constant Extractors : $B^{\ell,i} = B^{\ell}$ for $i = 1 : \nu_\ell$
Scaled Extractors :$B^{\ell,i} = \alpha_i B^{\ell}$ for $i = 1 : \nu_\ell$
Variable Extractors : $B^{\ell,i}$

This brief framework gives us the basic principle on designing a CNN models for classification. All models are seen as the special choice of data-feature mapping A^{ℓ}, feature extractors $B^{\ell,i}$ and the pooling operators $\Pi^{\ell}_{\ell+1}$ with $R^{\ell}_{\ell+1}$.

10.2 MgNet, pre-act ResNet, variants and generalizations

The MgNet model algorithm is one very basic and it can be generalized in many different ways. It can also be used as a guidance to modify and extend many existing CNN models.

The following result show how MgNet is related to the pre-act ResNet [**?**].

Theorem 22. *The MgNet model Algorithm 21, admits the following identities*

$$r^{\ell,i} = r^{\ell,i-1} - A^{\ell} \circ \sigma \circ B^{\ell,i} \circ \sigma(r^{\ell,i-1}), \quad i = 1 : \nu_\ell, \tag{10.22}$$

where

$$r^{\ell,i} = f^{\ell} - A^{\ell} * u^{\ell,i}. \tag{10.23}$$

Furthermore, (10.22) *represents pre-act ResNet [**?**] as shown before.*

Proof. Because of the linearity of A^ℓ and invariant within the same grid ℓ, we can apply A^ℓ on both sides of (10.3) and minus with f^ℓ, thus we have

$$f^{\ell} - A^{\ell} * u^{\ell,i} = f^{\ell} - A^{\ell} * u^{\ell,i-1} - A^{\ell} * \sigma \circ B^{\ell,i} \circ \sigma(f^{\ell} - A^{\ell} * u^{\ell,i-1}).$$

This finish the proof with definition in (10.23). □

The above result is very simple but critically important. In view of Theorem 22, it shows how multigrid and CNN are intimately related. Furthermore, it provides a different version of iResNet, which can be viewed as the dual version of the original pre-act ResNet. This relation is quit similar with the dual relation of u and f in multigrid method [**?**].

Lemma 31. *The ResNet [**?**] step as in* (9.47) *admits the following relation:*

$$\tilde{r}^{\ell,i+1} = \sigma(\tilde{r}^{\ell,i}) - A^{\ell,i} * \sigma \circ B^{\ell,i} * \sigma(\tilde{r}^{\ell,i}), \tag{10.24}$$

where

$$\tilde{r}^{\ell,i} = r^{\ell,i-1} - A^{\ell,i} * \sigma \circ B^{\ell,i} * r^{\ell,i-1}. \tag{10.25}$$

Proof. First, we apply $A^{\ell,i+1} \circ \sigma \circ B^{\ell,i+1}$ on the both sides of (9.47) and get

$$A^{\ell,i+1} * \sigma \circ B^{\ell,i+1} * r^{\ell,i} = A^{\ell,i+1} * \sigma \circ B^{\ell,i+1} * \sigma(\tilde{r}^{\ell,i}). \tag{10.26}$$

Minus by $r^{\ell,i}$ on the both sides and recall the definition in (10.25), we have

$$\tilde{r}^{\ell,i+1} = r^{\ell,i} - A^{\ell,i+1} * \sigma \circ B^{\ell,i+1} * \sigma(\tilde{r}^{\ell,i}).$$

By the definition of $r^{\ell,i} = \sigma(\tilde{r}^{\ell,i})$, we finish this proof. □

We call the above form (10.24) as σ-ResNet, similar to the MgNet we replace $A^{\ell,i}$ by A^ℓ and get the next Mg-ResNet form as:

$$r^{\ell,i} = \sigma(r^{\ell,i-1}) - A^{\ell} * \sigma \circ B^{\ell,i} * \sigma(r^{\ell,i-1}). \tag{10.27}$$

Table 10.1. Comparison for all iterative forms

Primal-Dual	Model	Iterative form
Feature space	Abstract-MgNet	Solving $A^\ell(u^\ell) = f^\ell$
	General-MgNet	$u^{\ell,i} = u^{\ell,i-1} + B^{\ell,i}(f^\ell - A^\ell(u^{\ell,i-1}))$
	MgNet	$u^{\ell,i} = u^{\ell,i-1} + \sigma \circ B^{\ell,i} \circ \sigma(f^\ell - A^\ell(u^{\ell,i-1}))$
Data space	pre-act ResNet	$r^{\ell,i} = r^{\ell,i-1} - A^{\ell,i} * \sigma \circ B^{\ell,i} * \sigma(r^{\ell,i-1})$
	Mg pre-act ResNet	$r^{\ell,i} = r^{\ell,i-1} - A^{\ell} * \sigma \circ B^{\ell,i} * \sigma(r^{\ell,i-1})$
	Mg-ResNet	$r^{\ell,i} = \sigma(r^{\ell,i-1}) - A^{\ell} * \sigma \circ B^{\ell,i} * \sigma(r^{\ell,i-1})$
	σ-ResNet	$r^{\ell,i} = \sigma(r^{\ell,i-1}) - A^{\ell,i} * \sigma \circ B^{\ell,i} * \sigma(r^{\ell,i-1})$
	ResNet	$r^{\ell,i} = \sigma(r^{\ell,i-1} - A^{\ell,i} * \sigma \circ B^{\ell,i} * r^{\ell,i-1})$

If we take these pooling and prolongation operators as discussed in the previous sections and focus on the iterative forms on a certain grid ℓ, we may compare them all as: We can have these connections for all iterative scheme in data space:

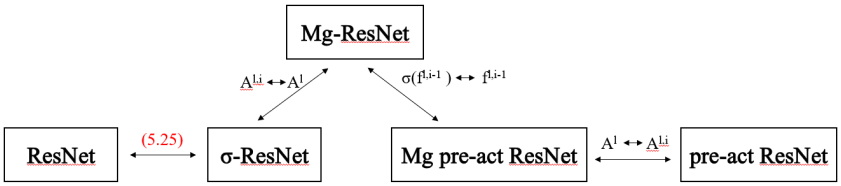

In this sense, these MgNet related models can be understood as models between pre-act ResNet and ResNet. And all these models can be understood as iteration in the data space as a dual relationship with feature space as MgNet.

The rationality of replacing $A^{\ell,i}$ by layer independent A^ℓ may be justified by the following theorem.

Theorem 23. *On each grid $\mathcal{T}_\ell$,*

1. Any CNN model with

$$f^{\ell,i} = \chi^{\ell,i} \circ \sigma(f^{\ell,i-1}), \tag{10.28}$$

can be written as

$$f^{\ell,i} = \sigma(f^{\ell,i-1}) - \xi^{\ell} \circ \sigma \circ \eta^{\ell,i} \circ \sigma(f^{\ell,i-1}). \tag{10.29}$$

2. *Any CNN model with*

$$f^{\ell,i} = \sigma \circ \chi^{\ell,i}(f^{\ell,i-1}). \tag{10.30}$$

can be written as

$$f^{\ell,i} = \sigma\left(f^{\ell,i-1} - \xi^{\ell} \circ \sigma \circ \eta^{\ell,i}(f^{\ell,i-1})\right). \tag{10.31}$$

Proof. Let use prove the first case as an example, the second case can be proven with the same process.

With similar structure in MgNet, we can take

$$\xi^{\ell} = \hat{\delta}^{\ell} := [\hat{\delta}_1, \cdots, \hat{\delta}_{c_\ell}], \tag{10.32}$$

and

$$\eta^{\ell,i} = [\mathrm{id}_{c_\ell}, -\mathrm{id}_{c_\ell}] \circ (\chi^{\ell,i} - \mathrm{id}_{c_\ell}). \tag{10.33}$$

Here

$$\mathrm{id}_{c_\ell} : \mathbb{R}^{n_\ell \times n_\ell \times c_\ell} \mapsto \mathbb{R}^{n_\ell \times n_\ell \times c_\ell}, \tag{10.34}$$

is the identity map and

$$\hat{\delta}_k : \mathbb{R}^{n_\ell \times n_\ell \times 2c_\ell} \mapsto \mathbb{R}^{n_\ell \times n_\ell}, \tag{10.35}$$

with

$$\hat{\delta}_k([X, Y]) = -([X]_k + [Y]_k), \tag{10.36}$$

for any $X, Y \in \mathbb{R}^{n_\ell \times n_\ell \times c_\ell}$ and $[X, Y] \in \mathbb{R}^{n_\ell \times n_\ell \times 2c_\ell}$.

First, we see that $\eta^{\ell,i}$ with the above form is a convolution from $\mathbb{R}^{n_\ell \times n_\ell \times c_\ell}$ to $\mathbb{R}^{n_\ell \times n_\ell \times 2c_\ell}$. Following the identity

$$ReLU(x) + ReLU(-x) = x, \tag{10.37}$$

and the definition of ξ^{ℓ} i.e.

$$\xi^{\ell} = \hat{\delta}^{\ell}, \tag{10.38}$$

as a special case in MgNet. For more details, we can give a exact form of $\hat{\delta}_k$ as in (10.36) with

$$\hat{\delta}_k = [0, \cdots, 0, -\delta, \cdots 0; 0, \cdots, 0, -\delta, \cdots 0], \quad k = 1 : c_\ell, \tag{10.39}$$

where δ is the identity kernel during one channel.

At last, we have

$$\left[\xi^\ell \circ \sigma \circ [\mathrm{id}_{c_\ell}, -\mathrm{id}_{c_\ell}](x)\right]_k = \left[\xi^\ell \circ \sigma \circ [x, -x]\right]_k, \tag{10.40}$$

$$= \hat{\delta}_k([\sigma(x), \sigma(-x)]), \tag{10.41}$$

$$= -\delta([\sigma(x)]_k) - \delta([\sigma(-x)]_k), \tag{10.42}$$

$$= -(\sigma([x]_k) + \sigma(-[x]_k)), \tag{10.43}$$

$$= -[x]_k \tag{10.44}$$

Thus to say,

$$\xi^\ell \circ \sigma \circ [\mathrm{id}_{c_\ell}, -\mathrm{id}_{c_\ell}] = -\mathrm{id}_{c_\ell}. \tag{10.45}$$

Then the modified dual form of MgNet in (10.24) becomes

$$f^{\ell,i} = \sigma(f^{\ell,i-1}) - \xi^{\ell,i} \circ \sigma \circ \eta^{\ell,i} \circ \sigma(f^{\ell,i-1}), \tag{10.46}$$

$$= \sigma(f^{\ell,i-1}) - \left(\xi^\ell \circ \sigma \circ [\mathrm{id}_{c_\ell}, -\mathrm{id}_{c_\ell}]\right) \circ (\chi^{\ell,i} - \mathrm{id}_{c_\ell}) \circ \sigma(f^{\ell,i-1}) \tag{10.47}$$

$$= \sigma(f^{\ell,i-1}) + (\chi^{\ell,i} - \mathrm{id}_{c_\ell}) \circ \sigma(f^{\ell,i-1}), \tag{10.48}$$

$$= \chi^{\ell,i} \circ \sigma(f^{\ell,i-1}). \tag{10.49}$$

This covers (10.29). □

Remark 7. Theorems 23 shows that general CNN in the forms of either (10.28) or (10.30) can be written recast as (10.29) or (10.31) with the data-feature mapping $A^\ell = \xi^\ell$ that is not only independent of the layers, but is actually given a priori as in (10.32). In view of Theorems 22 and 31, the classic CNN models can be essentially recovered from MgNet by choosing ξ^ℓ a priori as in (10.32). Since the classic CNN models have been extensively tested to be successful, the more general MgNet with more general ξ^ℓ (to be trained) are expected to be more efficient than the classic CNN models.

10.3 Constrained linear data-feature mapping from MgNet to interpret ResNet

In this section, we will establish a new understanding of pre-act ResNet by involving the idea that the pre-act ResNet block is an iterative scheme for solving some hidden model in each grid, which is also the fundamental assumption in MgNet. More details about this mathematical interpreting model for CNN can be found in [**?**].

The main point here is the introduction of the so-called data and feature space for CNN, which is analogous to the function space and its duality in the theory of multigrid methods [**?**]. Namely, following [**?**] we introduce the next data-feature mapping model in every grid level follows:

$$A^\ell * u^\ell = f^\ell, \tag{10.50}$$

where f^ℓ and u^ℓ belong to the data and feature space at ℓ-th grid. We now make the following two important observations for this data-feature mapping:

- The mapping in (10.50) is linear, more specifically it is just a convolution with multichannel, zero padding and stride one as in pre-act ResNet.
- In each level, namely between two consecutive pooling, there is only one data-feature mapping, or we say that A^ℓ only depends on ℓ, but not on number of layers.

We note that the assumption that these linear data-feature mapping depend only on the grid level ℓ is motivated from a basic property of multigrid methods [**? ? ?**].

Besides (10.50), we introducing an important constrained condition in feature space that

$$u^{\ell,i} \geq 0. \tag{10.51}$$

The rationality of this constraint in feature space can be interpreted as follows. First of all, from the real neural system, the real neurons will only be active if the electric signal is greater than certain thresholding value. Namely, we can think that human brains can only see features with certain threshold. On the other hand, the "shift" invariant property of feature space in CNNs, namely, $u+a$ will not change the classification results. This means that $u+a$ should have the same classification result with u. That is to say, we may assume that $u \geq 0$ to reduce some redundancy of u.

Based on these assumptions above, what we need to do next is to solve the data-feature mapping equation in (10.50). We will adopt some classical iterative methods [**?**] in scientific computing to solve the system (10.50) and obtain that

$$u^{\ell,i} = u^{\ell,i-1} + B^{\ell,i} * (f^\ell - A^\ell * u^{\ell,i-1}),\ i = 1 : \nu_\ell, \tag{10.52}$$

where $u^\ell \approx u^{\ell,\nu_\ell}$. For more details about iterative methods in numerical analysis, we refer to [**? ? ?**]. To preserve (10.51), we naturally use the ReLU activation function σ to modify (10.52) as follows

$$u^{\ell,i} = u^{\ell,i-1} + \sigma \circ B^{\ell,i} * \sigma(f^\ell - A^\ell * u^{\ell,i-1}), \quad i = 1 : \nu_\ell, \tag{10.53}$$

which leads the the basic iterative scheme in MgNet.

Now, let us consider the iteration for residual. Because of the linearity of convolution in data-feature mapping, if we consider the residual $r^{\ell,j} = f^\ell - A^\ell * u^{\ell,j}$, (10.53) leads to the next iterative forms for residuals

$$r^{\ell,i} = r^{\ell,i-1} - A^\ell * \sigma \circ B^{\ell,i} * \sigma(r^{\ell,i-1}). \tag{10.54}$$

This is the same as (9.48) under the constraint $A^{\ell,i} = A^\ell$ in pre-act ResNet.

We summarize the above derivation in the following simple theorem.

Theorem 24. *Under the assumption that there is only one linear data-feature mapping in each grid ℓ, i.e. $A^{\ell,i} = A^\ell$, the iterative form in feature space as in (10.52) is equivalent to (10.54) if A^ℓ is invertible where $r^{\ell,i} = f^\ell - A^\ell * u^{\ell,i}$.*

11

Initializations and Normalizations

11.1 Data normalization in DNNs and CNNs

The goal of data normalization is twofold:

1. Data normalization is the organization of data to appear similar across all records and fields.
2. It increases the cohesion of entry types leading to cleansing, lead generation, segmentation, and higher quality data.

Data normalization includes eliminating unstructured data and redundancy (duplicates) in order to ensure logical data storage. When data normalization is done correctly, you will end up with standardized information entry.

In this chapter, we use superscript i, j, l and ν to represent the i-th data, the j-th channel, the l-th depth and the ν-th iteration step, respectively.

11.1.1 Data normalization in DNNs

Consider that we have the all training data as

$$(X, Y) := \{(x^i, y^i)\}_{i=1}^N, \tag{11.1}$$

for $x^i \in \mathbb{R}^d$ and $y^i \in \mathbb{R}^k$. Here superscripte i represents the i-th data.

Before we input every data into a DNN model, we will apply the following normalization for all data x_i for each component. The notation $x \sim X$ means that x is a discrete random variable on X with probability

$$\mathbb{P}(x = x^i) = \frac{1}{N}, \tag{11.2}$$

for any $x^i \in X$. The expectation and the variance are

$$\mu_X = \mathbb{E}_{x\sim X}[x] = \frac{1}{N}\sum_{i=1}^N x^i, \quad \sigma_X = \mathbb{V}_{x\sim X}[x] = \frac{1}{N}\sum_{i=1}^N (x^i - \mu_X)^T(x^i - \mu_X). \tag{11.3}$$

Define new data

$$\tilde{x}^i = \frac{x^i - \mu_X}{\sqrt{\sigma_X}}, \tag{11.4}$$

where $x^i, \tilde{x}^i, \mu_X, \sigma_X \in \mathbb{R}^d$. Finally, we will have a "new" data set

$$\tilde{X} = \{\tilde{x}^1, \tilde{x}^2, \cdots, \tilde{x}^N\}, \tag{11.5}$$

with unchanged label set Y. To be specific, we rewrite the equation (11.4) into an elementwise form. Let denote

$$x^{i,j} \longleftrightarrow \text{ the j-th component of data } x^i. \tag{11.6}$$

Then we have following formula of for all $j = 1, 2, \cdots, d$

$$\tilde{x}^{i,j} = \frac{x^{i,j} - \mu_X^j}{\sqrt{\sigma_X^j}}, \tag{11.7}$$

where $\mu_X = (\mu_X^1, \mu_X^2, \cdots, \mu_X^d) \in \mathbb{R}^d$, $\sigma_X = (\sigma_X^1, \sigma_X^2, \cdots, \sigma_X^d) \in \mathbb{R}^d$ and

$$\mu_X^j = \mathbb{E}_{x\sim X}[x^j] = \frac{1}{N}\sum_{i=1}^N x^{i,j}, \quad \sigma_X^j = \mathbb{V}_{x\sim X}[x^j] = \frac{1}{N}\sum_{i=1}^N (x^{i,j} - \mu_X^j)^2. \tag{11.8}$$

Here we note that, by normalizing the data set, we have the next properties for new data $\tilde{x} = (\tilde{x}^1, \tilde{x}^2, \cdots, \tilde{x}^N) \in \tilde{X}$ with component $j = 1, 2, \cdots, d$,

$$\mathbb{E}_{\tilde{X}}[\tilde{x}] = \frac{1}{N}\sum_{i=1}^N \tilde{x}^i = 0, \tag{11.9}$$

and

$$\mathbb{V}_{\tilde{X}}[\tilde{x}] = \frac{1}{N}\sum_{i=1}^N (\tilde{x}^i - \mathbb{E}_{\tilde{X}}[\tilde{x}])^T(\tilde{x}^i - \mathbb{E}_{\tilde{X}}[\tilde{x}]) = 1. \tag{11.10}$$

For the next sections in this chapter, without special notices, we use X data set as the normalized one as default.

11.1.2 Data normalization for images in CNNs

For images, we have a color image data set $(X, Y) := \{(x^i, y^i)\}_{i=1}^N$. We further denote these the (s, t) pixel value for data x_i at channel j as:

$$x_{s,t}^{i,j} \longleftrightarrow (s, t) \text{ pixel value for } x^i \text{ at channel } j, \tag{11.11}$$

where $1 \le i \le N, 1 \le j \le 3, 1 \le s \le m$, and $1 \le t \le n$.

Then, the normalization for x^j is defined by

$$\tilde{x}_{s,t}^{i,j} = \frac{x_{s,t}^{i,j} - \mu_X^j}{\sqrt{\sigma_X^j}}, \tag{11.12}$$

where $x_{s,t}^{i,j}, \tilde{x}_{s,t}^{i,j}, \mu_X^j, \sigma_X^j \in \mathbb{R}$. This means that we need to normalize the data for each channel. Here

$$\mu_X^j = \frac{1}{m \times n \times N} \sum_{1 \le i \le N} \sum_{1 \le s \le m, 1 \le t \le n} x_{s,t}^{i,j}. \tag{11.13}$$

There are two common choices of σ_X^j:

1. Batch normalization also uses the formula below to compute the variance in CNN for each channel.

$$\sigma_X^j = \frac{1}{N \times m \times n} \sum_{1 \le i \le N} \sum_{1 \le s \le m, 1 \le t \le n} (x_{s,t}^{i,j} - \mu_X^j)^2. \tag{11.14}$$

2. Another way to compute the variance over each channel is to compute the standard deviation on each channel for every data, and then average them in the data direction.

$$\sqrt{\tilde{\sigma}_X^j} = \frac{1}{N} \sum_{1 \le i \le N} \left(\frac{1}{m \times n} \sum_{1 \le s \le m, 1 \le t \le n} (x_{s,t}^{i,j} - \mu_i^j)^2 \right)^{\frac{1}{2}}, \tag{11.15}$$

where $\mu_i^j = \frac{1}{m \times n} \sum_{1 \le s \le m, 1 \le t \le n} x_{s,t}^{i,j}$.

Example 7 (Comparison of $\sqrt{[\sigma_X]_j}$ and $\sqrt{[\tilde{\sigma}_X]_j}$ on CIFAR10.).
On CIFAR10, both ways share the same μ_X as

$$\mu_X = \Big(0.49140105\ 0.48215663\ 0.44653168\Big). \tag{11.16}$$

But they had different standard deviation estimates:

$$\begin{aligned} \sqrt{\sigma_X^j} &= \Big(0.24703284\ 0.24348499\ 0.26158834\Big) \\ \sqrt{\tilde{\sigma}_X^j} &= \Big(0.20220193\ 0.19931635\ 0.20086373\Big) \end{aligned} \tag{11.17}$$

This numerical shows that the two normalization are different.

11.2 Initialization for deep neural networks

To build a machine learning algorithm, we need to define an architecture (e.g. Logistic regression, Support Vector Machine, Neural Network) and train it to learn parameters. The training of neural network is actually the iteration of the above architecture. Then, the initial guess of the parameters is important in avoiding gradient vanishing or blowup. The initialization step deals with the initial guess of parameters, and can be critical to the model's ultimate performance.

11.2.1 Xavier's Initialization with $\sigma = id$

The goal of Xavier initialization [**?**] is to initialize the deep neural network to avoid gradient vanishing or blowup when the input is white noise.

Recall the DNN models in Section 7.3.2

$$\begin{cases} f^1(x) &= W^1 x + b^1 \\ f^\ell(x) &= W^\ell \sigma(f^{\ell-1}(x)) + b^\ell \quad \ell = 2:L\,, \\ f(x) &= f^L \end{cases} \tag{11.18}$$

with $x \in \mathbb{R}^{n_0}$ and $f^\ell \in \mathbb{R}^{n_\ell}$. More precisely, we have

$$W^\ell \in \mathbb{R}^{n_\ell \times n_{\ell-1}}. \tag{11.19}$$

We make the basic assumptions below:

- The initial weights W_{ij}^ℓ are i.i.d symmetric random variables with mean 0, namely the probability distribution of W_{ij}^ℓ is even.
- The initial bias $b^\ell = 0$.

The goal of Xavier's initialization is to ensure that the features f^ℓ and gradients do not blow up or vanish. Note that the mean of f^ℓ is zero, we only need to choose appropriate initial parameters to bound the variance of f^ℓ. To this end we have the following lemma.

Lemma 32. *Under the previous assumptions f_i^ℓ is a symmetric random variable with $\mathbb{E}[f_i^\ell] = 0$. Moreover, we have the following identity*

$$\mathbb{V}[f_i^\ell] = \mathbb{E}[(f_i^\ell)^2] = \sum_k \mathbb{E}[(W_{ik}^\ell)^2]\mathbb{E}[\sigma(f_k^{\ell-1})^2]. \tag{11.20}$$

where the subscript i of the notation f_i^ℓ represents the i-th component of f^ℓ.

Proof. For general activation function $\sigma(x)$, let first prove that f_i^ℓ is a symmetric random variable with $\mathbb{E}[f_i^\ell] = 0$. For any ℓ and $1 \le i \le n_\ell$, we have

$$f_i^\ell = \sum_k W_{ik}^\ell \sigma(f_k^{\ell-1}) + b_i^\ell, \tag{11.21}$$

Taking expectations, noting that W_{ik}^{ℓ} are independent of $f_k^{\ell-1}$ and that $b_i^{\ell} = 0$, we get

$$\mathbb{E}[f_i^{\ell}] = \sum_k \mathbb{E}[W_{ik}^{\ell}]\mathbb{E}[\sigma(f_k^{\ell-1})] = 0. \tag{11.22}$$

since $\mathbb{E}[W_{ik}^{\ell}] = 0$. Moreover, if the W_{ij}^{ℓ} are symmetric, it is clear that f_i^{ℓ} will be.

Next we calculate the variance of f_i^{ℓ}, we get

$$\begin{aligned}\mathbb{V}[f_i^{\ell}] = \mathbb{E}[(f_i^{\ell})^2] &= \mathbb{E}\left[\left(\sum_k W_{ik}^{\ell}\sigma(f_k^{\ell-1})\right)\left(\sum_l W_{il}^{\ell}\sigma(f_l^{\ell-1})\right)\right] \\ &= \sum_{k,l} \mathbb{E}[W_{ik}^{\ell} W_{il}^{\ell}\sigma(f_k^{\ell-1})\sigma(f_l^{\ell-1})].\end{aligned} \tag{11.23}$$

In the above sum we will have W_{ik}^{ℓ} and W_{il}^{ℓ} independent unless $k = l$. In this case the term will be 0. So the only terms which remain are those for which $k = l$ and we get

$$\mathbb{E}[(f_i^{\ell})^2] = \sum_k \mathbb{E}[(W_{ik}^{\ell})^2]\mathbb{E}[\sigma(f_k^{\ell-1})^2]. \tag{11.24}$$

□

Now, we assume $\sigma = id$. This assumption is pretty reasonably since most activation functions in use at the time (such as the hyperbolic tangent) were close to the identity near 0.

Lemma 33. *If $\sigma = id$,*

$$\mathbb{V}[f_i^L] = \left(\Pi_{\ell=2}^L n_{\ell-1}\mathrm{Var}[W_{st}^{\ell}]\right)\left(\mathbb{V}[W_{st}^1]\sum_j \mathbb{E}[(x^j)^2]\right), \tag{11.25}$$

where x^j represents the j-th component of data x.

Proof. Let us prove it this by induction. For $\ell = 1$,

$$\mathbb{V}[f_i^1] = \sum_j \mathbb{E}[(W_{ij}^1)^2]\mathbb{E}[(x^j)^2] = \mathbb{E}[(W_{ij}^1)^2]\left(\sum_j \mathbb{E}[(x^j)^2]\right), \tag{11.26}$$

for any $i = 1, 2, \cdots, n_1$. Since we already know that

$$\mathbb{V}[f_i^1] = \mathbb{E}[(W_{ij}^1)^2]\left(\sum_j \mathbb{E}[(x^j)^2]\right) = \mathbb{V}[f_k^1], \quad \forall i, k, \tag{11.27}$$

from derivation in $\ell = 1$. We will see that for $\ell = 2$,

$$\mathbb{V}[f_i^2] = n_1\mathbb{V}[W_{ij}^2]\mathbb{V}[f_j^1] = n_1\mathbb{V}[W_{st}^2]\left(\mathbb{V}[W_{st}^1]\sum_j \mathbb{E}[(x^j)^2]\right). \tag{11.28}$$

By induction,

$$\mathbb{V}[f_i^L] = \left(\Pi_{\ell=2}^L n_{\ell-1}\mathrm{Var}[W_{st}^\ell]\right)\left(\mathbb{V}[W_{st}^1]\sum_j \mathbb{E}[(x^j)^2]\right). \tag{11.29}$$

□

According to Theorem 33, one way to make sure the variance $\mathbb{V}[W_{ik}^\ell]$ does not blow up is to set

$$\mathbb{V}[W_{ik}^\ell] = \frac{1}{n_{\ell-1}}, \quad \forall \ell \geq 2. \tag{11.30}$$

In this case,

$$\mathbb{V}[f_i^L] = \mathbb{V}[f_j^{L-1}] = \cdots = \mathbb{V}[f_k^1] = \mathbb{V}[W_{st}^1]\sum_j \mathbb{E}[(x^j)^2]. \tag{11.31}$$

Thus, in pure DNN models, it is enough to just control $\sum_j \mathbb{E}[(x^j)^2]$. The choice (11.30) comes from the analysis of $\mathbb{V}[W_{ik}^\ell]$. We can also consider the propagation of the gradient $\frac{\partial L(\theta)}{\partial f^\ell}$. A similar analysis suggests the choice $\mathbb{V}[W_{ik}^\ell] = \frac{1}{n_\ell}$. Thus, the **Xavier's initialization** suggests to initialize W_{ik}^ℓ with variance as:

- To control $\mathbb{V}[f_i^\ell]$:

$$\mathrm{Var}[W_{ik}^\ell] = \frac{1}{n_{\ell-1}}. \tag{11.32}$$

- To control $\mathbb{V}[\frac{\partial L(\theta)}{\partial f_i^\ell}]$:

$$\mathrm{Var}[W_{ik}^\ell] = \frac{1}{n_\ell}. \tag{11.33}$$

- Trade-off to control $\mathbb{V}[\frac{\partial L(\theta)}{\partial W_{ik}^\ell}]$:

$$\mathrm{Var}[W_{ik}^\ell] = \frac{2}{n_{\ell-1}+n_\ell}. \tag{11.34}$$

Here we note that, this analysis works for all symmetric type distribution around zero. We often just choose uniform distribution $\mathcal{U}(-a,a)$ and normal distribution $\mathcal{N}(0,s^2)$. Since the expectation of W_{ik}^ℓ is zero and the variance is given above, the final version of Xavier's initialization takes the trade-off type as

$$W_{ik}^\ell \sim \mathcal{U}(-\sqrt{\frac{6}{n_\ell+n_{\ell-1}}}, \sqrt{\frac{6}{n_\ell+n_{\ell-1}}}), \quad \text{or} \quad W_{ik}^\ell \sim \mathcal{N}(0, \frac{2}{n_\ell+n_{\ell-1}}). \tag{11.35}$$

11.2.2 Variance analysis in backward propagation phase

Recall the loss function

$$L(\theta) = \mathbb{E}_{(x,y)\sim D}\ell\left(\text{softmax}\left(f^L\right), y\right),$$

where $f^L(x;\theta)$ is the DNN function defined by

$$\begin{cases} f^1(x) = W^1 x + b^1 \\ f^l(x) = W^l\sigma\left(f^{l-1}(x)\right) + b^l \quad \forall l = 2, \cdots L \end{cases}.$$

Then we have the following backward propagation ("BP") formula $\frac{\partial L(\theta)}{\partial W^l} = \frac{\partial L}{\partial f^l} \cdot \frac{\partial f^l}{\partial W^l}$, where $\frac{\partial L}{\partial f^l} \in \mathbb{R}^{n_e}$, $\frac{\partial f}{\partial W^l} \in \mathbb{R}^{n_e \times (n_e \times n_{e-1})}$. More Precisely,

$$\frac{\partial L(\theta)}{\partial W^l_{st}} = \sum_{i=1}^{n_l}\left(\frac{\partial L(\theta)}{\partial f^l_i} \cdot \frac{\partial f^l_i}{\partial W^l_{st}}\right).$$

Assume that

1. $\left\{\frac{\partial L(\theta)}{\partial f^l_i} \cdot \frac{\partial f^l_i}{\partial W^L_{st}}\right\}_{i=1}^{n_e}$ are independent
2. For each i, $\frac{\partial L(\theta)}{\partial f^l_i}$ and $\frac{\partial f^l_i}{\partial W^l_{st}}$ are independent

Actually, we can not such make general assumptions as $L(\theta), f^l_i, \frac{\partial f^l_i}{\partial W_{st}}\frac{\partial L(\theta)}{\partial f^l_i}$ are all fixed. We still make these assumption here to get some idea of the choice of W^l_{st}.

Lemma 34. *If $\sigma = id$ and the above assumption holds,*

$$\mathbb{V}\left[\frac{\partial L(\theta)}{\partial W^l_{st}}\right] = \prod_{j=l+1}^{L-1} n_j \mathbb{V}\left[W^j_{st}\right]\left(\mathbb{V}\left[W^L_{st}\right]\sum_{k=1}^{n_L}\mathbb{E}\left[\left(\frac{\partial L(\theta)}{\partial f^2_k}\right)^2\right]\right)\prod_{j=2}^{l-1} n_j \mathbb{V}\left[W^j_{st}\right]\left(\mathbb{V}\left[W^1_{st}\right]\sum_{R=1}^{d}\mathbb{E}\left[X^2_k\right]\right).$$

Proof. The assumption leads to

$$\mathbb{V}\left[\frac{\partial L(\theta)}{\partial W^l_{st}}\right] = \sum_{i=1}^{n_l}\left(\mathbb{E}\left[\left(\frac{\partial L(\theta)}{\partial f^l_i}\right)^2\right]\mathbb{E}\left[\left(\frac{\partial f^l_i}{\partial W^l_{st}}\right)^2\right] - \left(\mathbb{E}\left[\frac{\partial L(\theta)}{\partial f^l_i}\right]\mathbb{E}\left[\frac{\partial f^l_i}{\partial W^l_{st}}\right]\right)^2\right). \tag{11.36}$$

This implies that we only need to consider $\mathbb{E}\left[\left(\frac{\partial L(\theta)}{\partial f^l_i}\right)^2\right]$ and $\mathbb{E}\left[\left(\frac{\partial f^l_i}{\partial W^l_{st}}\right)^2\right]$.

1. Consider $\mathbb{E}\left[\left(\frac{\partial L(\theta)}{\partial f^l_i}\right)^2\right]$. By chain rule:

$$\frac{\partial L(\theta)}{\partial f_i^l} = \frac{\partial L(\theta)}{\partial f^{l+1}} \cdot \frac{\partial f^{l+1}}{\partial f_i^l} = \sum_{j=1}^{n_{l+1}} \frac{\partial L(\theta)}{\partial f_j^{l+1}} \frac{\partial f_j^{l+1}}{\partial f_i^l}$$
$$= \sum_{j=1}^{n_{l+1}} W_{ji}^{l+1} \sigma'\left(f_i^l\right) \frac{\partial L(\theta)}{\partial f_j^{l+1}} = \sum_{j=1}^{n_{l+1}} W_{ji}^{l+1} \frac{\partial L(\theta)}{\partial f_j^{l+1}} (\text{ if } \sigma = id)$$

Keep doing this:

$$\frac{\partial L(\theta)}{\partial f^l} = \left[W^{l+1}\right]^\top \cdot \left[W^{l+2}\right]^\top \cdots \left[W^L\right]^T \frac{\partial L(\theta)}{\partial f^L}$$

Assume the independence of $\frac{\partial L(\theta)}{\partial f^L}$ with $W^{l+i}, i = 1, 2, \ldots$. (Still we make this assumption although this can not be ture, as $\frac{\partial L(\theta)}{\partial f^l}$ contains W^{l+i}.) Then

$$\mathbb{E}\left[\frac{\partial L(\theta)}{\partial f_i^l}\right] = \sum_j \mathbb{E}\left[W_{ji}^{l+1}\right] \mathbb{E}\left[\frac{\partial L(\theta)}{\partial f_j^l}\right] = 0$$

(11.37)
$$\mathbb{E}\left[\left(\frac{\partial L(\theta)}{\partial f_i^l}\right)^2\right] = \mathbb{V}\left[\frac{\partial L(\theta)}{\partial f_i^l}\right] = \prod_{j=l+1}^{L-1} n_j \mathbb{V}\left[W_{st}^j\right] \cdot \left(\mathbb{V}\left[W_{st}^L\right] \sum_{i=1}^{n_L} \mathbb{E}\left[\left(\frac{\partial L(\theta)}{\partial f_i^L}\right)^2\right]\right)$$

2. Consider $\mathbb{E}\left[\left(\frac{\partial f_i^l}{\partial W_{st}^l}\right)^2\right]$. By definition, $\frac{\partial f_i^l}{\partial W_{st}^l} = \delta_{is}\sigma\left(f_t^{l-1}\right)$ namely, only $\frac{\partial f_s^l}{\partial W_{st}^l} \neq 0$, and $\frac{\partial f_s^l}{\partial W_{st}^l} = \sigma\left(f_t^{l-1}\right)$. If σ=id, apply the forward results
   a) Expectation:
$$\mathbb{E}\left[\left(\frac{\partial f_s^l}{\partial W_{st}^l}\right)\right] = 0.$$
   b) Variance:

(11.38)
$$\mathbb{E}\left[\left(\frac{\partial f_s^l}{\partial W_{st}^l}\right)^2\right] = \mathbb{E}\left[\left(f_t^{l-1}\right)^2\right] = \mathbb{V}\left[f_t^{l-1}\right]$$
$$= \prod_{j=2}^{l-1} n_{j-1} \mathbb{V}\left[W_{st}^j\right] \cdot \left(\mathbb{V}\left[W_{st}^1\right] \sum_{k=1}^{d} \mathbb{E}\left[X_k^2\right]\right).$$

A combination of (11.36), (11.37) and (11.38) completes the proof. □

Next we consider $\mathbb{V}\left[\frac{\partial L(\theta)}{\partial W_{st}^l}\right]$.

$$\mathbb{V}\left[\frac{\partial L(\theta)}{\partial W_{st}^l}\right] = \mathbb{V}\left[\frac{\partial L(\theta)}{\partial f_s^l}\right] \cdot \mathbb{V}\left[f_t^{l-1}\right]$$
$$= \prod_{j=l+1}^{L-1} n_j \mathbb{V}\left[W_{st}^j\right] \left(\mathbb{V}\left[W_{st}^L\right] \sum_{k=1}^{n_L} \mathbb{E}\left[\left(\frac{\partial L(\theta)}{\partial f_k^L}\right)^2\right]\right) \times \prod_{j=2}^{l-1} n_j V\left[W_{st}^j\right] \left(\mathbb{V}\left[W_{st}^1\right] \sum_{R=1}^{d} \mathbb{E}\left[X_k^2\right]\right),$$

where $\mathbb{V}_1 = \left(\mathbb{V}\left[W_{st}^1\right]\sum_{k=1}^{d}\mathbb{E}\left[X_k^2\right]\right)$, $\mathbb{V}_L = \mathbb{V}\left[W_{st}^L\right]\sum_{k=1}^{n_L}\mathbb{E}\left[(\frac{\partial L(\theta)}{\partial f_k^L})^2\right]$.

We consider

$$\mathbb{V}\left[W_{st}^l\right] = f\left(n_l, n_{l-1}\right).$$

We summarize Lemma 33 and Lemma 34 as below

1. $\mathbb{V}\left[f_i^l\right] = \prod_{j=2}^{l} n_{j-1} f\left(n_j, n_{j-1}\right)\left(\mathbb{V}\left[W_{st}^1\right]\sum_{k=1}^{d}\mathbb{E}\left[X_k^2\right]\right)$
2. $\mathbb{V}\left[\frac{\partial L(\theta)}{\partial f_i^2}\right] = \prod_{j=1+1}^{L-1} n_j f\left(n_j, n_{j-1}\right)\cdot\left(\mathbb{V}\left[W_{st}^L\right]\sum_{i=1}^{n_L}\mathbb{E}\left[\left(\frac{\partial L(\theta)}{\partial f_i^l}\right)^2\right]\right)$
3. $\mathbb{V}\left[\frac{\partial L(\theta)}{\partial W_{st}^l}\right] = \prod_{j=l+1}^{L-1} n_j \cdot f\left(n_j, n_{j-1}\right)\cdot\prod_{j=2}^{l-1} n_{j-1} f\left(n_j, n_{j-1}\right)\times\mathbb{V}_1\times\mathbb{V}_L$

Based on the equations above, we have different choice of $\mathbb{V}\left[W_{st}^l\right]$

1. If $f\left(n_1, n_{j-1}\right) = \frac{1}{n_{j-1}}$ (control $W[f_i^l]$), $\mathbb{V}\left[\frac{\partial L(\theta)}{\partial W_{st}^l}\right]$ will decrease as l grow up. (Notice that $n_l > n_k$ if $l > k$)
2. If $f\left(n_j, n_{j-1}\right) = \frac{1}{n_j}$ (control $V[\frac{\partial L(\theta)}{\partial f_i^L}]$), $\mathbb{V}\left[\frac{\partial L(\theta)}{\partial W_{st}^l}\right]$ still decrease!
3. If $f\left(n_j, n_{j-1}\right) = \frac{2}{n_j+n_{j-1}} (\leq \frac{1}{\sqrt{n_j n_{j-1}}})$, $\mathbb{V}\left[\frac{\partial L(\theta)}{\partial W_{st}^l}\right] = \frac{\sqrt{n_{L-1}}\cdot\sqrt{n_1}}{\sqrt{n_l}\cdot\sqrt{n_{l-1}}}\times\mathbb{V}_1\times\mathbb{V}_L$ decrease!

Question

Can we design some other choices of $\mathbb{V}\left[W_{st}^l\right]$ such that $\mathbb{V}\left[\frac{\partial L(\theta)}{\partial W_{st}^l}\right]$ admits the following properties:

- Keep constant,
- Increase,
- Change with certain scale.

11.2.3 Kaiming's initialization

In [**?**], Kaiming He and others extended this analysis to get an *exact* result when the activation function is the ReLU.

We first have the following lemma for symmetric distribution.

Lemma 35. *If $X_i \in \mathbb{R}$ for $i = 1 : n$ are i.i.d with symmetric probability density function $p(x)$, i.e. $p(x)$ is even. Then for any nonzero random vector $Y = (Y_1, Y_2, \cdots, Y_n) \in \mathbb{R}^n$ which is independent with X_i, the following random variable*

$$Z = \sum_{i=1}^{n} X_i Y_i, \tag{11.39}$$

is also symmetric.

Proof. Let us denote the joint distribution function for Y as $q(y_1, \cdots, y_n)$. Then the joint distribution density function for (X, Y) is

$$f(x_1, \cdots, x_n, y_1, \cdots, y_n) = p(x_1)p(x_2)\cdots p(x_n)q(y_1, y_2, \cdots, y_n). \tag{11.40}$$

Then we have the following probability function

$$\begin{aligned}
\mathbb{P}(Z < z) &= \int_{\sum_{i=1}^n x_i y_i < z} f(x_1, \cdots, x_n, y_1, \cdots, y_n)dxdy \\
&= \int_{\sum_{i=1}^n x_i y_i < z} p(x_1)p(x_2)\cdots p(x_n)q(y_1, y_2, \cdots, y_n)dxdy \\
&= \int_{\sum_{i=1}^n -x_i y_i > -z} p(x_1)p(x_2)\cdots p(x_n)q(y_1, y_2, \cdots, y_n)dxdy \\
&= \int_{\sum_{i=1}^n -x_i y_i > -z} p(-x_1)p(-x_2)\cdots p(-x_n)q(y_1, y_2, \cdots, y_n)dxdy \\
&= \int_{\sum_{i=1}^n \tilde{x}_i y_i > -z} p(\tilde{x}_1)p(\tilde{x}_2)\cdots p(\tilde{x}_n)q(y_1, y_2, \cdots, y_n)d\tilde{x}dy \\
&= \mathbb{P}(Z > -z).
\end{aligned} \tag{11.41}$$

□

Then state the following result for ReLU function and random variable with symmetric distribution around 0.

Lemma 36. *If X is a random variable on $\mathbb{R}$ with symmetric probability density $p(x)$ around zero, i.e.,*

$$p(x) = p(-x). \tag{11.42}$$

Then we have $\mathbb{E}X = 0$ and

$$\mathbb{E}[[\mathrm{ReLU}(X)]^2] = \frac{1}{2}\mathrm{Var}[X]. \tag{11.43}$$

Proof. By definition

$$\mathbb{E}X = \int_{-\infty}^{\infty} xp(x)d(x) = 0. \quad (\text{since } p(x) = p(-x)). \tag{11.44}$$

Furthermore,

$$\begin{aligned}
\mathbb{E}[[\mathrm{ReLU}(X)]^2] &= \int_{-\infty}^{\infty} (\mathrm{ReLU}(x))^2 p(x)dx \\
&= \int_0^{\infty} x^2 p(x)dx \\
&= \frac{1}{2}\int_{-\infty}^{\infty} (x - \mathbb{E}[x])^2 p(x)dx \\
&= \frac{1}{2}\mathbb{E}[[X - \mathbb{E}X]^2] \\
&= \frac{1}{2}\mathbb{V}[X].
\end{aligned} \tag{11.45}$$

□

Based on the previous Lemma 32, we know that $f_k^{\ell-1}$ is a symmetric distribution around 0. The most important observation in Kaiming's paper [**?**] is that:

$$\mathbb{V}[f_i^\ell] = n_{\ell-1}\mathbb{V}[W_{ij}^\ell]\mathbb{E}[[\sigma(f_j^{\ell-1})]^2] = n_{\ell-1}\mathbb{V}[W_{ik}^\ell]\frac{1}{2}\mathbb{V}[f_k^{\ell-1}],$$

if σ = ReLU. Thus, Kaiming's initialization suggests to take:

$$\mathbb{V}[W_{ik}^\ell] = \frac{2}{n_{\ell-1}},, \quad \forall \ell \geq 2. \tag{11.46}$$

For the first layer $\ell = 1$, by definition

$$f^1 = W^1 x + b^1, \tag{11.47}$$

there is no ReLU, thus it should be $\mathbb{V}[W_{ik}^1] = \frac{1}{d}$. For simplicity, they still use $\mathbb{V}[W_{ik}^1] = \frac{2}{d}$ in the paper [**?**]. Similarly, an analysis of the propagation of the gradient suggests that we set

$$\mathbb{V}[W_{ik}^\ell] = \frac{2}{n_\ell}. \tag{11.48}$$

However, in paper [**?**] authors did not suggest to take the trade-off version, they just chose

$$\mathbb{V}[W_{ik}^\ell] = \frac{2}{n_{\ell-1}}, \tag{11.49}$$

as default. Thus, the final version of Kaiming's initialization takes the forward type as

$$W_{ik}^\ell \sim \mathcal{U}(-\sqrt{\frac{6}{n_{\ell-1}}}, \sqrt{\frac{6}{n_{\ell-1}}}), \quad \text{or} \quad W_{ik}^\ell \sim \mathcal{N}(0, \frac{2}{n_{\ell-1}}). \tag{11.50}$$

11.3 Data normalization in CNNs

For CNN models, following the analysis above we have the next iterative scheme in CNNs

$$f^{\ell,\nu} = K^{\ell,\nu} * \sigma(f^{\ell,\nu-1}), \tag{11.51}$$

where the previous step $f^{\ell,\nu-1} \in \mathbb{R}^{c_\ell \times n_\ell \times m_\ell}$, the current step $f^{\ell,\nu} \in \mathbb{R}^{h_\ell \times n_\ell \times m_\ell}$ and $K \in \mathbb{R}^{(2k+1)\times(2k+1)\times h_\ell \times c_\ell}$. Thus we have

$$f_{h;p,q}^{\ell,\nu} = \sum_{c=1}^{c_\ell} \sum_{s,t=-k}^{k} K_{h,c;s,t}^{\ell,\nu} * \sigma(f_{c;p+s,q+t}^{\ell,\nu-1}). \tag{11.52}$$

Take variance on both sides, we will get

$$\mathbb{V}[f_{h;p,q}^{\ell,\nu}] = c_\ell(2k+1)^2\mathbb{V}[K_{h,o;s,t}^{\ell,\nu}]\mathbb{E}[(f_{o;p+s,q+t}^{\ell,\nu-1})^2], \tag{11.53}$$

thus we have the following initialization strategies:

Xavier's initialization

$$\mathbb{V}[K^{\ell,\nu}_{h,o;s,t}] = \frac{2}{(c_\ell + h_\ell)(2k+1)^2}. \tag{11.54}$$

Kaiming's initialization

$$\mathbb{V}[K^{\ell,\nu}_{h,o;s,t}] = \frac{2}{c_\ell(2k+1)^2}. \tag{11.55}$$

Here we can take this Kaiming's initialization as:

- Double the Xavier's choice, and get

$$\mathbb{V}[K^{\ell,\nu}_{h,o;s,t}] = \frac{4}{(c_\ell + h_\ell)(2k+1)^2}. \tag{11.56}$$

- Then pick c_ℓ or h_ℓ for final result

$$\mathbb{V}[K^{\ell,\nu}_{h,o;s,t}] = \frac{2}{c_\ell(2k+1)^2}. \tag{11.57}$$

And they have the both uniform and normal distribution type.

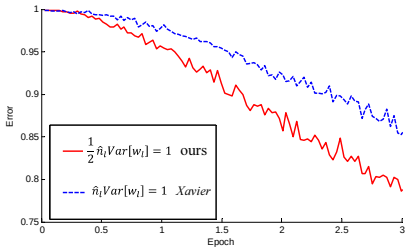

Fig. 11.1. The convergence of a **22-layer** large model. The x-axis is the number of training epochs. The y-axis is the top-1 error of 3,000 random val samples, evaluated on the center crop. Use ReLU as the activation for both cases. Both Kaiming's initialization (red) and "*Xavier's*" (blue) [**?**] lead to convergence, but Kaiming's initialization starts reducing error earlier.

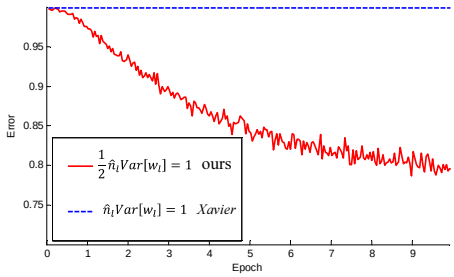

Fig. 11.2. The convergence of a **30-layer** small model (see the main text). Use ReLU as the activation for both cases. Kaiming's initialization (red) is able to make it converge. But "*Xavier's*" (blue) [**?**] completely stalls - It is also verified that that its gradients are all diminishing. It does not converge even given more epochs.

Given a 22-layer model, in Cifar10 both Kaiming's and Xavier's initialization are able to converge and the validation accuracies with two different initialization are about the same(error is 33.82,33.90). But the convergence with Kaiming's initialization is faster than Xavier's. With extremely deep model with up to 30 layers, Kaiming's initialization is able to make the model convergence. On the contrary, Xavier's method completely stalls the learning.

11.4 Batch Normalization in DNN and CNN

Recall the classical (fully connected) artificial deep neural network (DNN) f^L in (7.23). We can define

$$\mathrm{DNN_L} := \{\mathrm{f^L(x;\Theta)} \mid \Theta \in \mathbb{R}^N\}. \tag{11.58}$$

Or, we have a more comprehensive notation for classical DNN models.

$$\begin{aligned}\mathrm{DNN_L} := \{f : f = \theta^L \circ \sigma \circ \theta^{L-1} \cdots \sigma \circ \theta^1(x),\\ \theta^\ell \in \mathbb{R}^{n^{\ell+1}\times(n^\ell+1)}, \quad n^0 = d, \quad n^L = 1, \quad n^\ell \in \mathbb{N}^+\}.\end{aligned} \tag{11.59}$$

Generally speaking, a deep learning problem consists of the next few components:

$$\text{Data} \to \text{Model} \to \text{Training} \to \text{Testing}. \tag{11.60}$$

We will try to give a different explanation for batch normalization based on the above outline.

11.4.1 Ideas Behind the BN for DNN: Internal Covariate Shift in Training

The Internal Covariate Shift is defined in [**?**] as the change in the distribution of network activations due to the change in network parameters during training.

For example, considering the training data with $X = \{(x^i, y^i) \mid i = 1, .., N\} \subset \mathcal{X} := \{(x, y) \mid x, \in \mathbb{R}^n, y \in \mathbb{R}^c\}$, then output of ν-th layer (the input of activation function in $\nu + 1$-the layer) $\{f^\nu(x^i)\}_{i=1}^N$ will satisfy different discrete distributions if you have different parameters Θ which always happened during training process.

More intuitively, fixed distribution of inputs to a sub-network would have positive consequences for the layers *outside* the sub-network, as well. Consider a layer with a sigmoid activation function $f = \sigma(Wx + b)$ where x is the layer input, the weight matrix W and bias vector b are the layer parameters to be learned, and $\sigma(x) = \frac{1}{1+e^{-x}}$. It is easy to see

$$\sigma'(x) \to 0 \quad \text{if} \quad |x| \to \infty.$$

This means that for all dimensions of $y = Wx+b$ except those with small absolute values, the gradient flowing down to x will vanish and the model will train slowly. However, since y is affected by W, b and the parameters of all the layers below, changes to those parameters during training will likely move many dimensions of y into the saturated regime of the nonlinearity and slow down the convergence. This effect is amplified as the network depth increases. In practice, the saturation problem and the resulting vanishing gradients are usually addressed by using $\mathrm{ReLU}(x) = \max(x, 0)$, careful initialization and small learning rates. However, if we could ensure that the distribution of nonlinearity inputs remains more stable as the network trains, then the optimizer would be less likely to get stuck in the saturated regime, and the training would accelerate.

In summary, the gradient vanishes in the following two situations:

- Saturated problem:

$$\sigma'(x) \to 0 \quad \text{for } x \text{ located in some saturated domain.}$$

- Instability from multiplication:

$$\nabla_{W^1} \ell(f^L(x^i;\Theta), y^i) \approx \Pi_{\ell=1}^{L} W^\ell \mathrm{Diag}(\sigma'(f^{\ell-1})) \to 0\,, \quad \text{if } L \text{ is big.}$$

Under this principle, it has been long known [**? ?**] that the network training converges faster if its inputs are whitened, i.e., linearly transformed to have zero means and unit variances, and decorrelated.

Thus to say, to improve the training, one may seek to reduce the internal covariate shift. By fixing the distribution of the layer inputs f^ℓ as the training progresses, it is expected to improve the training speed. As each layer observes the inputs produced by the layers below, it would be advantageous to achieve the same whitening of the inputs of each layer. By whitening the inputs to each layer, BN would take a step towards achieving the fixed distributions of inputs that would remove the ill effects of the internal covariate shift.

Within this framework, whitening the layer inputs is expensive, as it requires computing the covariance matrix

$$\mathrm{Cov}[f^\ell] = \mathbb{E}_{x\in X}[f^\ell(x)[f^\ell(x)]^T] - \mathbb{E}_{x\in X}[f^\ell(x)]\mathbb{E}_{x\in X}[f^\ell(x)]^T \tag{11.61}$$

and its inverse square root, to produce the whitened activations

$$\tilde{f}^\ell = \left(\mathrm{Cov}[f^\ell]\right)^{-1/2}\left(f^\ell - \mathbb{E}[f^\ell]\right), \tag{11.62}$$

as well as the derivatives of these transforms for backpropagation. However, this is impossible to take gradient for $\left(\mathrm{Cov}[f^\ell]\right)^{-1/2}$ w.r.t Θ as $f^\ell = f^\ell(x;\Theta)$.

The original version is to do whitening in Batch i.e. $\mathbb{E}_{x\in X}[\cdot]$, that. This is why this is called Batch Normalization not mini-batch normalization which is the practical version of batch normalization.

11.4.2 Practical batch normalization: assume i.i.d and add scale and shift

Since the full whitening of each layer's inputs is costly and not everywhere differentiable, BN makes two necessary simplifications.

Take batch normalization for each scalar feature (neuron).

The first is that instead of whitening the features in layer inputs and outputs **jointly**, batch normalization will normalize each **scalar feature (neuron)** independently, by making it have the mean of zero and the variance of 1. Assume the distribution of scalar features to be i.i.d.

For a layer with n^ℓ-dimensional input $f^\ell = (f_1^\ell, \ldots, f_{n^\ell}^\ell)$, we will normalize each dimension

$$\hat{f}_k^\ell = \frac{f_k^\ell - \mathbb{E}[f_k^\ell]}{\sqrt{\mathrm{Var}[f_k^\ell]}}$$

where the expectation and variance are computed over the training data set. As shown in [**?**], such normalization speeds up convergence, even when the features are not decorrelated.

Add scale and shift into batch normalization.

Note that simply normalizing each input of a layer may change what the layer can represent. For instance, normalizing the inputs of a sigmoid would constrain them to the linear regime of the nonlinearity. To address this, we make sure that *the transformation inserted in the network can represent the identity transform*. To accomplish this, we introduce, for each activation $\hat{f}_k^\ell$, a pair of parameters $\gamma_k^\ell, \beta_k^\ell$, which scale and shift the normalized value:

$$\tilde{f^\ell}_k = \gamma_k^\ell \hat{f^\ell}_k + \beta_k^\ell. \tag{11.63}$$

These parameters are learned along with the original model parameters, and restore the representation power of the network. Indeed, by setting $\gamma_k^\ell = \sqrt{\mathrm{Var}[f_k^\ell]}$ and $\beta_k^\ell = \mathbb{E}[f_k^\ell]$, we could recover the original activations, if that were the optimal thing to do.

11.4.3 Batch normalization for DNN

Definition of batch normalization operation based on the batch

Following the idea in (11.60), we consider that we have the all training data as

$$(X, Y) := \{x^i, y^i\}_{i=1}^N. \tag{11.64}$$

Since the normalization is applied to each activation independently, let us focus on a particular activation f_k^ℓ and omit k as f^ℓ for clarity. We have N values of this activation in the batch,

$$X = \{x_1, \cdots, x_N\}.$$

Let the normalized values be $\hat{f}^\ell$, and their linear transformations be $\tilde{f}^\ell$.

(11.65)

$$\mu_X^\ell \leftarrow \mathbb{E}_{x\sim X}[f^\ell(x)] = \frac{1}{N}\sum_{i=1}^N f^\ell(x^i) \qquad \text{batch mean}$$

$$\sigma_X^\ell \leftarrow \mathbb{E}_{x\sim X}\left[(f^\ell(x) - \mathbb{E}_{x\sim X}[f^\ell(x)])^2\right] = \frac{1}{N}\sum_{i=1}^N (f^\ell(x^i) - \mu_X^\ell)^2 \qquad \text{batch variance}$$

$$\hat{f}^\ell(x) \leftarrow \frac{f^\ell(x) - \mu_X^\ell}{\sqrt{\sigma_X^\ell + \epsilon}} \qquad \text{normalize}$$

$$\tilde{f}^\ell(x) \leftarrow \gamma^\ell \hat{f}^\ell(x) + \beta^\ell \qquad \text{scale and shift}$$

Here we note that all these operations in the previous equation are defined element-wise. Then at last, we define the batch normalization operation based on the batch set as

$$\mathrm{BN}_X(f^\ell(x)) = \tilde{f}^\ell(x) := \gamma^\ell \frac{f^\ell(x) - \mu_X^\ell}{\sqrt{\sigma_X^\ell + \epsilon}} + \beta^\ell, \tag{11.66}$$

where $\tilde{f}^\ell(x)$, μ_X^ℓ and σ_X^ℓ are given above.

Model with batch normalization

Then we have the new DNN model with batch normalization as:

$$\begin{cases} \tilde{f}^1(x^i) & = (\theta^1(x^i)), \\ \tilde{f}^\ell & = \theta^\ell \circ \sigma \circ \mathrm{BN}_X(\tilde{f}^{\ell-1}), \quad \ell = 2, ..., L. \end{cases} \tag{11.67}$$

For a more comprehensive notation, we can use the next notation

$$\sigma_{\mathrm{BN}} := \sigma \circ \mathrm{BN}_X. \tag{11.68}$$

We can remove the basis b^ℓ in θ^ℓ, thus to say the real model we use should be

$$\begin{cases} \tilde{f}^1(x^i) & = W^1 x^i, \\ \tilde{f}^\ell & = W^\ell \sigma_{\mathrm{BN}}(\tilde{f}^{\ell-1}), \quad \ell = 2, ..., L. \end{cases} \tag{11.69}$$

Combine the two definitions, we note

$$\tilde{\Theta} := \{W, \gamma, \beta\}, \tag{11.70}$$

where $W = \{W^1, \cdots, W^l\}$, $\gamma := \{\gamma^2, \cdots, \gamma^L\}$ and $\beta := \{\beta^2, \cdots, \beta^L\}$. Finally, we have the loss function

$$\mathcal{L}(\tilde{\Theta}) = \mathbb{E}_{(x,y)\sim(X,Y)} \approx \frac{1}{N} \sum_{i=1}^{N} \ell(\tilde{f}^L(x^i; \tilde{\Theta}), y^i). \tag{11.71}$$

A key observation in (11.71) and the new BN model (11.69) is that

$$\begin{aligned} \mu_X^\ell &= \mathbb{E}_{x\sim X}[f^\ell(x)], \\ \sigma_X^\ell &= \mathbb{E}_{x\sim X}\left[(f^\ell(x) - \mathbb{E}_{x\sim X}[f^\ell(x)])^2\right], \\ \mathcal{L}(\tilde{\Theta}) &= \mathbb{E}_{(x,y)\sim(X,Y)}\left[\ell(\tilde{f}^L(x^i; \tilde{\Theta}), y^i)\right]. \end{aligned} \tag{11.72}$$

Here we need to mention that

$$x \sim X$$

means x subjects to the discrete distribution of all data X.

11.4.4 Batch normalization: some "modified" SGD training algorithm

Following the key observation in (11.72), and recall the similar case in SGD, we do the the sampling trick in (11.71) and obtain the mini-batch SGD:

$$x \sim X \approx x \sim \mathcal{B}, \tag{11.73}$$

here $\mathcal{B}$ is a mini-batch of batch X with $\mathcal{B} \subset X$.

However, for problem in (11.71), it is very difficult to find some subtle sampling method because of the composition of μ_X^ℓ and $[\sigma_X^\ell]$. However, one simple way for sampling (11.71) can be chosen as taking (11.73) for all the expectation case in (11.71) and (11.72). This is to say, in training process (t-th step for example), once we choose $B_t \subset X$ as the mini-batch, then the model becomes

$$\begin{cases} \tilde{f}^1(x^i) &= W^1 x^i, \\ \tilde{f}^\ell &= W^\ell \sigma_{\mathrm{BN}}(\tilde{f}^{\ell-1}), \quad \ell = 2, ..., L. \end{cases} \tag{11.74}$$

where

$$\sigma_{\mathrm{BN}} := \sigma \circ \mathrm{BN}_{\mathcal{B}_t}, \tag{11.75}$$

or we can say that X is replaced by $\mathcal{B}_t$ in this case. Here $\mathrm{BN}_{\mathcal{B}_t}$ is defined by

$$\begin{aligned} \mu_{\mathcal{B}_t}^\ell &\leftarrow \frac{1}{m}\sum_{i=1}^m f^\ell(x^i) && \text{mini-batch mean} \\ \sigma_{\mathcal{B}_t}^\ell &\leftarrow \frac{1}{m}\sum_{i=1}^m (f^\ell(x^i) - \mu_{\mathcal{B}_t})^2 && \text{mini-batch variance} \\ \hat{f}^\ell(x) &\leftarrow \frac{f^\ell(x) - \mu_{\mathcal{B}_t}^\ell}{\sqrt{\sigma_{\mathcal{B}_t}^\ell + \epsilon}} && \text{normalize} \\ \mathrm{BN}_{\mathcal{B}_t}(\tilde{f}^\ell) := \tilde{f}^\ell(x) &\leftarrow \gamma^\ell \hat{f}^\ell(x) + \beta^\ell && \text{scale and shift} \end{aligned} \tag{11.76}$$

Here batch normalization operation introduces some new parameters such as γ and β. Thus to say, for training phase, if we choose mini-batch as $\mathcal{B}_t$ in t-th training step, we need to take gradient

$$\frac{1}{m}\nabla_{\tilde{\Theta}} \sum_{i \in \mathcal{B}_t} \ell(\tilde{f}^L(x^i; \tilde{\Theta}), y^i), \tag{11.77}$$

which requires the gradient of $\mu_{B_t}^\ell$ or $[\sigma_{B_t}^\ell]$ w.r.t W^i for $i \le \ell$. To derive the new gradient formula for batch normalization step,

$$\mu_{\mathcal{B}_t}^\ell, \quad \text{and} \quad \sigma_{\mathcal{B}_t}^\ell,$$

contain the output of $\tilde{f}^{\ell-1}$. This is exact the batch normalization method described in [**?**].

11.4.5 Final model with BN in DNN after training

One key problem is that, in the batch normalization operator, we need to compute the mean and variance in a data set (batch or mini-batch). However, in the inference step, we just input one data into this DNN, how to compute the batch normalization operator in this situation.

Actually, the γ and β parameter is fixed after training, the only problem is to compute the mean μ and variance σ. All the mean $\mu_{\mathcal{B}_t}$ and variance $\sigma_{\mathcal{B}_t}$ during the training phase are just the approximation of the mean and variance of whole batch i.e. μ_X and σ_X as shown in (11.72).

One natural idea might be just use the batch normalization operator w.r.t to the whole training data set, thus to say just compute μ_X and σ_X by definition in (11.65).

However, there are at least the next few problems:

- computation cost,
- ignoring the statistical approximation (don't make use of the $\mu_{\mathcal{B}_t}$ and $\sigma_{\mathcal{B}_t}$ in training phase).

Considering that we have the statistical approximation for μ_X and σ_X during each SGD step, moving average might be a more straightforward way. Thus to say, we define the μ^ℓ and $[\sigma^\ell]$ for the inference (test) phase as

$$\mu^\ell = \frac{1}{T}\sum_{t=1}^{T}\mu^\ell_{\mathcal{B}_t}, \quad \sigma^\ell = \frac{1}{T}\frac{m}{m-1}\sum_{t=1}^{T}\sigma^\ell_{\mathcal{B}_t}. \tag{11.78}$$

Here we take Bessel's correction for unbiased variance. The above moving average step is found in the original paper of batch normalization in [**?**].

Another way to do this is to call the similar idea in momentum. At each time step we update the running averages for mean and variance using an exponential decay based on the momentum parameter:

$$\begin{aligned}\mu^\ell_{\mathcal{B}_t} &= \alpha\mu^\ell_{\mathcal{B}_{t-1}} + (1-\alpha)\mu^\ell_{\mathcal{B}_t},\\ \sigma^\ell_{\mathcal{B}_t} &= \alpha\sigma^\ell_{\mathcal{B}_{t-1}} + (1-\alpha)\sigma^\ell_{\mathcal{B}_t}.\end{aligned} \tag{11.79}$$

α is close to 1, we can take it as 0.9 generally. Then we all take bath mean and variance as $\mu^\ell_X \approx \mu^\ell_{\mathcal{B}_T}$ and $\sigma^\ell_X \approx \sigma^\ell_{\mathcal{B}_T}$.

Many people argue that the variance here should also use Bessel's correction.

11.4.6 Batch Normalization for CNN

One key idea in batch normalization is to do normalization with each scalar features (neurons) separately along a mini-batch. Thus to say, we need to identify what is neuron in CNN. This is a historical problem, some people think neuron in CNN should be the pixel in each channel, some other people think that each channel is just one neuron. Batch normalization chooses the later one. One important reason for this choice is the fact of computation cost.

For convolutional layers, batch normalization additionally requires the normalization to obey the convolutional property so that different elements of the same feature map, at different locations, are normalized in the same way. To compute $\mu^{\ell}_{\mathcal{B}_t}$, we take mean of the set of all values in a feature map across both the elements of a mini-batch and spatial locations, so for a mini-batch of size m and feature maps of size $m_\ell \times n_\ell$ (image geometrical size), we use the effective mini-batch of size $mm_\ell n_\ell$. We learn a pair of parameters γ_k and β_k per feature map (k-th channel), rather than per activation.

For simplicity, then have the following batch normalization scheme for CNN

(11.80)
$$\begin{aligned}
\mu^{\ell,j}_{\mathcal{B}_t} &\leftarrow \frac{1}{m \times m_\ell \times n_\ell} \sum_{i=1}^{m} \sum_{1\le s\le m_\ell, 1\le t\le n_\ell} f^{\ell,j}_{s,t}(x^i) && \text{mean on channel } j\\
\sigma^{\ell,j}_{\mathcal{B}_t} &\leftarrow \frac{1}{m \times m_\ell \times n_\ell} \sum_{i=1}^{m} \sum_{1\le s\le m_\ell, 1\le t\le n_\ell} (f^{\ell,j}_{s,t}(x^i) - \mu^{\ell,j}_{\mathcal{B}_t})^2 && \text{variance on channel } j\\
\hat{f}^{\ell,j}_{s,t}(x) &\leftarrow \frac{f^{\ell,j}_{s,t}(x)] - \mu^{\ell,j}_{\mathcal{B}_t}}{\sqrt{\sigma^{\ell,j}_{\mathcal{B}_t} + \epsilon}} && \text{normalize}\\
[\mathrm{BN}_{\mathcal{B}_t}(\tilde{f}^{\ell})]_{j;st} := \tilde{f}^{\ell,j}_{s,t}(x) &\leftarrow \gamma^{\ell,j} \hat{f}^{\ell,j}_{s,t}(x) + \beta^{\ell,j} && \text{scale and shift on channel}
\end{aligned}$$

11.4.7 Batch normalization for MgNet

When we train MgNet, we also adopt the batch normalization mechanism. This means that, when we do training for MgNet, we apply the following basic block in MgNet

(11.81) $$u^{\ell,\nu} \leftarrow u^{\ell,\nu-1} + \mathrm{ReLU} \circ \mathrm{BN}_{\mathcal{B}_t} \circ B^{\ell,\nu} * \mathrm{ReLU} \circ \mathrm{BN}_{\mathcal{B}_t}(f^\ell - A^\ell * u^{\ell,\nu-1}),$$

or simply

(11.82) $$u^{\ell,\nu} \leftarrow u^{\ell,\nu-1} + \mathrm{ReLU}_{\mathrm{BN}} \circ B^{\ell,\nu} * \mathrm{ReLU}_{\mathrm{BN}}(f^\ell - A^\ell * u^{\ell,\nu-1}),$$

where

(11.83) $$\mathrm{ReLU}_{\mathrm{BN}} = \mathrm{ReLU} \circ \mathrm{BN}_{\mathcal{B}_t}.$$